FLEXIBLE ELECTRIC BOILERS AS PART OF THE ENERGY SYSTEM OF THE FUTURE

Lappeenranta–Lahti University of Technology LUT

Master's programme in Energy Technology

2026

Chieh-en Chou

Examiner(s): Associate professor Aki Grönman

Associate Professor Antti Uusitalo

ABSTRACT

Lappeenranta–Lahti University of Technology LUT

LUT School of Energy Systems

Energy Technology

Double Degree Programme in cooperation with: Leibniz University Hannover

Chieh-en Chou

Flexible electric boilers as part of the energy system of the future

Master's thesis

2026

98 pages, 27 figures, 13 tables

Examiner(s): Associate professor Aki Grönman and Associate Professor Antti Uusitalo

Keywords: district heating, electrification, electric boiler, thermal energy storage, combined heat and power, linear programming, techno-economic analysis.

Decarbonising district heating through electrification is widely advocated, but its value within a carbon-neutral biomass combined heat and power (CHP) system is ambiguous. This thesis examines the cost and emissions effects of partial and full electrification of the Lappeenranta district heating system, and the role of the existing thermal energy storage (TES). An hourly linear programming model covering 1 March 2025 to 9 March 2026 is built using operational data from Lappeenrannan Energia, Nord Pool spot prices, and Fingrid hourly grid CO2 intensity. Five configurations are compared, from the current biomass CHP system with natural gas boilers to full electrification; the model is validated against measured operation and tested through sensitivity sweeps.

Partial electrification combined with the existing TES is the only configuration cheaper than the current system on total cost, saving 0.33 MEUR per year while reducing emissions by roughly 33%. This advantage is robust to plausible variation in electricity and gas prices. Full electrification achieves the lowest operating cost but, owing to its capital cost, requires a carbon price of 219 EUR/tCO2 to break even, while electrification without storage requires 511 EUR/tCO2. The emissions reduction comes from the fuel switch away from natural gas, not from storage, and full electrification emits more than the partial configurations because grid electricity displaces carbon-neutral biomass heat. The value of TES grows approximately 2.6-fold under electrification. The case for full electrification strengthens as carbon prices rise and the grid decarbonises.

SYMBOLS AND ABBREVIATIONS

Roman characters

c	Cost coefficient per unit of heat (fuel, electricity, slack penalty, cycling)	EUR/MWh
c_co2	Carbon price	EUR/tCO2
C_op	Total annual operating cost (LP objective)	EUR
ef	Emission factor of fuel input	kgCO2/MWh
I_0	Lump-sum investment cost	EUR
i	Production unit index	–
n	Technical lifetime	a
P	TES charging or discharging power	MW
Q	Heat output or heat demand	MW
r	Discount rate	–
SOC	State of charge of the thermal energy storage	MWh
t	Hourly time index	h
T	Optimisation time horizon	h

Greek characters

α_chp	CHP electricity credit
η	Efficiency (unit conversion; TES charge, discharge, standing loss)

Subscripts

ch / charge	TES charging
chp	Combined heat and power unit
demand	Heat demand
dis / discharge	TES discharging
eb	Electric boiler
gas	Gas boiler
i	Production unit
loss	Standing heat loss
max	Maximum limit (capacity or power rating)
min	Minimum limit
oil	Oil boiler
op	Operating (cost)
pellet	Pellet boiler
slack	Unmet heat demand (slack variable)
t	Hour
t_0	First hour of storage operation

Abbreviations

ACC	Annualised capital cost
aFRR	Automatic Frequency Restoration Reserve

CHP	Combined heat and power
COP	Coefficient of performance
CRF	Capital recovery factor
DEA	Danish Energy Agency
DSO	Distribution system operator
EB	Electric boiler
ETS	Emissions Trading System (EU)
FCR	Frequency Containment Reserve
HP	Heat Pump
LP	Linear programming
mFRR	Manual Frequency Restoration Reserve
MILP	Mixed-integer linear programming
O&M	Operation and maintenance
P2H	Power-to-heat
RMSE	Root-mean-square error
SOC	State of charge
TES	Thermal energy storage
TSO	Transmission system operator
VRE	Variable Renewable Energy

DECLARATIONS

Turnitin

The originality of this thesis has been reviewed with the Turnitin similarity checking service.

AI usage

The author of the thesis, Chieh-en Chou, used the following AI-tools during the preparation of the thesis:

1. Claude
    a. Purpose of use: brainstorming sources, MATLAB support, interpretation review, structuring writing points, grammar and clarity.
    b. Explanation of the use of the tool: the tool was used interactively throughout the project; all thesis text was written by the author, with the tool used to check and revise drafts for grammar, clarity and consistency, to verify literature sources, and to assist in debugging the MATLAB optimisation code; all suggestions were reviewed, edited and verified by the author before use.
2. Copilot
    a. Purpose of use: draft schedule, refine research questions
    b. Explanation of the use of the tool: In the initial phase, the tool was used to refine the research questions based on the project description and to draft a rough six-month schedule.

Responsibility

The author, Chieh-en Chou, takes full responsibility for the content of this thesis and has reviewed and edited the content generated by the possible use of AI tools.

Table of contents

Abstract

Symbols and abbreviations

Declarations

1 Introduction 11
1.1 Background and motivation 11
1.2 Research objectives and questions 11
1.3 Scope and delimitations 12
1.4 Structure of the thesis 13
2 Literature review 13
2.1 Need for flexibility in renewable-based power systems 13
2.1.1 The changing generation mix 13
2.1.2 From controllable to variable supply 14
2.1.3 The resulting need for flexibility 14
2.1.4 Flexibility options and sector coupling 15
2.2 Electric boilers as flexible power-to-heat technology 15
2.2.1 Working principles and types 15
2.2.2 Performance characteristics 16
2.2.3 Operational limitations 16
2.2.4 Technology selection: comparison with heat pumps 17
2.3 Electric boilers in CHP-based district heating systems 18
2.3.1 District heating fundamentals 18
2.3.2 CHP operation and its limits in high-VRE systems 19
2.3.3 Integrating the EB: roles and functions 20
2.3.4 Thermal energy storage as the enabler 21
2.4 Electric boilers in electricity and reserve markets 21
2.4.1 Electricity market structure 21
2.4.2 EB in energy markets 22
2.4.3 EB in reserve markets 23
2.4.4 Revenue streams and system-level value 23

2.5 Identified research gap and motivation 24
3 Methodology 25
3.1 Case study: the Lappeenranta district heating system 27
3.1.1 Network overview and heat demand 27
3.1.2 Production unit portfolio and merit order 27
3.1.3 Thermal energy storage (TES) specification 28
3.2 Data collection 29
3.2.1 Operational data 29
3.2.2 Open data sources 29
3.2.3 Temporal resolution and study period 30
3.3 Scenario design 30
3.3.1 Definition of Scenarios A–E 30
3.3.2 Scenario B as the baseline 31
3.3.3 The slack variable and its cost 32
3.4 Optimisation model 33
3.4.1 Decision variables and constraints 34
3.4.2 Objective function 35
3.4.3 Thermal energy storage dynamics 36
3.4.4 Cost treatment: capital, O&M, and carbon price 38
3.4.5 Justification of linear programming over MILP 40
3.4.6 Perfect foresight and the absence of a rolling horizon 41
3.5 Parameters and assumptions 42
3.5.1 CHP electricity credit 42
3.5.2 Emission factors and grid CO2 intensity 43
3.5.3 Summary of model parameters and inputs 44
3.6 Sensitivity analysis design 46
3.6.1 Price sweeps 47
3.6.2 Thermal energy storage sweeps 47
3.6.3 CHP electricity credit and carbon price sweep 47
3.7 Model validation 48
3.7.1 Electric boiler validation 48
3.7.2 Thermal energy storage validation 51
3.7.3 CHP validation 55

4 Results 57
4.1 Overview 57
4.2 Dispatch behaviour 57
4.3 Cost results 60
4.3.1 Operating cost ordering 61
4.3.2 Total cost ordering 62
4.3.3 Cost savings against the baseline 63
4.4 Emissions results 63
4.4.1 Emissions by scenario 63
4.4.2 The roles of fuel switching and storage 64
4.4.3 Emissions of full electrification 65
4.4.4 Emissions intensity of electric boiler operation 65
4.4.5 Emissions under grid decarbonisation 66
4.5 Sensitivity analysis 67
4.5.1 Sensitivity to electricity and gas prices 67
4.5.2 Sensitivity to TES power limits 71
4.5.3 Optimal TES capacity 73
4.5.4 Sensitivity to TES conversion efficiency 75
4.5.5 Sensitivity to CHP electricity credit and carbon price 76
4.5.6 Carbon price break-even for investment 79
4.6 Summary of results 80
5 Discussion 81
5.1 Role and optimal capacity of electric boilers 82
5.2 Economic value of thermal energy storage 83
5.3 Decoupling decarbonisation from economics 84
5.4 The emissions trade-off of electrification in a biomass-CHP system 85
5.5 Sensitivity to carbon price and key assumptions 86
5.6 Comparison with existing literature 87
5.7 Practical implications for Lappeenrannan Energia and study limitations 89
6 Conclusion 90
6.1 Answers to the research questions 90
6.2 Practical recommendations 91
6.3 Future research 92

References.....93

1 Introduction

1.1 Background and motivation

Global warming is driving an urgent, worldwide search for ways to reduce greenhouse gas emissions. Heating is an essential part of daily life and accounts for a major share of society's carbon footprint, which makes it central to reaching carbon neutrality. At the same time, the rapid growth of variable renewable energy (VRE) generation is making electricity supply more variable and less predictable, so consumption must become more flexible than before to keep production and demand in balance. This shift also creates an opportunity to decarbonise end-use sectors by switching from fossil fuels to electricity. The European Union has set a target of net-zero greenhouse gas emissions by 2050 (European Commission, 2026), and Finland has adopted the more ambitious goal of carbon neutrality by 2035 (Finnish Ministry of the Environment, 2022). Within this policy context, district heating is well placed to contribute: combined with an electric boiler (EB) and thermal energy storage (TES), it can use inexpensive low-carbon electricity to cut emissions and lower operating cost. This thesis examines how a biomass combined heat and power (CHP) based district heating system in South Karelia, Finland, can be decarbonised further. This thesis was carried out as part of a wider research collaboration on flexible electric boilers in the South Karelia region.

1.2 Research objectives and questions

The objective of this thesis is to assess, on techno-economic grounds, how electric boilers (EB) and thermal energy storage (TES) can be integrated into the Lappeenranta district heating system, which is currently based on biomass CHP. The current system is compared against partially and fully electrified configurations, with and without storage, in order to evaluate their cost, emissions and the conditions under which each becomes justified. This leads to the following central research question:

How can electric boilers and thermal energy storage be integrated into the Lappeenranta biomass-CHP district heating system to improve its cost-efficiency and reduce emissions, and under what conditions does each configuration become justified?

The main question is addressed through four sub-questions:

1. What role can the electric boiler play in the system, and how does its capacity affect heat dispatch, cost and emissions?
2. What is the economic value of thermal energy storage, what storage size is appropriate, and how does that value change when the system is electrified?
3. How do partially and fully electrified configurations compare with the current system including existing storage, the baseline of this study, in operating cost, total cost and emissions?
4. At what carbon price does each electrified configuration become cost-competitive with the baseline?

1.3 Scope and delimitations

This study focuses on the linear programming (LP) optimisation of five defined scenarios, based on one year of operational data from the Lappeenranta district heating system. Electricity is priced at the day-ahead spot price throughout.

Four elements are deliberately placed outside the scope of this work. First, reserve-market revenue from EBs is excluded, since the district heating company does not treat it as a main source of operational income. Second, heat pumps are not modelled, as the local district heating system does not include them. Third, the detailed impact on the electricity grid and transmission network is not assessed, since it is addressed by other work packages within the same project. Fourth, the model assumes perfect foresight of electricity prices, whereas in practice the operator knows prices only up to the day-ahead stage; a rolling forecast could not be incorporated within the project timeframe, and the implications are discussed in Section 3.4.6 .

1.4 Structure of the thesis

The remainder of this thesis is structured as follows. Chapter 2 reviews the literature on the need for flexibility in renewable-based power systems, the characteristics of electric boilers as a power-to-heat technology, their integration into CHP-based district heating systems, and their role in electricity and reserve markets, and it identifies the research gap this thesis addresses. Chapter 3 presents the methodology, including the case study, the data, the scenario design, and the optimisation model. Chapter 4 reports the results of the optimisation. Chapter 5 discusses these results and their implications, and Chapter 6 concludes the thesis and outlines directions for future work.

2 Literature review

2.1 Need for flexibility in renewable-based power systems

2.1.1 The changing generation mix

Modern power systems have changed rapidly in recent years, and the transformation is still ongoing. The main change lies in the increase of VRE, especially for wind and solar energy, which have grown at unprecedented speed (Impram, Varbak Nese and Oral, 2020; Sinsel, Riemke and Hoffmann, 2020). The transformation is driven by policy. At the European level, the European Climate Law sets a legally binding target of climate neutrality by 2050, requiring every sector to move away from fossil fuels (European Commission, 2026). Finland legislated one of the earliest national targets, carbon neutrality by 2035, in its Climate Act (Finnish Ministry of the Environment, 2022). The Finnish generation mix itself reflects the shift: wind power capacity has grown from around 200 MW in 2012 to over 9,400 MW at the end of 2025, and wind now accounts for roughly 28% of the electricity produced in Finland (Renewables Finland, 2026). The energy security concerns that followed the events of 2022 have further reinforced the move away from imported fossil fuels (European Commission, 2022). Heating plays a particular part in this transformation: electrification of heating serves a double purpose, replacing fossil fuel combustion in the

heat sector while simultaneously offering the power system a large and flexible demand, which is why power-to-heat has received growing attention (Bloess et al., 2018).

2.1.2 From controllable to variable supply

The traditional way of producing electricity by burning fossil fuel allows production to follow demand, whereas renewable generation is fully dependent on the weather, which does not follow consumption (Sinsel, Riemke and Hoffmann, 2020). The growing share of VRE also brings both variability, as output changes over time, and uncertainty, as output cannot be exactly predicted (Impram, Varbak Nese and Oral, 2020). The first challenge is the temporal supply and demand mismatch, with surpluses in high-wind hours and shortfalls at peak demand, which leads to frequency instability (Impram, Varbak Nese and Oral, 2020). The second challenge is curtailment: when the system cannot absorb further VRE surpluses, the excess output must be curtailed, and the amount of curtailment tends to grow with the penetration level (Bird et al., 2016). The third challenge is in the market, where renewable generators bid at near-zero marginal cost, which lowers the average electricity price but increases its volatility, producing more frequent very low and even negative prices (Ketterer, 2014; Cramton, 2017). In the Nordic market, this growing price volatility is precisely what makes flexible electricity use in heating economically interesting (Trømborg et al., 2017).

2.1.3 The resulting need for flexibility

As described in the previous section, power systems now require greater flexibility to maintain the balance between supply and demand and to cope with uncertainty on both sides, and this need grows directly with the penetration of VRE (Impram, Varbak Nese and Oral, 2020). Flexibility also allows renewable production that exceeds demand at the time to be used or stored rather than curtailed, which improves the utilisation of renewable energy and lowers system cost (Lund et al., 2015; Yilmaz et al., 2018). Flexibility measures exist on the supply side, in storage, and on the demand side, and the choice between them is ultimately an economic one (Lund et al., 2015). The available measures are examined in the next section.

2.1.4 Flexibility options and sector coupling

Flexibility can be provided through different measures, including flexible generation on the supply side, energy storage, grid expansion and demand-side measures (Lund et al., 2015).

Coupling the power sector with other energy sectors expands the flexibility space beyond what electricity-only solutions offer, since flexibility may already be embedded in the other sector, sometimes at lower cost (Lund et al., 2012; Bloess, Schill and Zerrahn, 2018).

Among sector coupling strategies, one of the most accessible is to convert surplus renewable electricity into heat (power-to-heat, P2H), and the value of EBs and heat pumps for wind power integration was recognised in the Nordic system early on (Meibom et al., 2007). P2H technologies such as the electric boiler and the heat pump are technically mature and well suited to providing flexibility, with EBs among the cheapest per unit of ramping capability (Witkowski et al., 2020). The heating sector is particularly well placed to host this flexibility: heat demand is large, especially in the Nordic context, buildings and networks carry considerable thermal inertia, and heat can be stored far more cheaply than electricity (Ibrahim, Ilinca and Perron, 2008; Bloess, Schill and Zerrahn, 2018). These properties motivate the technology examined in the remainder of this chapter, the electric boiler.

2.2 Electric boilers as flexible power-to-heat technology

2.2.1 Working principles and types

An electric boiler converts electricity directly into heat and can be categorised into two main types based on the heating principle: heating by resistance elements (resistance boiler) or by passing current directly through the water (electrode boiler) (Pini et al., 2018; Novikov et al., 2023).

In an electrical resistance boiler, the heating elements are integrated within a hot water tank, and heat is produced by the electrical resistance of the heating wire as current passes through it. Resistance boilers operate at low voltage with capacities up to a few MW, since the capacity is limited by the number of heating elements required. Electrode boilers, in contrast, connect at medium to high voltage (approximately 4 to 24 kV), where capacities can reach

tens of MW, which makes them the relevant type for district heating (Ivanova, Sauhats and Linkevics, 2017; Danish Energy Agency, 2026b). The type therefore also determines the performance envelope of the unit, which is examined next.

2.2.2 Performance characteristics

Within the context of integration with district heating, as mentioned above, the electrode boiler is the type whose scale suits sector coupling in district heating. For EBs to provide flexibility, there are a few key characteristics, including efficiency, ramp rate, response time, capacity range, controllability, and minimum load. The EB is a mature technology and its efficiency has almost reached unity (Pini et al., 2018; Danish Energy Agency, 2026b). The main advantage of EB is that it can ramp effectively without technical limitation and start in seconds to minutes regardless of the capacity, making them the fastest heating technology (Witkowski et al., 2020; Javanshir et al., 2023). Efficiency determines the operating cost per MWh of heat, ramp rate and response time determine how fast the unit can follow prices and qualify for fast markets, and the wide controllable range with a minimal load floor means output can track the price signal almost continuously. Capacity ranges, minimum loads and controllability differ by type. Table 1 tabulates the EB performance characteristics.

Table 1. Flexibility characteristics of Electrode EB (Ivanova, Sauhats and Linkevics, 2017; Pini et al., 2018; Danish Energy Agency, 2026b)

Flexibility characteristics	Range
Capacity range	5-60 MWth
Connection voltage	4-24 kV
Net thermal Efficiency	99%
Ramp rate up/down	100 % nom power/min
Response time (cold / hot start up time)	Cold: 5 min Hot: < 0.5 min
Controllability (controllable range)	1-100%
Minimum load	1-5%

2.2.3 Operational limitations

The flexibility of the EB comes with limitations that follow directly from its working principle. First, an EB relies on electricity to produce heat and is therefore fully exposed

economically to the electricity price, taxes, and grid tariffs (Soysal et al., 2016). Grid tariff design alone can decide whether operation is profitable, as tariffs raise the effective electricity cost and shift the price threshold below which the EB is competitive (Kirkerud, Trømborg and Bolkesjø, 2016). Second, for EB operation, heat demand or storage has to exist, otherwise the heat goes to waste and cheap electricity hours cannot be exploited (Trømborg et al., 2017; Bloess, Schill and Zerrahn, 2018). Third, in order to enable the very fast ramp up time, a minimal electrical load (about 1% nominal capacity) is required to keep the EB operational (Witkowski et al., 2020). Fourth, grid connection is a further practical constraint owing to the voltage requirements of EBs: large-scale units impose a considerable load on local networks, and the terms of connection and operation are set by the distribution system operator (DSO) (Sinha, Jensen and Radhakrishnan Pillai, 2018). When an EB constitutes a relatively large load within the network, power flows on individual lines may exceed their limits during peak consumption periods, affecting grid stability (Sun et al., 2022). Moreover, investment in new EB capacity is ultimately limited by the physical capacity of the available grid connection (Danish Energy Agency, 2026b).

Beyond the boiler itself, integration into the district heating (DH) system is subject to the thermal inertia of the network: the thermal mass and storage within the network respond on considerably slower timescales than the EB. This mismatch further constrains how quickly the overall system can follow changes in EB heat production without compromising delivered heat or comfort (Borsche, Oldewurtel and Andersson, 2014; Lu et al., 2023).

These limitations define the conditions under which EB deployment is feasible and underpin the comparison with alternative power-to-heat technologies in the following section.

2.2.4 Technology selection: comparison with heat pumps

The advantages of the EB are that it is a mature technology, structurally simple, with low capital cost and fast response (Danish Energy Agency, 2026b). Among thermal flexibility options it has the lowest cost of reactivity, defined as the specific investment divided by the ramp rate (Witkowski et al., 2020), and it offers excellent controllability.

Its main alternative as a power-to-heat technology is the large-scale heat pump. The two differ in how they use electricity: an EB uses electricity to produce heat directly, so its ratio

of heat output to electricity input is close to one, whereas a heat pump uses electricity to transport heat and can therefore reach a coefficient of performance (COP) of 2 to 4. The heat pump is consequently more efficient and often more profitable per MWh of heat, but at the price of higher capital cost, slower response and tighter operational constraints (Blarke, 2012; Gao et al., 2023; Knorr, Schlosser and Meschede, 2023).

System studies find that both power-to-heat technologies add value in systems with a growing share of VRE, and that the choice between them depends on the price pattern and the district heating operating profile rather than one dominating. Heat pumps are favoured for high utilisation of a base heat load, whereas EBs are favoured for intermittent, price-driven operation in the hours when electricity is cheap (Blarke, 2012; Nielsen et al., 2016; Javanshir, Syri and Hiltunen, 2024).

This study focuses on the EB for two reasons. First, the district heating operator already has an EB in operation, which makes its expansion the relevant marginal investment. Second, its low capital cost, unrestricted ramping and suitability for spot-price-driven operation match the investment question examined here, in which the unit runs only when the electricity price makes it the cheapest heat source. A full comparison with heat pumps is outside the scope of this thesis.

2.3 Electric boilers in CHP-based district heating systems

2.3.1 District heating fundamentals

District heating is a mature technology in which heat is produced centrally and distributed to residential, commercial and industrial users, normally through insulated water pipe networks (Henchoz et al., 2016; Werner, 2017). Compared with local boilers, this reduces heat production cost, increases energy efficiency and allows better control of pollution (Frederiksen and Werner, 2013). The heat sources for district heating have also evolved, from traditional fossil fuel combustion, CHP plants, waste-to-energy and industrial processes towards renewable heat sources such as geothermal and solar energy, and a combination of sources is now seen as the way to achieve lower environmental impact (Werner, 2017). Furthermore, to support a future energy system based fully on renewable

energy, modern district heating systems are evolving to integrate with fluctuating renewable energy sources (Lund et al., 2014), with the aim of making the entire system carbon-free and sustainable (Mazhar, Liu and Shukla, 2018).

In the Finnish context, district heating covers 46% of the total heat demand (Werner, 2017; Finnish Energy, 2026). Its production has historically relied on fossil-fuelled plants, much of it CHP, but has since shifted towards biomass, and operators are now electrifying their systems (Javanshir, Syri and Hiltunen, 2024). Research in the Finnish context also shows that an electrified heating system is cost-competitive even under extreme circumstances such as the 2022 European energy crisis (Javanshir, Syri and Hiltunen, 2024). In such a system, the CHP plant serves as the base-load producer, and its operating logic is the constraint around which the other units operate.

2.3.2 CHP operation and its limits in high-VRE systems

The operation of CHP plants in district heating is heat-led, meaning that electricity production is tied to the heat demand the plant must serve, even in periods of low electricity demand. This constrains the flexibility of CHP towards the power market (Nuytten et al., 2013).

A further operational limitation is the technical part-load minimum imposed by the boiler and turbine, and CHP units cannot be shut down and restarted quickly or frequently without efficiency losses (Danish Energy Agency, 2026a). This restricts the operating range further: when heat demand falls persistently below the minimum load, the CHP unit must be shut down.

In systems with a high share of VRE, the electricity price becomes considerably more volatile, which favours the integration of power-to-heat (P2H) in district heating. Periods of low electricity prices erode CHP electricity revenue, while heat obligations force the plant to remain in must-run operation exactly when prices are lowest (Böttger et al., 2015; Gao et al., 2023). In such hours, must-run CHP also adds electricity to a system that is already in surplus, depressing prices further and increasing the excess that must be absorbed or curtailed (Böttger et al., 2015).

This development points to a technology that converts low-priced electricity into heat, turning low-price hours from a burden into an opportunity.

2.3.3 Integrating the EB: roles and functions

The EB plays several key roles when integrated into district heating in a power system with a growing share of VRE. The first role is low-price and surplus heating: the EB absorbs electricity when the price is favourably low or production is in surplus, turning curtailed wind power into useful heat. Some systems operate the EB only on curtailed wind power (Yang, Zhang and Gao, 2018), while others optimise EB operation to absorb the curtailment (Cheng et al., 2021).

The second role is the decoupling of heat and electricity. Adding an EB with storage breaks the rigid link between heat and power in CHP operation, which further improves the dispatch economics of the system (Zhou and Zhong, 2019; Liu et al., 2020).

The third role is covering the sub-minimum shoulder load. When heat demand falls below the CHP minimum load, the EB can carry the load instead of forcing the CHP into inefficient operation or shutdown (Nuytten et al., 2013; Dancker et al., 2019). This role is directly relevant to the system examined in this thesis, in which the CHP unit operates under a minimum load constraint (Section 3.4.1).

The fourth role is complementing the existing system rather than replacing it. Hybrid configurations with biomass as base load and an EB perform better than purely biomass-based or purely electric configurations; one study found the hybrid system cheapest in five of the six years examined (Taylor, Atkins and Walmsley, 2025). The relative prices of fossil fuels and biomass further drive the viability of EB integration with CHP (Ivanova, Sauhats and Linkevics, 2017).

The fifth role, reported mainly outside the Nordic context, is peak shaving: an EB combined with thermal storage can shift consumption away from peak hours, relieving system stress and increasing local consumption of surplus wind (Sun et al., 2022). This role is not applicable in the Finnish setting, however, because heat demand and electricity price are positively correlated: the cold periods that drive peak heat demand also drive the highest electricity prices, so EB operation in those hours is uneconomical.

To summarise, across system studies, adding an EB consistently reduces operating cost, curtailment of renewable energy and fuel use (Liu et al., 2016; Zhang et al., 2024). Almost all the studies reviewed above pair the EB with storage, because storage is what allows the EB to operate independently of the instantaneous heat load.

2.3.4 Thermal energy storage as the enabler

Thermal energy storage enables heat to be supplied without being bound to the moment demand occurs. It decouples the timing of heat production from the timing of heat demand, allowing each production unit to run in its best hours (Guelpa and Verda, 2019). Integrating TES with CHP widens the feasible operating window, since production can be delayed or advanced (Nuytten et al., 2013). For the EB, TES extends the harvesting of cheap electricity beyond the instantaneous heat demand (Wang, Gui and Cai, 2023). The combination of EB and TES outperforms either technology alone, in both wind integration and operating cost (Yang, Zhang and Gao, 2018; Zhang et al., 2024). TES also enables market participation, since held heat allows capacity to be offered to the market while the heat supply remains secured for the delivery period (Boldrini et al., 2022; Javanshir et al., 2022). The remaining question is how these operational roles translate into economic value, which the following section examines through the electricity markets.

2.4 Electric boilers in electricity and reserve markets

2.4.1 Electricity market structure

Electricity is traded in several marketplaces according to the timeline before delivery, and the markets can be divided into the day-ahead, intraday, and balancing and reserve markets. Most of the electricity volume is traded in the day-ahead market, in which the prices for each delivery period of the following day are set through an auction held at noon on the preceding day. The market traditionally operated at hourly resolution, but since October 2025 day-ahead prices have been set in 15-minute periods (Nord Pool, 2025). The intraday market follows as delivery approaches, allowing participants to adjust their positions as demand and supply forecasts improve. Any remaining imbalance during the delivery period is managed

by the transmission system operator (TSO) through the balancing and reserve markets, in which capacity is procured as products categorised by their response speed: the frequency containment reserve (FCR), the automatic frequency restoration reserve (aFRR) and the manual frequency restoration reserve (mFRR) (Cramton, 2017; Javanshir et al., 2023).

In the Nordic region, the day-ahead and intraday markets are operated by Nord Pool, while the reserve products in Finland are procured by the TSO Fingrid (Javanshir et al., 2023; Fingrid, 2025). For a heat producer with an electric boiler, the day-ahead price is the primary operating signal, and its role is examined in the following section. Figure 1 shows the sequence of the electricity marketplaces in which the EB participates.

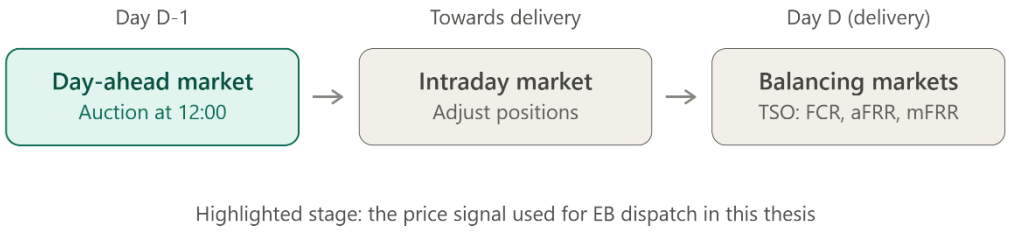

Figure 1. Sequence of the electricity marketplaces from day-ahead auction to delivery

2.4.2 EB in energy markets

In the energy markets, EB dispatch follows price-driven operation, also called price-threshold logic: the EB runs only when the electricity price falls below the marginal cost of the alternative heat source (Trømborg et al., 2017). The threshold itself is not fixed, since the taxes and grid tariffs applied to the electricity input shift the effective price the EB faces (Kirkerud, Trømborg and Bolkesjø, 2016). The rising VRE share increases the number of hours in which the electricity price falls below such thresholds, at times even below zero, which strengthens the economic case for EB dispatch over time; this effect was identified early in studies of wind integration in the Nordic system (Meibom et al., 2007) and is confirmed by more recent Nordic analyses (Trømborg et al., 2017). Intraday adjustment can add further value on top of day-ahead scheduling (Javanshir et al., 2023). This price-driven operating logic is the mechanism implemented in the optimisation model of this thesis, in which the EB is dispatched against the day-ahead price series.

2.4.3 EB in reserve markets

Beyond the energy markets, the EB has increasing potential to play a role in the reserve markets. In systems with high shares of VRE generation, more reserve capacity is needed to ensure grid stability, and demand-side resources in district heating are well placed to provide it (Boldrini et al., 2022; Fingrid, 2025). Each reserve product carries technical requirements, of which activation time is the most restrictive. EBs meet even the fastest requirements because their output can be adjusted across the full range without ramping restrictions, whereas large heat pumps are limited to the slower products (Javanshir et al., 2023). Power-to-heat units are particularly cost-effective in down-regulation, since absorbing surplus electricity as heat simultaneously relieves must-run generation, and Nordic analyses find EBs strongest precisely in the down-regulation products (Böttger et al., 2015; Javanshir and Syri, 2023). Reserve revenues have been a significant driver of EB investment in district heating, in some cases justifying installations that energy-market operation alone would not (Javanshir and Syri, 2023; Danish Energy Agency, 2026b). Reserve participation is thus one of several value streams available to an EB, which the next section assembles.

2.4.4 Revenue streams and system-level value

The value of an EB in a district heating system accumulates from several streams: arbitrage against the electricity price, the avoided fuel cost of the heat source it displaces, reserve-market payments where the operator participates, and, at system level, reduced curtailment of renewable generation (Boldrini et al., 2022; Sun et al., 2022; Javanshir and Syri, 2023).

At larger deployment scales these effects feed back into the power system itself: widespread EB capacity raises electricity demand in low-price hours, which influences prices and dispatch and can even increase the electricity output of bio-CHP plants (Hiltunen, Lindroos and Rämä, 2025).

Within this study, the local district heating operator Lappeenrannan Energia participates in the reserve markets only to a limited extent, offering mFRR capacity, as the response capability of the existing EB restricts it to the slowest product. Reserve operation is therefore not a central revenue stream in the current system, although district heating operators elsewhere participate more actively, and new EB capacity would make faster products

accessible (Javanshir and Syri, 2023). This study accordingly models spot-driven operation against the day-ahead price only; any reserve revenue would be additive to the value reported. What the literature reviewed above does not resolve is the specific configuration examined in this study, which the next section formalises.

2.5 Identified research gap and motivation

From the literature review, three points are relevant to this thesis. First, the EB is a mature power-to-heat technology with a simple structure and a high ramp rate, and is therefore well suited to absorbing surplus renewable electricity (Witkowski et al., 2020; Danish Energy Agency, 2026b). Second, in a district heating system with CHP as the base load, which is the case in this study, the EB can decouple heat from electricity and cover sub-minimum heat load when the electricity price is favourably low, which reduces the dispatch cost (Dancker et al., 2019; Liu et al., 2020). Third, thermal energy storage is the enabler that integrates the EB into the district heating system: it unbinds heat production from the timing of demand, which allows the EB to follow market signals (Nuytten et al., 2013; Guelpa and Verda, 2019).

The existing literature generally evaluates electrification against a fossil-fuelled base system. In that setting, replacing fossil combustion with electricity both lowers emissions and reduces exposure to volatile fossil fuel prices, so the remaining question is mainly one of cost (Bloess, Schill and Zerrahn, 2018; Javanshir et al., 2022). The EB itself is often framed through reserve-market revenue, with its operation optimised for that purpose (Böttger et al., 2015; Javanshir and Syri, 2023). The flexibility provided by the EB and the sizing of the TES are also commonly treated as separate topics.

For an existing biomass-CHP base load system, this framing does not hold. Under EU and Finnish accounting, biomass heat is treated as a carbon-neutral source, so the accounted emissions do not reflect actual combustion emissions. The effect of electrifying a biomass-based system on emissions is therefore not as straightforward as electrifying a fossil-based one: the EB can displace the carbon-neutral biomass source with grid electricity that does carry real emissions. Notably, the fossil-free configuration can then emit more than a partially electrified one. Because the TES is already in operation in this case, the baseline includes storage, which makes the decision a marginal one rather than a greenfield design.

For this real network, EB capacity and TES sizing are resolved jointly, including how the value of the TES changes once the system is electrified. Explicit carbon-price thresholds are also derived for when each electrified configuration becomes competitive. The scope of this study is spot-driven, covering electricity-market and fuel-displacement value, since the operator does not participate in reserve markets. This isolates a value stream that the reserve-focused literature usually leaves bundled in.

This research develops an hourly linear programming (LP) model for the techno-economic optimisation of the Lappeenranta district heating system over a full year. Five scenarios are designed, spanning the current biomass-CHP system through to full electrification, with and without TES. The main outputs are operating cost, total cost, emissions, and their sensitivity to carbon, gas, and electricity prices. The following section presents the methodology developed to address this gap.

3 Methodology

This chapter describes the modelling approach used in this study. Figure 2 gives an overview of the full workflow, from input data through model construction, scenario definition, validation, and sensitivity analysis to the final results. The dashed feedback loop indicates the calibration of the model against real operational data. The remainder of the chapter details each stage in turn: the case study system and data (Sections 3.1 and 3.2), the scenario design and optimisation model (Sections 3.3 and 3.4), the parameter assumptions (Section 3.5), the sensitivity analysis (Section 3.6), and the model validation (Section 3.7).

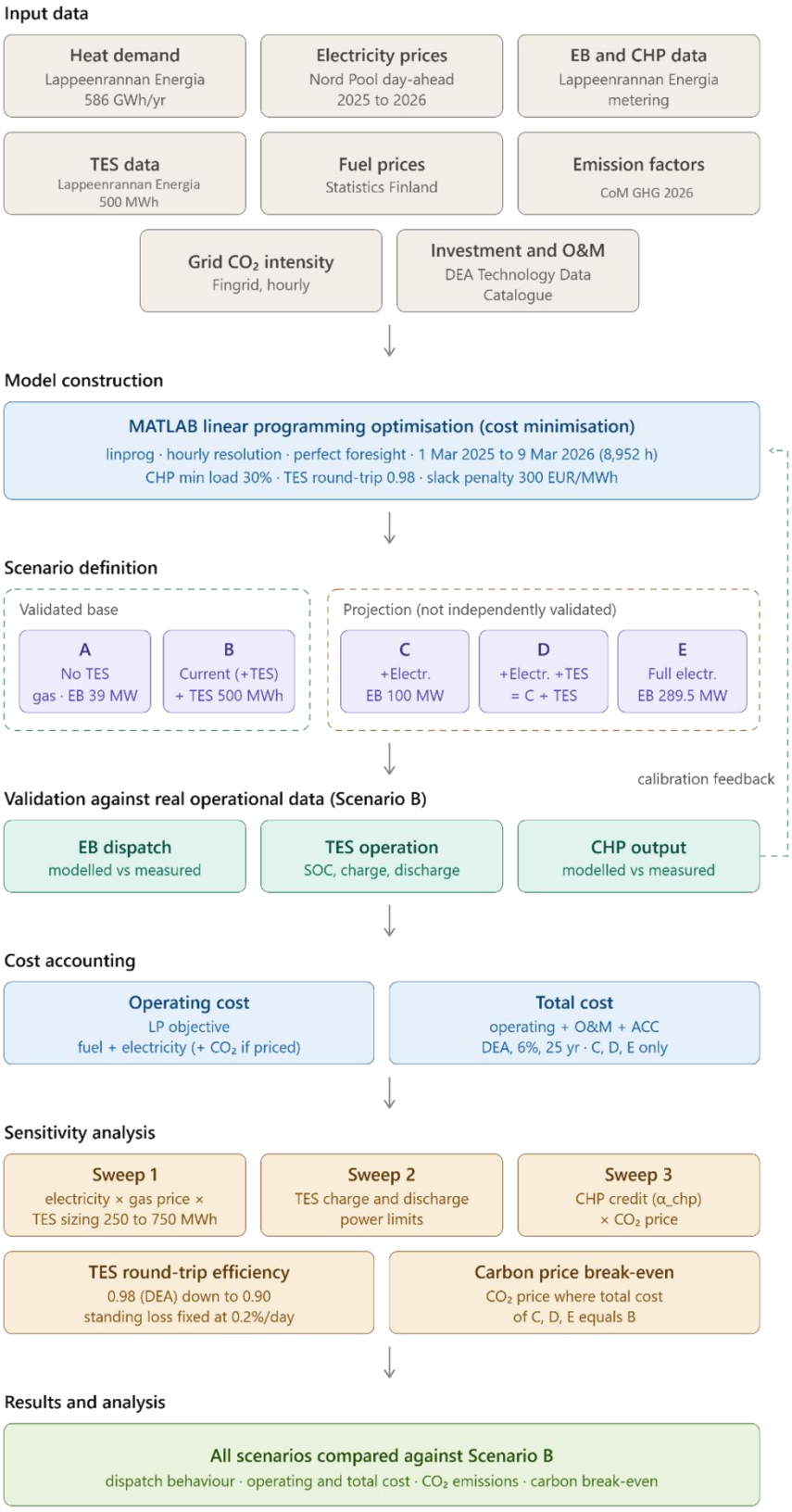

Figure 2. Overview of the modelling workflow

3.1 Case study: the Lappeenranta district heating system

3.1.1 Network overview and heat demand

This study focuses on the district heating network of Lappeenranta, operated by Lappeenrannan Energia. The total annual heat demand of the network is 586 GWh.

The heat demand used in the model is the demand measured at network level, which includes distribution losses. It was provided at fifteen-minute resolution and aggregated to hourly resolution for the optimisation (Section 3.2.3). The study period runs from 1 March 2025 to 9 March 2026, a full year that captures the seasonal variation in heat demand and the commissioning of the thermal energy storage in May 2025.

3.1.2 Production unit portfolio and merit order

The Lappeenranta network is supplied by four heat production sources: a biomass CHP plant, gas boilers, pellet boilers, and an electric boiler. Their rated heat capacities are summarised in Table 2. In this study the production units are grouped by heating source rather than as individual boilers: the gas and pellet capacities each represent the combined total of several units, aggregated by fuel type to simplify the dispatch model. The merit-order logic operates on the cost of each heating source, so this aggregation does not affect the dispatch results.

Table 2. Nominal heat production capacities of the Lappeenranta district heating network

Unit	Heat capacity (MW)
Biomass CHP	110.0
Gas boilers	250.5
Electric boiler	38.0
Pellet boilers	14.0

The biomass CHP, with a capacity of 140 MW, is the principal unit and operates as baseload. As with the electric boiler, the CHP capacity is taken from the operational data rather than from the nominal rating: the company's unit listing gives 110 MW, but the operational data from Lappeenrannan Energia show CHP output reaching and sustaining 140 MW during

periods of high heat demand, so 140 MW is adopted as the capacity in the model. The gas boilers (250.5 MW combined) provide peak and backup capacity, the pellet boilers (14 MW combined) serve as secondary biomass units, and the electric boiler converts grid electricity to heat. The electric boiler's nominal capacity is given as 38 MW in the company's listing and was originally rated at 40 MW, but the operational data show a maximum observed output of 39 MW, which is the value adopted in the model.

The units are dispatched in order of increasing variable heat cost (merit order). The biomass CHP operates as a baseload unit when heat demand exceeds its minimum load, supplemented by the heat-only boilers as demand rises. The electric boiler is dispatched opportunistically, running when the spot electricity price falls low enough that its heat production cost undercuts that of the biomass units. This dispatch logic, in which cogeneration provides baseload and flexible units follow demand and price, is characteristic of Nordic district heating systems and is well documented in the literature (Beiron, Normann and Johnsson, 2023; Javanshir, Syri and Hiltunen, 2024).

The CHP unit is subject to a minimum heat output of 30% of rated capacity during the heating season, consistent with the operational lower bound of large steam turbines reported in the literature (Danish Energy Agency, 2026a), and confirmed by the operational data, which show CHP output during the heating season remaining above this threshold. Outside the heating season, as described in Section 3.4.1 4.4.2 , this minimum does not apply, and the data show the plant running at low part-load in the shoulder month of May.

3.1.3 Thermal energy storage (TES) specification

The thermal energy storage is the Mertaniemi heat accumulator, an insulated steel tank 40 metres tall containing 10,000 m³ of district heating water. When fully charged, the water reaches approximately 90°C (Lappeenrannan Energia, 2025). The storage was commissioned in May 2025. It has charging and discharging power of approximately 40 MW and an energy capacity of 250 to 500 MWh depending on the operating temperature. In this study the storage is modelled at its upper capacity of 500 MWh, with charge and discharge power limits of 34 MW and 28 MW respectively (Section 3.4.3).

3.2 Data collection

The data used in this study come from two categories of source: operational data from the local district heating company, and openly available Finnish datasets.

3.2.1 Operational data

The following operational data for the Lappeenranta district heating system were provided by Lappeenrannan Energia under a confidentiality agreement and are used as model inputs only:

- hourly heat demand profile (March 2025 to March 2026)
- current production-unit capacities and characteristics
- CHP heat supply (January 2025 to March 2026)
- thermal energy storage usage profile and characteristics (from commissioning in late May 2025 to March 2026)
- electric boiler usage profile (January 2025 to March 2026)

The study period is determined by the availability of the heat demand profile, and in particular by the commissioning of the thermal energy storage in May 2025, which marks the point from which storage supports increased electric boiler use and reduced gas consumption. The heat demand profile was provided at fifteen-minute resolution as network-level heat, inclusive of distribution losses. These raw operational values are not reproduced in this thesis; with the permission of Lappeenrannan Energia, only results derived from them (production cost, dispatch behaviour, and emissions) are presented in the figures and tables that follow.

3.2.2 Open data sources

The following datasets are publicly available:

- hourly day-ahead electricity prices (Nord Pool, 2026)

- real-time CO2 intensity of the Finnish grid (Fingrid, 2026)
- emission factors (Bastos, Monforti-Ferrario and Melica, 2026)
- heat production unit efficiencies (Danish Energy Agency, 2026b)
- thermal energy storage characteristics, including standing loss (Danish Energy Agency, 2024)
- outdoor temperature, 2021 to 2025, used for comparison (Finnish Meteorological Institute, 2026)

Fuel prices are taken from Statistics Finland (Statistics Finland, 2026b). The plant uses forest chips as the primary CHP fuel, with pellet dust serving as a secondary fuel under certain operating conditions. In the absence of data on the fuel mixing ratio, a forest chip price of 39 EUR/MWh is used as the representative CHP fuel cost. Access details and retrieval dates for all open datasets are given in the reference list.

3.2.3 Temporal resolution and study period

The optimisation model operates at hourly resolution over the full study period (March 2025 to March 2026). Although some input data, such as the heat demand profile, were available at fifteen-minute resolution, not all datasets shared this granularity; in particular, the day-ahead electricity prices are defined hourly. Hourly resolution was therefore chosen as the finest resolution consistent across all inputs. This resolution is sufficient to capture the daily and seasonal dynamics of heat demand and electricity price that drive dispatch and storage operation, while keeping the optimisation computationally tractable over a full year.

3.3 Scenario design

3.3.1 Definition of Scenarios A–E

Table 3. Definition of five scenarios

Scenario	Label	CHP* (MW)	Pellet (MW)	Gas boiler (MW)	EB* (MW)	TES	Grid status

A	No TES	140	14	250.5	39	No	Existing
B	Current (+TES)	140	14	250.5	39	Yes	Existing
C	+Electr.	140	14	0	100	No	Grid-constrained, deployable
D	+Electr. +TES	140	14	0	100	Yes	Grid-constrained, deployable
E	Full electr.	140	14	0	289.5	Yes	Requires 400 kV upgrade, reference only

*In Scenarios C, D, and E the gas boiler is removed. In Scenario C, a slack term represents unmet demand met as a last resort (Section 3.3.3); it is not a production unit.
* The modelled CHP and EB capacities are calibrated from operational data, and therefore differ slightly from the nominal capacities of the Lappeenrannan Energia production units presented in section 3.1.2 .

Table 3 defines the five scenarios modelled in this study. Scenario B is the current system, combining the existing mix of heat production units with the thermal energy storage, and serves as the baseline (Section 3.3.2). Scenario A is identical to B but without the storage, and is used to isolate the effect of the thermal energy storage.

Scenario C is partially electrified: the gas boiler is removed and the electric boiler capacity is raised from the existing 39 MW to 100 MW. The 100 MW figure is the grid connection capacity that Lappeenrannan Energia can operate without significant investment or construction, and is used here as the upper limit for near-term electrification. Because Scenario C has no storage, a slack term is included to represent any unmet demand in peak or high-price hours (Section 3.3.3). Scenario D adds the existing thermal energy storage to Scenario C.

Scenario E is fully electrified, with the electric boiler scaled to 289.5 MW to replace the entire gas boiler capacity and meet peak demand without fossil backup. This would require a 400 kV grid upgrade for Lappeenranta and is therefore treated as a reference case, included to show the effect of complete electrification on the system rather than as a near-term option.

3.3.2 Scenario B as the baseline

All scenario comparisons in this study are made against Scenario B, the current system together with the thermal energy storage, rather than against Scenario A, the same system without storage. This choice reflects the actual decision faced by Lappeenrannan Energia.

The thermal energy storage was commissioned in 2025 and is already in operation, so its capital cost is sunk: it has been incurred regardless of any subsequent decision about electrification. The relevant question for the company is therefore not whether to build storage, but what further electrification adds to a system that already includes it. Scenario B represents that starting point, and is the appropriate reference against which the incremental value of electrification is measured.

Using A as the baseline would instead frame the analysis as a decision about whether to add storage, which is no longer a live question, and would attribute to electrification the savings that storage alone already delivers. Comparing against B isolates the marginal effect of each further step. This framing is also more demanding, and therefore more honest: because B already captures the cost and emission benefits of storage, an electrified scenario must improve on a stronger reference rather than on the unimproved fossil system, so any advantage it shows is genuinely additional.

Scenario A is retained, but as a reference point rather than a baseline. The comparison from A to B isolates the effect of the storage itself, which is useful for understanding how much of the system's performance is attributable to storage as opposed to electrification. The effect of electrification is then assessed through the comparisons from B to C (partial electrification without additional storage) and from B to D (partial electrification combined with the existing storage), and the effect of full electrification through the comparison from B to E. In this way each scenario isolates a distinct effect: A to B the value of storage, B to C and B to D the value of electrification with and without the storage buffer, and B to E the value of complete fossil-free operation.

3.3.3 The slack variable and its cost

The model includes a slack variable, representing unmet heat demand in a given hour, as a last-resort term that guarantees the optimisation always has a feasible solution. It is not a physical production unit: it allows demand to go unmet at a high penalty cost, so that the model remains solvable even in hours where the available units cannot meet demand, whether because of a capacity shortfall or because production would be prohibitively expensive. Penalising unserved demand through a slack term in this way is standard practice in energy system optimisation. Chaudry et al. (2023), for example, apply penalty costs for

unserved energy demand in both the national and local systems of an integrated energy system model of Great Britain.

The penalty cost is set to 300 EUR/MWh. This value is chosen to sit just above the effective cost ceiling of the electric boiler, so that the optimiser resorts to slack only when running the electric boiler would be more expensive still. Because the electric boiler cost per unit of heat is the electricity price divided by its efficiency, the slack penalty of 300 EUR/MWh corresponds to an electricity price of approximately 297 EUR/MWh (300 multiplied by the boiler efficiency of 0.99). Below this electricity price the electric boiler is the cheaper option and is dispatched; above it, accepting the slack penalty is cheaper than running the boiler. The penalty therefore acts as an implicit price ceiling on electric boiler operation, and can be interpreted as a value-of-lost-load proxy: the cost the system is willing to bear to avoid shedding heat.

In the results this design causes slack to appear only in genuine price-spike hours. In Scenario C, for example, total slack amounts to 378 MWh, equivalent to 0.06% of annual demand, occurring in only 38 hours, all of which coincide with electricity prices above the 297 EUR/MWh threshold. The dispatchable capacity is never the binding limit, confirming that the shortfalls are price-driven rather than capacity-driven, and that the system is otherwise able to meet demand in every hour. The slack variable thus serves a dual purpose: it guarantees feasibility, and its volume acts as a diagnostic distinguishing price-driven from capacity-driven shortfalls.

One consequence is that the slack cost is a modelling parameter rather than a measured price. Its exact value is therefore a modelling choice; however, because slack is negligible at base conditions (a fraction of a percent of demand), the results are not sensitive to the precise figure, provided it is set high enough to act as a genuine last resort.

3.4 Optimisation model

This section formalises the linear optimisation model used to dispatch and cost each scenario, solved at hourly resolution over the full study period and independently for each scenario. The modelled system is shown in Figure 3.

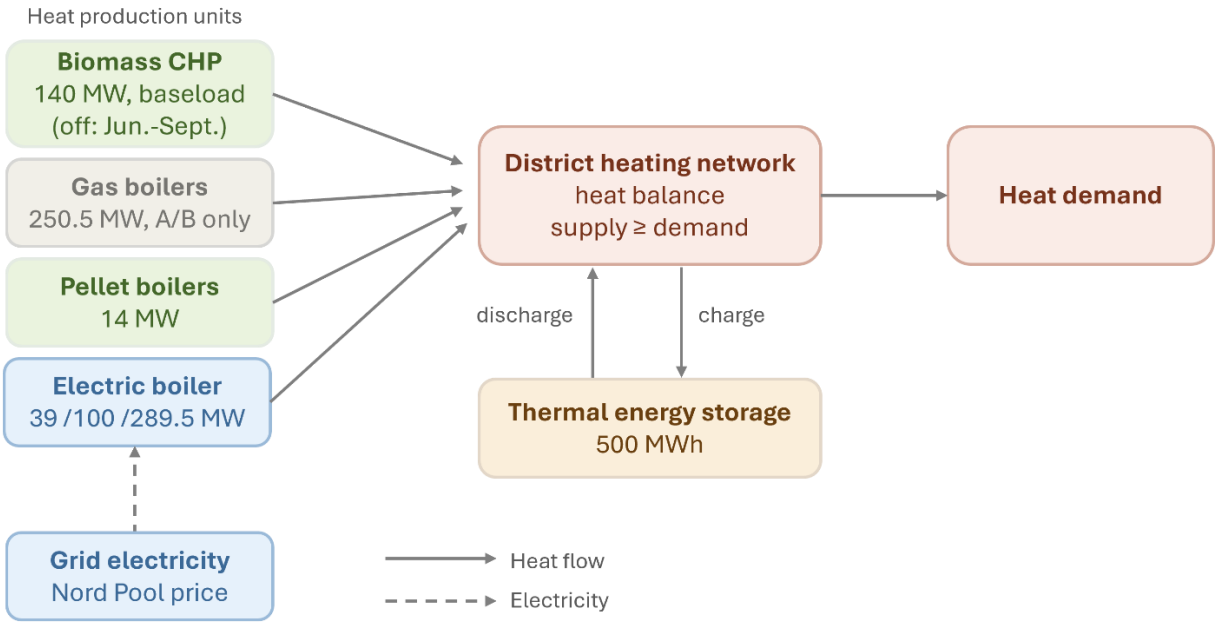

Figure 3. Schematic of the modelled district heating system

3.4.1 Decision variables and constraints

The model determines the hourly dispatch of each production unit and the operation of the thermal energy storage over the full time horizon T. For each hour t, the decision variables are the heat output of each production unit, namely the CHP unit Q_chp,t, the gas boiler Q_gas,t, the oil boiler Q_oil,t, the pellet boiler Q_pellet,t, and the electric boiler Q_eb,t, all in MW. An additional slack variable Q_slack,t represents unmet heat demand (Section 3.3.3). For the storage-enabled scenarios, three further variables describe the TES: the charging power P_charge,t, the discharging power P_discharge,t, and the state of charge SOC_t (in MWh). All variables are non-negative. The oil boiler is retained in the formulation for completeness but assigned zero capacity, as it has been removed from the system.

The central constraint is the hourly heat balance, which requires that total heat supplied meets demand in every hour:

$$Q_{\text{chp},t} + Q_{\text{gas},t} + Q_{\text{oil},t} + Q_{\text{pellet},t} + Q_{\text{eb},t} + Q_{\text{slack},t} + P_{\text{dis},t} - P_{\text{ch},t} \geq Q_{\text{demand},t} \quad \forall t \in T \quad (1)$$

Heat discharged from the TES (P_dis,t) adds to supply, while heat charged into the TES (P_ch,t) is a withdrawal from the network and so enters with a negative sign. The constraint is formulated as an inequality (≥) rather than an equality: this permits oversupply, which can occur when the CHP unit is held above demand by its minimum-load requirement, while the

slack variable guarantees feasibility when supply would otherwise fall short. The use of an inequality with a penalised slack variable avoids the infeasibility that a strict equality can cause under rounding or binding capacity limits.

Each production unit is bounded by its rated capacity:

$$Q_{i,t} \leq Q_{i,max} \quad \forall i, \forall t \in T \tag{2}$$

The capacities differ by scenario, as defined in Table 3; for example, the gas boiler capacity is set to zero in the electrified scenarios, and the electric boiler capacity is raised from its existing 39 MW to 100 MW (Scenarios C and D) or 289.5 MW (Scenario E).

The CHP unit is subject to two additional operational constraints. During the heating season (October to April) it must operate at or above a minimum load of 30% of rated capacity (Danish Energy Agency, 2026a):

$$Q_{\text{chp},t} \geq 0.30 \cdot Q_{\text{chp},max} \quad \forall t \in \text{heating season} \tag{3}$$

and during the summer months (June to September) it is forced offline, reflecting the operational practice of Lappeenrannan Energia:

$$Q_{\text{chp},t} = 0 \quad \forall t \in \text{June-September} \tag{4}$$

Outside these periods, in the shoulder month of May, CHP output is left unconstrained. This reflects the operational data, which show the plant running at a low part-load in May, below its nominal heating-season minimum; a fixed minimum-load constraint would therefore misrepresent actual shoulder operation.

3.4.2 Objective function

The objective function minimises the total annual operating cost of heat production, summed over all hours in the modelling horizon. For each scenario it comprises the fuel cost of each production unit, the electricity cost of the electric boiler, and the slack penalty:

$$min\ C_{\text{op}} = \sum_{t \in T} \big(c_{\text{chp}} Q_{\text{chp},t} + c_{\text{gas}} Q_{\text{gas},t} + c_{\text{oil}} Q_{\text{oil},t} + c_{\text{pellet}} Q_{\text{pellet},t} + c_{\text{eb},t} Q_{\text{eb},t} + c_{\text{slack}} Q_{\text{slack},t} \big) \tag{5}$$

The electric boiler cost coefficient ($c_{eb,t}$) is time-varying, set by the hourly electricity price divided by the boiler efficiency, whereas the fuel cost coefficients (c_{gas}, c_{oil}, c_{pellet}) are treated as constant over the modelling horizon. Each coefficient expresses the cost per unit of heat delivered, so that fuel costs are divided by the respective unit efficiency.

The CHP cost coefficient reflects the fuel cost of heat production, adjusted by a credit parameter α_{chp} that governs how much of this cost is offset by electricity sales revenue from the back-pressure turbine. In the base case $\alpha_{chp} = 0$, treating heat as the primary product and allocating the full fuel cost to heat. This is a stakeholder-confirmed cost-allocation convention rather than a physical calibration, and its influence on the scenario cost ranking is examined in the sensitivity analysis (Section 3.6.3).

The slack variable $Q_{slack,t}$ represents unmet heat demand and is assigned a high penalty cost c_{slack}, set well above any real production cost (Section 3.3.3). This guarantees model feasibility in every hour while ensuring that slack is used when available heat production is either insufficient or more expensive than the specified unmet-demand penalty; in the dispatch results it therefore acts as a diagnostic for capacity- or price-driven shortfalls rather than a genuine supply option.

In the storage-enabled scenarios, the objective additionally includes small penalty terms on thermal energy storage cycling and on violation of the soft minimum state of charge. These terms are included for numerical regularisation only, to discourage unnecessary cycling and to keep the state of charge well defined, and are excluded from the reported costs.

The objective above contains only the marginal operating costs that drive hourly dispatch. For the scenarios representing potential future investment (C, D, and E), the comparison of total cost additionally includes the annualised capital cost and the fixed and variable O&M of the new electric boiler capacity. The treatment of these investment-related costs, and the rationale for excluding them from the dispatch optimisation, is described in Section 3.4.4 .

3.4.3 Thermal energy storage dynamics

The thermal energy storage is modelled through its state of charge, which evolves across consecutive hours according to the charging and discharging decisions and a standing heat loss. For each hour t after the TES comes online, the state of charge is given by:

$$\mathrm{SOC}_t = \mathrm{SOC}_{t-1}(1 - \eta_{\mathrm{loss}}) + \eta_{\mathrm{ch}} P_{\mathrm{ch},t} - P_{\mathrm{dis},t}/\eta_{\mathrm{dis}} \quad (6)$$

where η_loss is the fractional standing loss per hour (0.0000833, corresponding to approximately 0.2% per day (Danish Energy Agency, 2024)), and η_ch and η_dis are the charging and discharging efficiencies. Both are set to √0.98 (Danish Energy Agency, 2024), so that the combined round-trip efficiency of the TES is 0.98: charging retains a fraction η_ch of the input power as stored heat, and recovering a given quantity of heat requires dividing the discharged power by η_dis. Splitting the round-trip loss symmetrically between charging and discharging reflects the conversion losses incurred on both filling and emptying the TES. The standing-loss term (1 − η_loss) applied to the previous hour's content represents the gradual cooling of the stored water between hours, and is modelled separately from the round-trip conversion loss.

In the first hour of operation the TES begins empty, so the initial state of charge is set by that hour's charging and discharging alone:

$$\mathrm{SOC}_{t_0} = \eta_{\mathrm{ch}} P_{\mathrm{ch},t_0} - P_{\mathrm{dis},t_0}/\eta_{\mathrm{dis}} \quad (7)$$

The storage is bounded in both energy and power. The state of charge must remain between a minimum and the rated capacity:

$$\mathrm{SOC}_{min} \leq \mathrm{SOC}_t \leq \mathrm{SOC}_{max} \quad (8)$$

SOC_max is 500 MWh in the base case and SOC_min is 10% of capacity. The minimum is implemented as a soft constraint: a non-negative slack variable permits the floor to be violated at a small penalty cost, which preserves feasibility in edge cases without materially affecting dispatch. The charging and discharging powers are limited to their rated values:

$$P_{\mathrm{ch},t} \leq P_{\mathrm{ch,max}} \quad (9)$$

$$P_{\mathrm{dis},t} \leq P_{\mathrm{dis,max}} \quad (10)$$

with base-case limits of 34 MW and 28 MW respectively. A further constraint restricts simultaneous charging and discharging, which the round-trip loss and cycling cost render uneconomic in any case:

$$P_{\mathrm{ch},t} + P_{\mathrm{dis},t} \leq P_{\mathrm{ch,max}} \quad (11)$$

Finally, before the storage comes online (prior to late May 2025), both charging and discharging are fixed to zero, so that the TES contributes to dispatch only from its actual commissioning date onward.

3.4.4 Cost treatment: capital, O&M, and carbon price

The model distinguishes two cost levels: operating cost and total cost. Operating cost comprises the marginal costs that drive hourly dispatch and is the quantity the optimisation minimises. Total cost adds the investment-related costs borne by each configuration, namely annualised capital and fixed and variable O&M. Only operating cost enters the optimisation; the total-cost components are assembled in postprocessing for the scenario comparison.

Costs in the optimisation. The objective function (Section 3.4.2) contains only the marginal costs that vary with dispatch: fuel costs, the time-varying electricity cost of the electric boiler, and the slack penalty. Costs that are incurred regardless of how the units are dispatched, namely fixed operation and maintenance (O&M) and capital, are deliberately excluded from the objective. Including a constant in the objective would not alter any dispatch decision, as the optimiser minimises cost by choosing when to run each unit, and a fixed cost is unaffected by that choice. These dispatch-invariant costs are therefore added only when comparing the total cost of each scenario.

Capital cost. For the scenarios representing potential future investment (C, D, and E), the capital cost of the new electric boiler capacity is annualised using the capital recovery factor (CRF) method:

$$\mathrm{CRF} = \frac{r(1+r)^n}{(1+r)^n - 1} \tag{12}$$

with a discount rate r of 6% and a technical lifetime n of 25 years, giving a CRF of approximately 0.078. The annualised capital cost (ACC) is the product of this factor and the total investment. The unit investment cost is taken from the DEA data sheet (Danish Energy Agency, 2026a), interpolated to a 2025 commissioning year, and applied only to the new capacity above the existing 39 MW, since the existing electric boiler is already installed. This gives an incremental capacity of 61 MW for Scenarios C and D and 250.5 MW for

Scenario E, and an ACC of approximately 0.33 MEUR per year for C and D and 1.35 MEUR per year for E.

Operation and maintenance. Fixed and variable O&M costs for the new electric boiler capacity are taken from the same DEA catalogue (Danish Energy Agency, 2026a). Fixed O&M scales with the installed new capacity and is added, like the capital cost, only in the scenario comparison. Variable O&M is charged per unit of heat produced by the new capacity, that is, on electric boiler output above the existing 39 MW threshold; output from the existing boiler carries no variable O&M charge in the model, as the existing unit's O&M is a constant present in all scenarios and does not affect the comparison. O&M for all other production units is excluded on the same basis: it is identical across scenarios and so cancels in any comparison between them.

Carbon price. The base case applies no explicit carbon price (c_co2 = 0); the carbon price is instead introduced as a dedicated sensitivity dimension (Section 3.6.3). This choice keeps the base-case results anchored to directly observed market conditions, namely fuel prices, spot electricity prices, and heat demand, rather than embedding a forecast of a volatile and uncertain carbon price into the headline figures. It is also appropriate for this system for two reasons. First, day-ahead electricity prices partly internalise the carbon costs faced by fossil-based marginal generators through the EU Emissions Trading System, so electricity-related carbon is implicitly priced; an explicit carbon cost would apply only to direct fuel combustion. Second, the electrified scenarios remove direct fossil combustion almost entirely, so a carbon price has little to act on in those scenarios and influences mainly the gas-using baseline. The principal effect of a carbon price is therefore not on dispatch but on the investment decision, namely the carbon price at which removing the baseline's gas use justifies the electric boiler investment, which is examined directly through the break-even analysis in Section 3.6.3 and the results of Section 4.5.6 4.5.4 .

When the carbon price is non-zero in the sensitivity analysis, it enters the gas and oil cost coefficients as the product of the carbon price and the unit's emission factor, converted to a cost per unit of heat. It therefore raises the marginal cost of the fossil units and affects their dispatch, while leaving the biomass and electric units unaffected.

3.4.5 Justification of linear programming over MILP

The dispatch problem is formulated as a linear program (LP), with continuous decision variables and linear constraints. A mixed-integer linear program (MILP) would additionally represent discrete on/off commitment through binary variables, including a minimum stable load enforced only when a unit is committed. Both formulations are established in district heating dispatch modelling: comparing the two for the CHP-based system of eastern Denmark, Ommen, Markussen and Elmegaard (2014) describe the LP model as the frequently used benchmark type, while noting that mixed-integer optimisation represents unit commitment more accurately. Gonzalez-Salazar et al. (2023) compared merit order and MILP models for district heating portfolio optimisation and found that combining the two approaches could enable faster and more robust decision-making. For this system, the CHP minimum load and seasonal shutdown are instead imposed directly: a must-run lower bound on CHP output during the heating season (October to April) and a forced shutdown in summer (June to September).

To assess whether this simplification affects the results, an equivalent MILP with binary CHP and gas commitment, including a minimum-load-when-committed constraint, was solved and compared with the LP on representative weekly horizons. During the heating season, when CHP is must-run above its minimum, the two formulations produced identical costs, as the commitment is fixed and no discrete decision remains. They diverged only in the shoulder month of May, where the comparison favoured the LP: the operational data show that the real CHP unit runs at a low part-load in May (a monthly mean of 11.4 MW, below its nominal minimum), which the continuous LP reproduces closely, whereas a binary minimum-load formulation cannot represent it, as it would force CHP either offline or above its minimum stable output. The divergence therefore reflects the MILP imposing a minimum-load rule that the real plant does not observe in shoulder operation, rather than a limitation of the LP.

The LP formulation is therefore used throughout. It reproduces the observed dispatch behaviour across all seasons, including the sub-minimum shoulder operation that a unit-commitment model would misrepresent, and it solves quickly enough to run the full set of scenarios required for the sensitivity analysis.

3.4.6 Perfect foresight and the absence of a rolling horizon

The optimisation is solved over the full study horizon in a single pass, so the model has perfect foresight of electricity prices, heat demand, and grid CO2 intensity for the entire period. This differs from real operation, where the day-ahead electricity market reveals prices only about 24 hours in advance, and a system operator must therefore commit dispatch decisions without knowledge of prices beyond the current horizon. In practice this is commonly represented by a rolling-horizon approach, in which the optimisation is solved repeatedly over a short look-ahead window (for example 24 to 48 hours) that advances through the period, with only the first hours of each solution implemented.

A rolling-horizon formulation was attempted in this study, but it could not be integrated with the existing optimisation structure within the project timeframe, and the model was therefore solved with full foresight. The principal consequence is that the thermal energy storage is dispatched with complete knowledge of future prices, which may allow it to capture favourable price windows that a 24-hour-ahead operator would not anticipate. The reported storage savings should therefore be read as an upper bound on what perfect price forecasting could achieve, rather than as the saving realisable under day-ahead information alone.

This simplification is acceptable for the purpose of this study for two reasons. First, the analysis is a comparative one: all five scenarios are solved under the same foresight assumption, so any optimism introduced by perfect foresight applies consistently across them and does not distort the comparison between configurations, which is the basis for the conclusions. Second, the day-ahead market already provides a 24-hour price horizon, which covers a full daily charge and discharge cycle of the storage; since the storage in this system operates as a short-term, sub-daily buffer rather than a seasonal storage, much of its value derives from price variation within a horizon that an operator can in fact see. A rolling-horizon implementation remains a clear avenue for future work, and would allow the realisable storage value under realistic information constraints to be quantified.

3.5 Parameters and assumptions

3.5.1 CHP electricity credit

The CHP unit produces heat and electricity together, so a question arises in cost accounting as to how much of its fuel cost should be attributed to heat. The model represents this through a credit parameter, alpha_chp, which specifies the fraction of the CHP fuel cost offset by revenue from the cogenerated electricity. A higher credit lowers the effective heat-production cost of the CHP unit, reflecting greater electricity revenue, while a credit of zero allocates the entire fuel cost to heat.

The base case uses alpha_chp = 0, treating heat as the primary product and assigning the full fuel cost to heat production. This is a cost-allocation convention confirmed by Lappeenrannan Energia rather than a physical property of the plant; it reflects how the company accounts for CHP heat cost, and is not a calibration of the unit's actual electricity yield. Setting the credit to zero is also the conservative choice for this study, because it gives the CHP unit its highest possible heat-production cost. Any electricity credit would make the biomass CHP cheaper to run relative to the electric boiler, which would favour the baseline scenarios over the electrified ones. By assigning no credit, the analysis avoids overstating the relative cost of electrification, so the case for electrification is not flattered by the assumption.

Because alpha_chp is an accounting convention rather than a measured quantity, its influence on the results is examined directly in the sensitivity analysis (Section 4.5.5), across the full range from zero to 0.95. The scenario cost ranking is robust across most of this range: at the stakeholder-confirmed value of zero, and across the great majority of the tested interval, Scenario D remains cheaper than the baseline B, and the principal conclusions hold. Only at very high credit values, above approximately 0.87, does the baseline become cheaper than D on operating cost, a level far above the value confirmed for this system. The credit affects the absolute cost of all scenarios, but does not change the relative conclusions within the realistic range.

3.5.2 Emission factors and grid CO2 intensity

Emissions in this study are accounted for using two distinct methods, depending on where the emissions arise. Emissions from direct fuel combustion are calculated using fixed emission factors (Bastos, Monforti-Ferrario and Melica, 2026), since the emissions per unit of fuel are a property of the fuel and do not vary with external conditions. Emissions from electric boiler operation are instead calculated using the real-time hourly CO2 intensity of the electricity grid (Fingrid, 2026), because the carbon content of grid electricity varies substantially from hour to hour with the generation mix. Applying a fixed factor to grid electricity would misrepresent these emissions, whereas applying real-time intensity captures the correlation between when the electric boiler operates and how carbon-intensive the grid is at that time.

The fixed emission factors are taken from the Covenant of Mayors (CoM) GHG Emission factors 2026 table (Bastos, Monforti-Ferrario and Melica, 2026): 202 kg CO2/MWh for natural gas and 267 kg CO2/MWh for light fuel oil, expressed per unit of fuel input. These are direct combustion CO2 factors rather than lifecycle greenhouse-gas factors; the analysis uses combustion factors because it concerns the operational emissions of heat production rather than the full supply-chain footprint of the fuels. The slack term, which represents unmet demand met as a last resort, is assigned the natural gas emission factor, treating it as an emergency gas-fired backup; this is a conservative choice, as slack is negligible in all scenarios.

Biomass combustion is treated as carbon-neutral, with an emission factor of zero. This follows Finnish and EU accounting practice (European Union, 2018; Statistics Finland, 2026a), under which the CO2 released when sustainably sourced biomass is burned is considered to be offset by the carbon absorbed during regrowth, and is therefore not counted at the point of combustion. As a result, the CHP unit, which burns forest chips, and the pellet boiler, which burns wood pellets, contribute no CO2 emissions in the model. It should be noted that this is an accounting convention based on national policy; the combustion of biomass does release CO2 at the stack, and a full lifecycle assessment would attribute some emissions to biomass through its supply chain. The carbon-neutral treatment is applied here for consistency with the regulatory framework under which the system operates.

For the electric boiler, the hourly grid CO2 intensity is taken from Fingrid data (Fingrid, 2026), for the study period. This intensity is not constant but varies considerably, as shown in Figure 4. Hourly values range from approximately 10 to 77 kg CO2/MWh, with an annual mean of 26.75 kg CO2/MWh. The distribution is strongly right-skewed: the majority of hours fall well below the mean, concentrated around 15 to 20 kg CO2/MWh, while a smaller number of high-intensity hours form a long upper tail that raises the mean above the median. These higher-intensity periods occur predominantly in the colder months, with sustained elevated values through winter and pronounced spikes in spring, although they appear as short-duration peaks rather than a smooth seasonal cycle. Because electric boiler operation concentrates in winter, when both heat demand and grid intensity tend to be higher, a single annual average factor would understate the emissions associated with grid electricity. Weighting emissions by actual hourly operation therefore captures a correlation that a constant factor would obscure, which motivates the real-time intensity method used throughout this study.

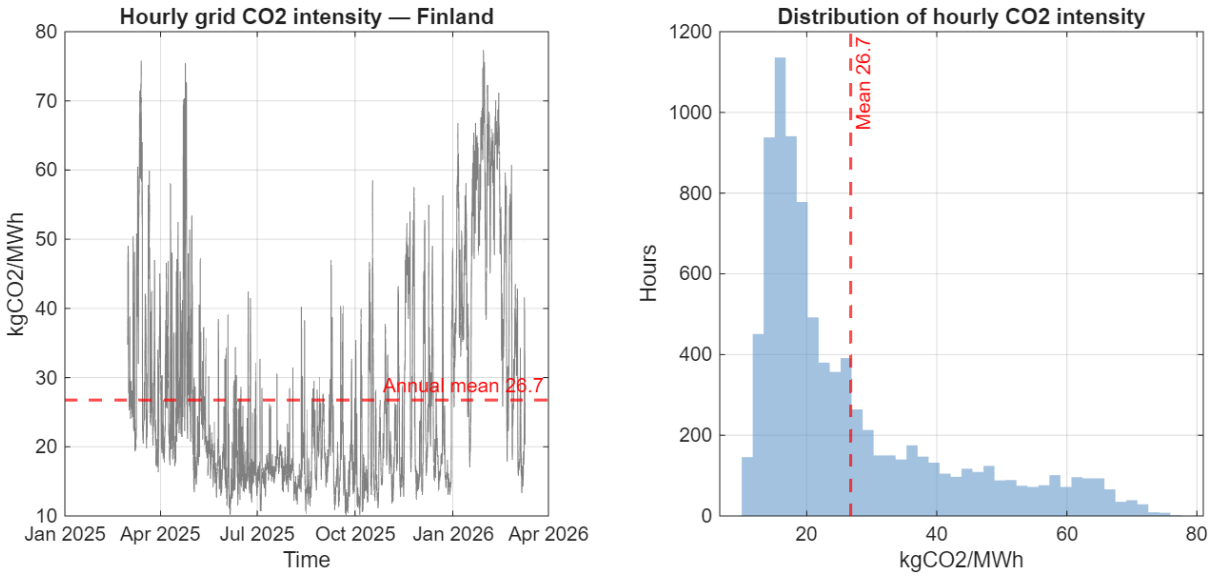

Figure 4. Hourly grid CO2 intensity for Finland over the study period (left) and its distribution (right); dashed line: annual mean 26.75 kgCO2/MWh.

3.5.3 Summary of model parameters and inputs

Table 4. Modelled unit capacities and efficiencies

Unit	Heat capacity (MW)	Efficiency	Efficiency source

Biomass CHP	140	0.83	Danish Energy Agency, 2026a
Gas boilers	250.5	0.91	Danish Energy Agency, 2026a
Pellet boilers	14	0.82	Danish Energy Agency, 2026a
Electric boiler (existing)	39	0.99	Danish Energy Agency, 2026a
Electric boiler (Scenarios C, D)	100	0.99	Grid connection limit (Lappeenrannan Energia)
Electric boiler (Scenario E)	289.5	0.99	Full electrification

Table 5. Fuel prices and cost parameters

Parameter	Value	Source
CHP fuel (forest chips)	39.00 EUR/MWh	Statistics Finland, 2026b
Natural gas	49.83 EUR/MWh	Statistics Finland, 2026b
Wood pellet	85.00 EUR/MWh	Statistics Finland, 2026b
Electricity	Hourly, time-varying	Nord Pool, 2026
Slack penalty	300 EUR/MWh	Modelling parameter (Section 3.3.3)
Carbon price (base case)	0 EUR/tCO2	Base case (Section 3.4.4)
CHP electricity credit (α_chp)	0	Confirmed by Lappeenrannan Energia (Section 3.5.1)

Table 6. Emission factors

Fuel	Emission factor (kg CO2/MWh fuel)	Treatment	Source
Forest chips (CHP)	0	Carbon-neutral	European Union, 2018; Statistics Finland, 2026a (Section 3.5.2)
Wood pellet	0	Carbon-neutral	European Union, 2018; Statistics Finland, 2026a
Natural gas	202	Direct combustion	Bastos, Monforti-Ferrario and Melica, 2026
Light fuel oil	267	Direct combustion	Bastos, Monforti-Ferrario and Melica, 2026
Grid electricity	Hourly, time-varying (mean 26.75)	Real-time intensity	Fingrid, 2026 (Section 3.5.2)

Table 7. Thermal energy storage parameters

Parameter	Value
Energy capacity	500 MWh
Minimum state of charge	10% of capacity (50 MWh)
Charge power limit	34 MW
Discharge power limit	28 MW

Charge efficiency (η_ch)	√0.98 ≈ 0.99
Discharge efficiency (η_dis)	√0.98 ≈ 0.99
Round-trip efficiency	0.98
Standing loss (η_loss)	0.0000833 per hour (0.2%/day)

Table 8. Investment cost parameters

Parameter	Value	Source
EB unit investment cost	0.0691 MEUR/MW	Danish Energy Agency, 2026a
Discount rate	6%	Section 3.4.4
Technical lifetime	25 years	Danish Energy Agency, 2026a
Capital recovery factor (CRF)	0.0782	Derived
Fixed O&M (new EB capacity)	1,111 EUR/MW/yr	Danish Energy Agency, 2026a
Variable O&M (new EB capacity)	0.5317 EUR/MWh	Danish Energy Agency, 2026a
New capacity, Scenarios C and D	61 MW	Above existing 39 MW
New capacity, Scenario E	250.5 MW	Above existing 39 MW
Annualised capital cost (ACC), C and D	329,900 EUR/yr	Derived
Annualised capital cost (ACC), E	1,354,400 EUR/yr	Derived
TES unit investment cost	3,000 EUR/MWh capacity	Danish Energy Agency, 2024
TES technical lifetime / CRF	40 years / 0.0665	Danish Energy Agency, 2024
TES fixed O&M	8.8 EUR/MWh capacity/yr	Danish Energy Agency, 2024

* TES investment costs apply only to the storage-sizing analysis (Section 4.5.3); the existing 500 MWh storage is treated as sunk in all scenario comparisons.

3.6 Sensitivity analysis design

The base-case results rest on a number of input values and assumptions, several of which are uncertain or represent modelling choices rather than measured quantities. To test the robustness of the conclusions, three sensitivity sweeps are carried out, each varying the parameters most likely to influence the results. In each sweep, the selected parameters are varied over a defined range while the others are held at their base values, and all five scenarios are re-optimised for every combination. The sweeps examine operating cost, since this is the quantity the optimisation determines directly; where a sweep bears on the investment decision, the total-cost implications are considered separately. The results of the three sweeps are presented in Section 4.5 .

3.6.1 Price sweeps

The first sweep varies the two market prices to which the system is most exposed, the electricity price and the gas price, together with the thermal energy storage capacity. The electricity price and the gas price are each scaled from 70% to 250% of their base levels. These ranges are chosen to span plausible market variation, with the gas range extended further upward to reflect the greater volatility of gas prices and the possibility of sustained high prices. Sensitivity analyses in comparable district heating studies are commonly limited to varying prices by around plus or minus 50% of base values, often one parameter at a time (Dahl, Brun and Andresen, 2019). A wider, jointly swept range is used here because the cost crossovers between scenarios lie outside such a band (Section 4.5.1), and because the 2022 energy crisis showed that Finnish spot prices can sustain multiples of their historical levels (Javanshir, Syri and Hiltunen, 2024). The storage capacity is varied across 250, 500, and 750 MWh, spanning the uncertain operating capacity of the existing storage (250 to 500 MWh) and a larger hypothetical storage. This sweep tests whether the cost ranking of the scenarios, and in particular the position of the electrified scenarios relative to the baseline, is robust to the prices that drive dispatch.

3.6.2 Thermal energy storage sweeps

The second sweep varies the charge and discharge power limits of the thermal energy storage independently, each from 50% to 200% of its base value (charge from 17 to 68 MW, discharge from 14 to 56 MW). Varying the two limits separately allows the distinct contributions of charging and discharging capability to be identified, since the value of storage may depend asymmetrically on how quickly it can absorb cheap electricity versus how quickly it can release stored heat. This sweep tests how sensitive the value of storage is to its power rating, and which of the two power limits is the binding constraint.

3.6.3 CHP electricity credit and carbon price sweep

The third sweep varies the two parameters that most affect the cost accounting but cannot be measured directly for this case study: the CHP electricity credit (alpha_chp) and the CO2

price. The credit is varied from 0 to 0.95, spanning the full range from no credit (the stakeholder-confirmed base case, allocating all CHP fuel cost to heat) to almost full allocation to electricity. The CO2 price is varied from 0 to 400 EUR/tCO2, spanning the base case of no explicit carbon price through to values well above current and near-term projected levels. This sweep tests how the scenario ranking responds to these two assumptions, and underpins the break-even analysis of the carbon price at which further electrification becomes cost-competitive with the baseline (Section 4.5.6).

3.7 Model validation

Before the optimisation results are interpreted, the model is validated against real operational data from Lappeenrannan Energia to confirm that it reproduces the actual behaviour of the system. The validation compares the modelled dispatch of the three key components, the electric boiler, the thermal energy storage, and the CHP unit, against their measured (real) operation over the study period. The purpose is not to reproduce the historical dispatch hour by hour, since the model optimises cost under simplifying assumptions rather than replicating every operational decision, but to confirm that the model responds to the same drivers as the real system and produces dispatch of comparable magnitude and pattern.

3.7.1 Electric boiler validation

The electric boiler is dispatched in the model on the basis of the electricity price, running when the price is low enough for electric heat to undercut the alternatives. Figure 5 compares the modelled electric boiler output against the measured output over the study period, both in absolute terms and against the electricity price. The modelled and measured output show good agreement in pattern: the model produces a total of 171,482 MWh against a measured 138,507 MWh, and a mean output of 19.1 MW against a measured 15.4 MW. The modelled maximum is 39.0 MW, and the measured output also concentrates at 39.0 MW, briefly reaching 40.9 MW. The model dispatches the boiler about 24% more than the real operation, but in fewer hours: it is active for 4,778 hours against the measured 5,122, running at rated power whenever electricity is cheap enough, whereas the real plant spreads its operation

across more hours at partial load, reflecting operational constraints not represented in the model.

The price-driven behaviour is reproduced clearly. In the measured data, the boiler runs at a mean electricity price of 19.7 EUR/MWh and is idle at a mean price of 96.6 EUR/MWh; in the model, the corresponding figures are 10.9 and 100.2 EUR/MWh. Both the real and modelled boiler therefore concentrate operation in low-price hours and shut down when prices are high, confirming that the model captures the price-responsive dispatch that is central to the electrified scenarios. The model's slightly sharper price discrimination, running at a lower mean price when on, reflects its cost-optimal dispatch, whereas the real plant occasionally operates at higher prices for operational reasons.

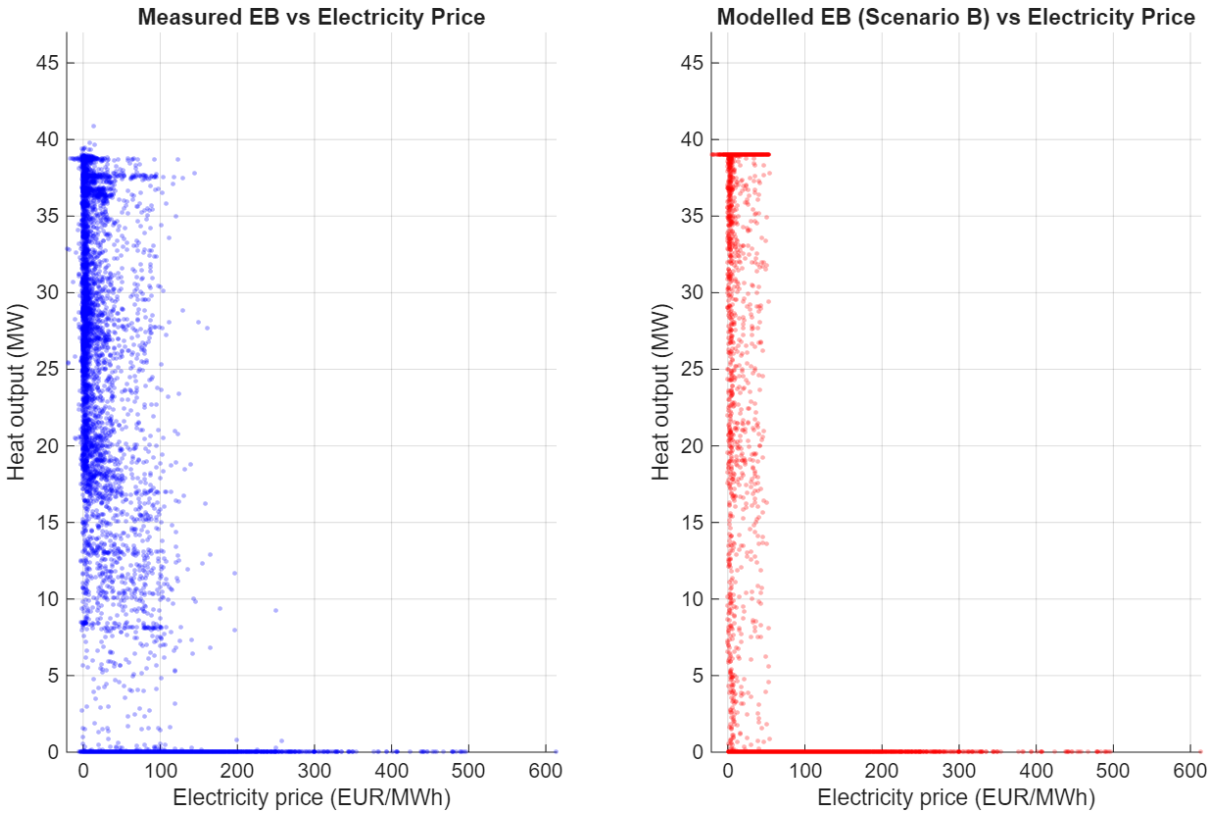

Figure 5. EB heat output against electricity price (left: measured; right: modelled).

Figure 6 presents the comparison over the study period. In the hourly series (Figure 6, top), the modelled dispatch follows the same seasonal structure as the measured operation: near-continuous operation through the low-price months from May to July, intermittent operation in the shoulder seasons, and an almost complete shutdown in the high-price period of late January and February 2026. The measured output plotted against the electricity price (Figure 6, middle) makes the driver of this pattern visible, with output rising whenever the price falls

and the boiler standing idle through sustained price peaks, most clearly in February 2026, when the monthly mean price reached 137 EUR/MWh. The monthly means (Figure 6, bottom) quantify where model and measurement diverge. Agreement is closest in high summer, with July and August differing by less than 1 MW, and September is the only month in which the measured output exceeds the modelled. The model dispatches the boiler more heavily in the shoulder months, most notably April, October and November, where the gap reaches 6 to 8 MW: at moderate average prices of around 48 EUR/MWh these months contain many hours in which electric heat is marginally economic, all of which the cost-optimal model captures but the real operation only partly uses. This is the expected signature of the difference between cost-optimal and operational dispatch, and is consistent with the price-threshold comparison below.

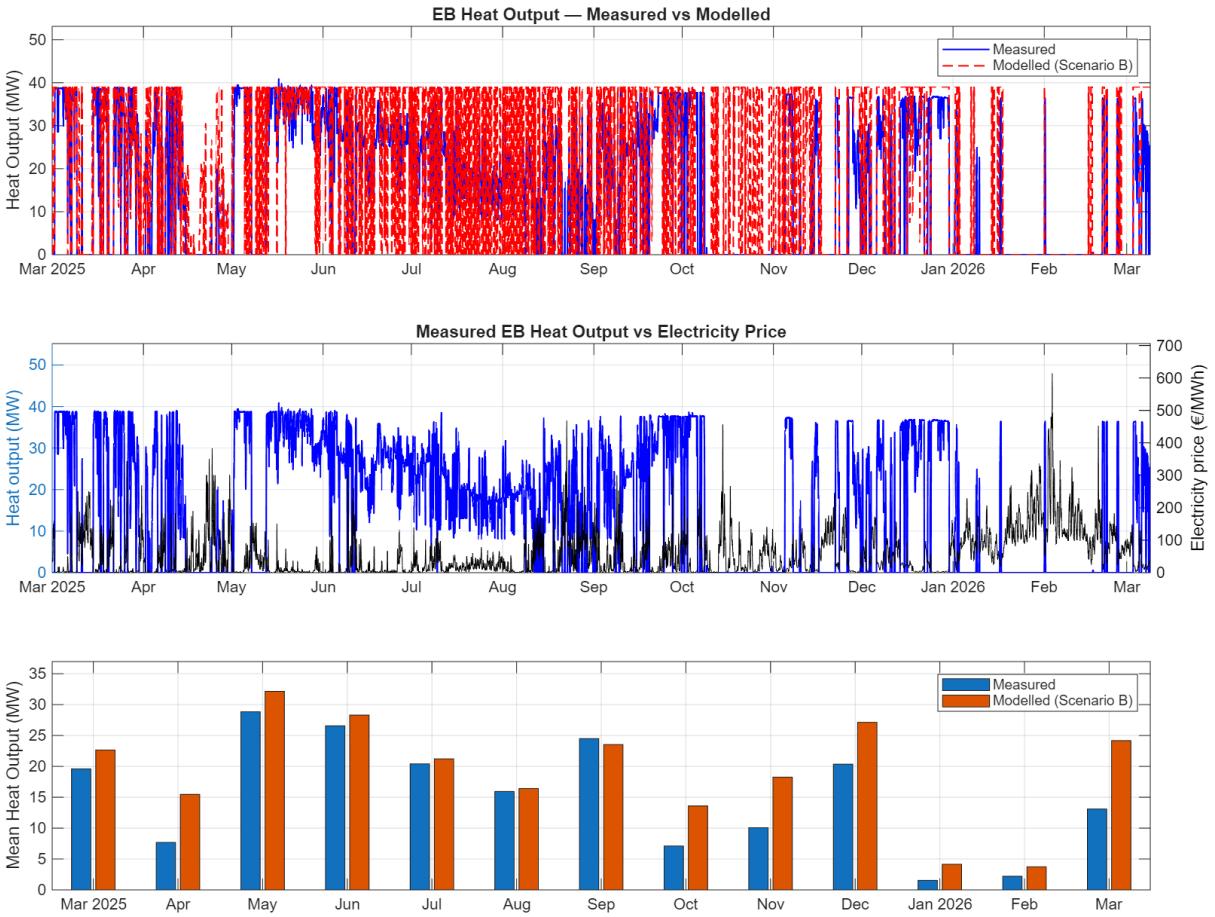

Figure 6. Electric boiler heat output, measured against modelled (Scenario B): hourly series (top), measured output against price (middle), and monthly means (bottom)

3.7.2 Thermal energy storage validation

Real operation characterisation. Before validating the model, the measured operation of the TES was characterised to establish how the unit is used in practice. Figure 7 shows the measured (real) charge and discharge power against the day-ahead electricity price, together with the monthly count of charging and discharging hours, over the operational window of 27 May 2025 to 9 March 2026 (6,875 hours). The TES is idle for roughly two thirds of the period (4,608 hours), and when active it responds to price: charging occurs at a mean price of 40.5 EUR/MWh and discharging at a mean of 80.0 EUR/MWh. Both charging and discharging occur within every operational month rather than concentrating charging in summer and discharging in winter. This sub-monthly cycling, rather than the seasonal drift in the mean state of charge (SOC), identifies the unit as a short-term price-responsive buffer rather than a seasonal storage, behaviour that the optimisation model is built to represent.

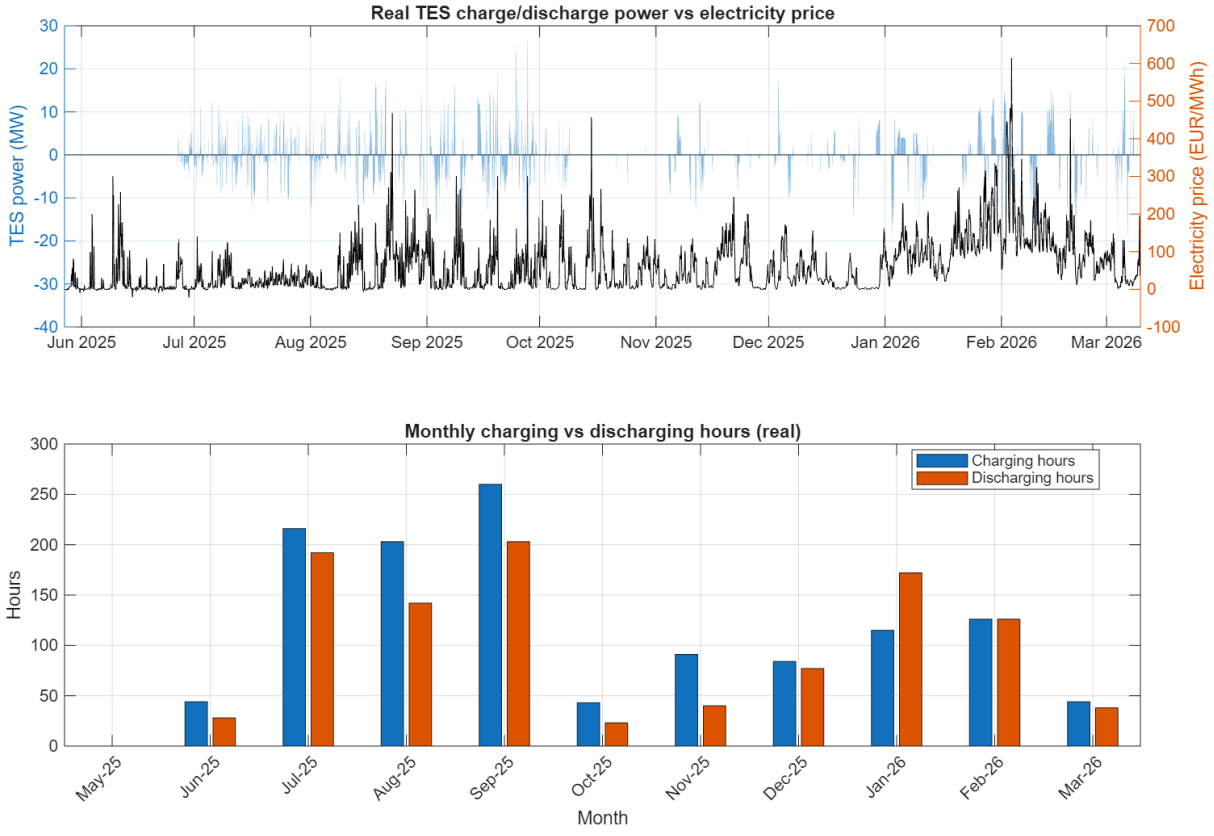

Figure 7. Measured TES charge and discharge power against day-ahead price (top) and monthly active hours (bottom); positive: discharging, negative: charging.

Storage model validation. The storage model was then validated against the same measured data. The modelled SOC was reconstructed by replaying the metered charge and discharge power through the storage energy balance, using the same efficiency and standing-loss parameters as the optimisation model, and was compared against the measured SOC. This comparison establishes whether the modelled TES reproduces the behaviour of the real system. Because the reconstruction uses the real charge and discharge decisions, it isolates the storage physics rather than the dispatch logic. To keep the reconstruction physically valid, the SOC was bounded to the range 0 to 500 MWh, since the real TES cannot fall below empty; without this bound, the reconstruction accumulates a spurious one-way offset whenever the measured TES rests at zero.

Both storage parameters were taken from the DEA Technology Data catalogue: a round-trip efficiency of 0.98, applied symmetrically as a charge and discharge efficiency of sqrt(0.98) on each side, and a standing loss of 0.2% per day (equivalent to 8.3e-5 per hour). Under these values, the reconstructed SOC follows the measured trajectory closely (Figure 8, top), with a correlation of 0.953 and a root-mean-square error (RMSE) of 47.8 MWh, or 9.6% of the 500 MWh capacity. The error series (Figure 8, middle) is concentrated in the first weeks of operation and in an isolated discontinuity in September, consistent with the periods in which the modelled and measured trajectories diverge in the top panel. Over the settled period from October onwards, the model tracks the measured SOC to within approximately 50 MWh. The mean bias is 14.9 MWh, and falls to 0.5 MWh when the standing loss is set to zero, indicating that the model carries no material systematic offset.

The standing-loss assumption was verified independently through calibration (Figure 8, bottom). The standing-loss coefficient was swept from -0.001 to 0.003 per hour, in increments of 0.00005, and the value minimising the SOC RMSE against the measured data was identified. The best-fit standing loss was approximately 0.0001 per hour, effectively identical to the catalogue value of 0.2% per day. This minimum lies in the interior of the search range rather than at a boundary, indicating that the metered data resolve a standing loss that aligns with the independent catalogue figure. This agreement between two independent sources, the technology catalogue and the measured operation, provides direct empirical support for the storage parameters adopted in the model.

The residual RMSE of 9.6% is attributable to two sources that do not indicate model error. First, the maximum absolute error of 218 MWh arises from the isolated metering

discontinuities noted above rather than from storage dynamics, and is most likely due to measurement noise or disturbance. Second, the apparent round-trip efficiency of the raw data, computed as total discharged over total charged energy, is 0.937, below the modelled 0.98. This figure combines conversion and standing losses, and is further reduced by the TES finishing the window at a higher SOC than it began, so it overstates the true conversion loss. The residual gap between the catalogue efficiency and this apparent operational figure is examined as a conversion-efficiency sensitivity case in Section 4.5.4 , and the headline results are shown to be robust to it.

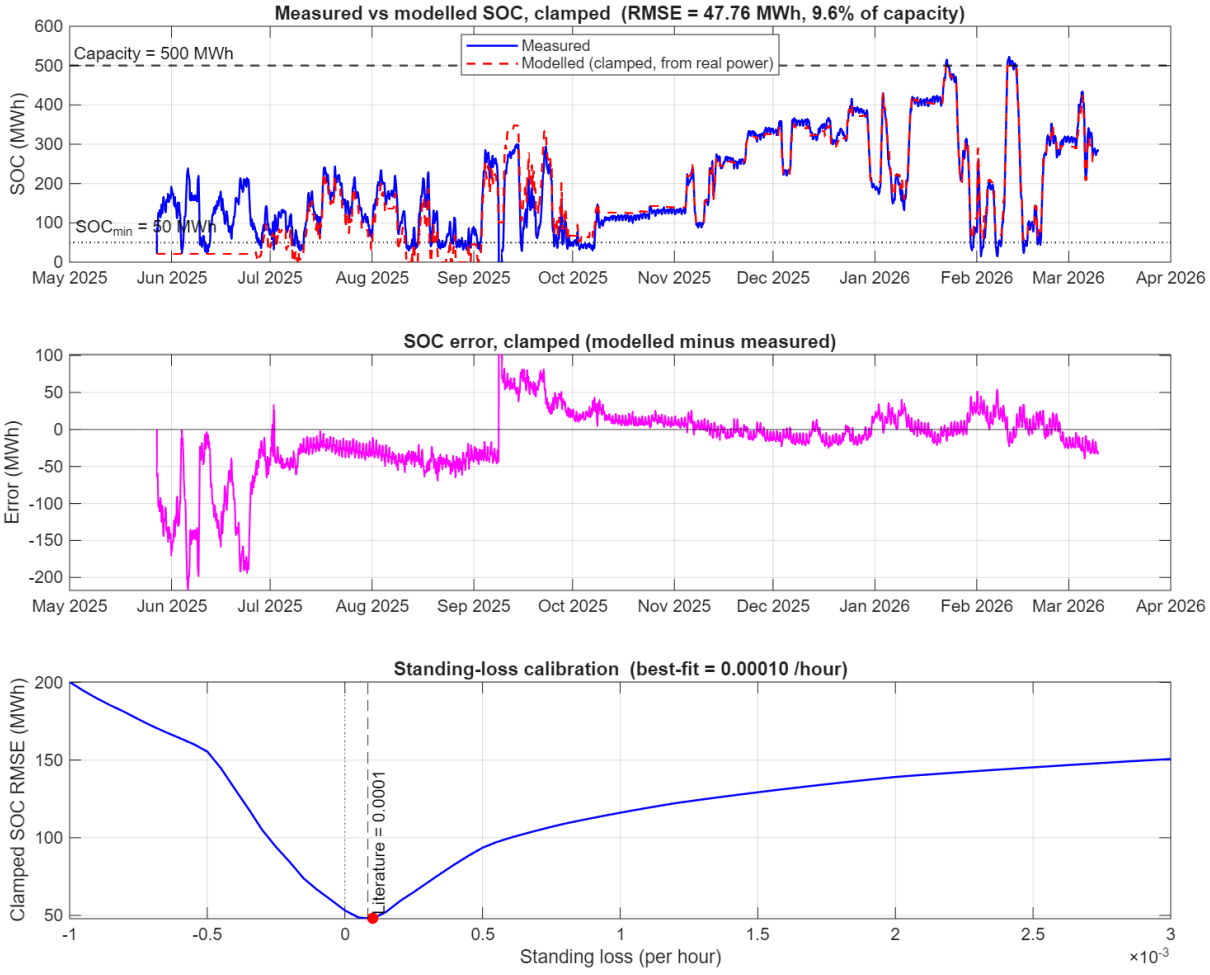

Figure 8. Measured against reconstructed SOC (top), SOC error (middle), and standing-loss calibration with the catalogue value marked (bottom).

Dispatch benchmark (not validation). As a separate exercise, the cost-optimal dispatch produced by the linear programme was compared against the real operation over the same window (Figure 9). This comparison is a benchmark rather than a validation: the

optimisation dispatches the TES cost-optimally with perfect foresight, whereas the real operation follows the operator's own rules, so the two are not expected to coincide. The difference therefore measures the value of optimal control rather than any model error.

The optimised TES runs far more cycles, moving approximately five times the metered energy volume and using the full 0 to 500 MWh range, and it charges at substantially lower prices (a mean of 19.2 against 40.5 EUR/MWh). The price spread it captures between charging and discharging (42.7 EUR/MWh) is only slightly larger than that of the real operation (39.6 EUR/MWh), indicating that the existing operation already exploits the price signal effectively. The difference lies in the intensity of TES use rather than in the timing of charging and discharging. The mean discharge price is not a reliable indicator in this comparison, since the optimisation discharges across many more hours and therefore averages into mid-priced periods; the meaningful measure of the optimisation advantage is total system cost, reported in Section 4.3.1 . In the baseline configuration, the electricity price is only a partial proxy for the marginal heat cost, because the existing electric boiler is small and the marginal producer is frequently the CHP plant or gas. The spread figures are therefore indicative here and become more directly meaningful in the electrified scenarios.

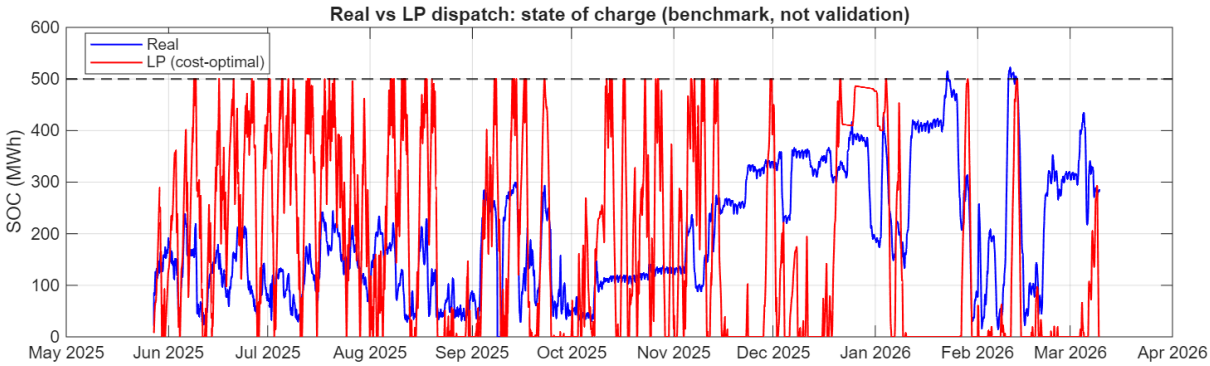

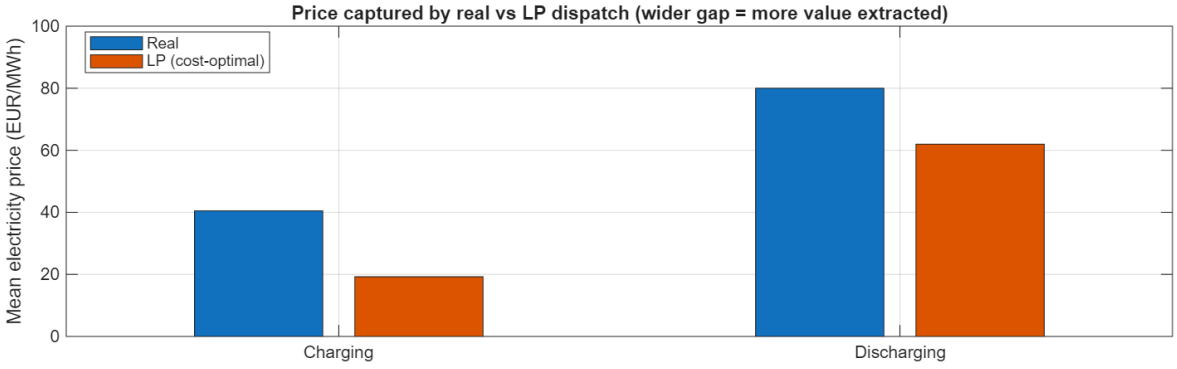

Figure 9. Real against cost-optimal TES dispatch: SOC trajectories (top) and mean prices during charging and discharging (bottom).

3.7.3 CHP validation

The CHP unit is validated by comparing its modelled monthly heat output against the measured output over the study period (Figure 10). The model reproduces the observed seasonal pattern, as shown in Table 9: high output through the heating season, the enforced shutdown in summer, and low part-load operation in the shoulder months. Over the year, the model produces a total of 392,709 MWh against a measured 373,862 MWh, with a mean output of 44.6 MW against a measured 44.4 MW, and modelled maxima of 140 MW against measured 143.0 MW. The monthly means track the real plant closely across the year.

Of particular note is the shoulder month of May, in which the real CHP unit operates at a low part-load, with a monthly mean output of 11.4 MW, below its nominal heating-season minimum of 30% of capacity. The model reproduces this behaviour, with a modelled mean of 14.0 MW. This confirms that the continuous linear formulation captures the real plant's sub-minimum shoulder operation, a behaviour that a binary minimum-load formulation could not represent, as it would force the unit either offline or above its minimum stable output. This finding supports the choice of a linear rather than a mixed-integer formulation (Section 3.4.5): in the one regime where the two formulations diverge, the linear model is the more faithful to the observed operation.

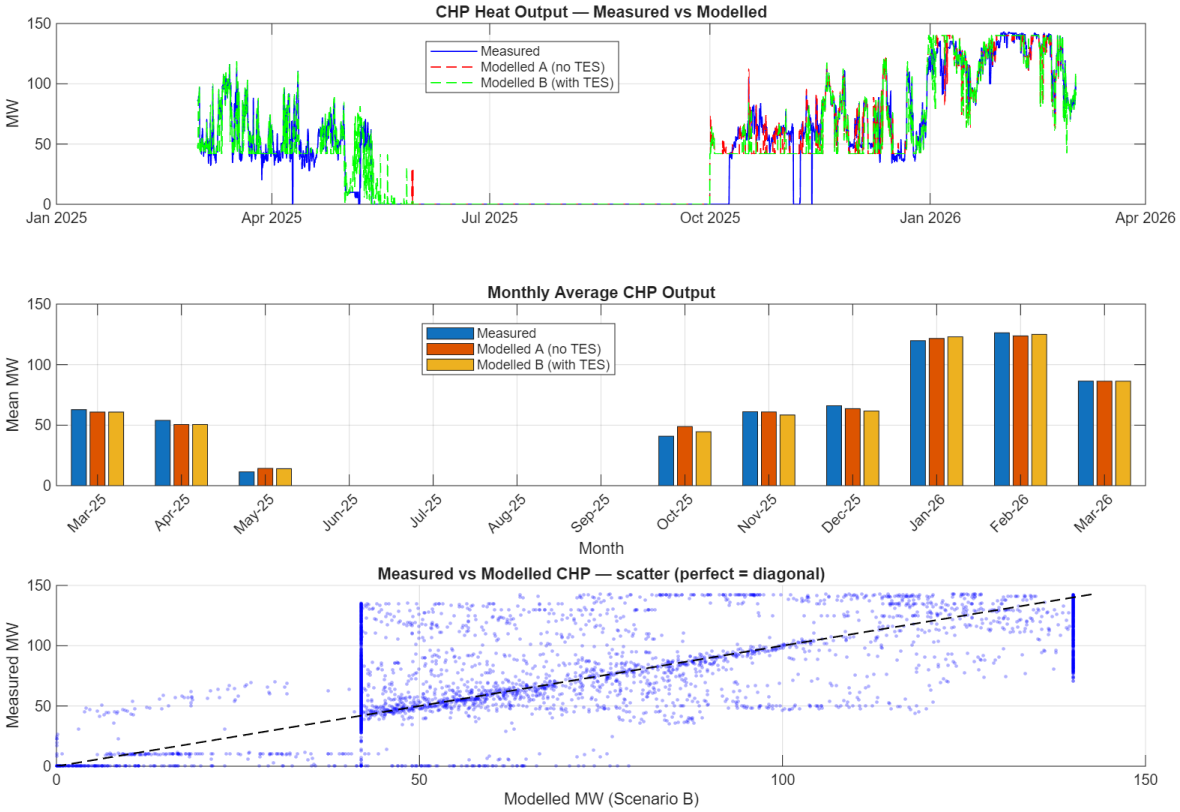

Figure 10. CHP validation charts (top: CHP heat output comparison measured vs modelled, middle: monthly average CHP output, bottom: measured vs modelled CHP power output)

Table 9. Monthly mean CHP heat output, measured versus modelled (MW)

Month	Measured	Modelled (B)
Mar 2025	62.8	60.8
Apr 2025	53.9	50.5
May 2025	11.4	14.0
Jun–Sep 2025	0.0	0.0
Oct 2025	40.9	44.6
Nov 2025	61.1	58.4
Dec 2025	66.0	61.7
Jan 2026	119.8	123.0
Feb 2026	126.3	125.0
Mar 2026	86.4	86.3

4 Results

4.1 Overview

Scenario A represents the current system without TES; Scenario B is the current system with the existing TES in operation; Scenario C replaces gas with an EB capped at 100 MW; Scenario D adds TES to Scenario C; and Scenario E is the fully electrified system with storage, in which the EB is scaled to 289.5 MW to meet peak demand without fossil backup.

In this chapter, all scenario comparisons are made against Scenario B, the current system with the TES already in operation, rather than against Scenario A, which shares the same heat production technologies but lacks storage. Because the TES is already operational, its capital cost is treated as sunk. The focus is therefore not whether storage should be added, but how electrification of the district heating system can be integrated with the existing TES, and under what conditions this becomes economically feasible. Scenario A is retained to isolate the effect of the TES (A→B), while the effect of electrification is assessed through the comparisons B→C and B→D, and full electrification through B→E. Scenario A does not serve as the reference point for the chapter's conclusions. The comparison of these results with the existing literature is presented in Section 5.6 .

4.2 Dispatch behaviour

Before comparing costs and emissions, this section describes how the modelled system operates under the observed 2025 to 2026 electricity prices. Unlike the sensitivity analysis in Section 4.5 , which scales prices to hypothetical levels, the results here reflect the actual price series used in the optimisation. The focus is on how the system runs, not on what it costs.

The EB operates in strong response to electricity price (Figure 11, top). In all scenarios its output is highest when prices are low and falls sharply as prices rise, approaching zero above roughly 50 EUR/MWh. The electrified scenarios C, D, and E reach much higher peak output than the current system (A and B), reflecting their larger EB capacity, but all five share the

same price-driven pattern: the EB is dispatched only when electricity is cheap relative to the alternative heat sources, consistent with the price-threshold operation described in the literature (Trømborg et al., 2017).

The TES charging behaviour follows the same price signal (Figure 11, bottom). Across the storage-enabled scenarios, charging (heat into the storage) concentrates in low-price hours, while discharging (heat out) occurs as prices rise, so the storage absorbs cheap electricity and releases it when running the EB would be expensive. This charge-low, discharge-high pattern is the mechanism through which TES lowers operating cost, and it is most pronounced in Scenarios D and E, where the larger EB provides more scope to exploit price variation. A slight increase in discharging is also visible for D and E at very high electricity prices (above 120 EUR/MWh): the price series for the study period contains a substantial number of hours in this range, and in those hours the model relies on TES discharge to avoid running the EB at prohibitive cost.

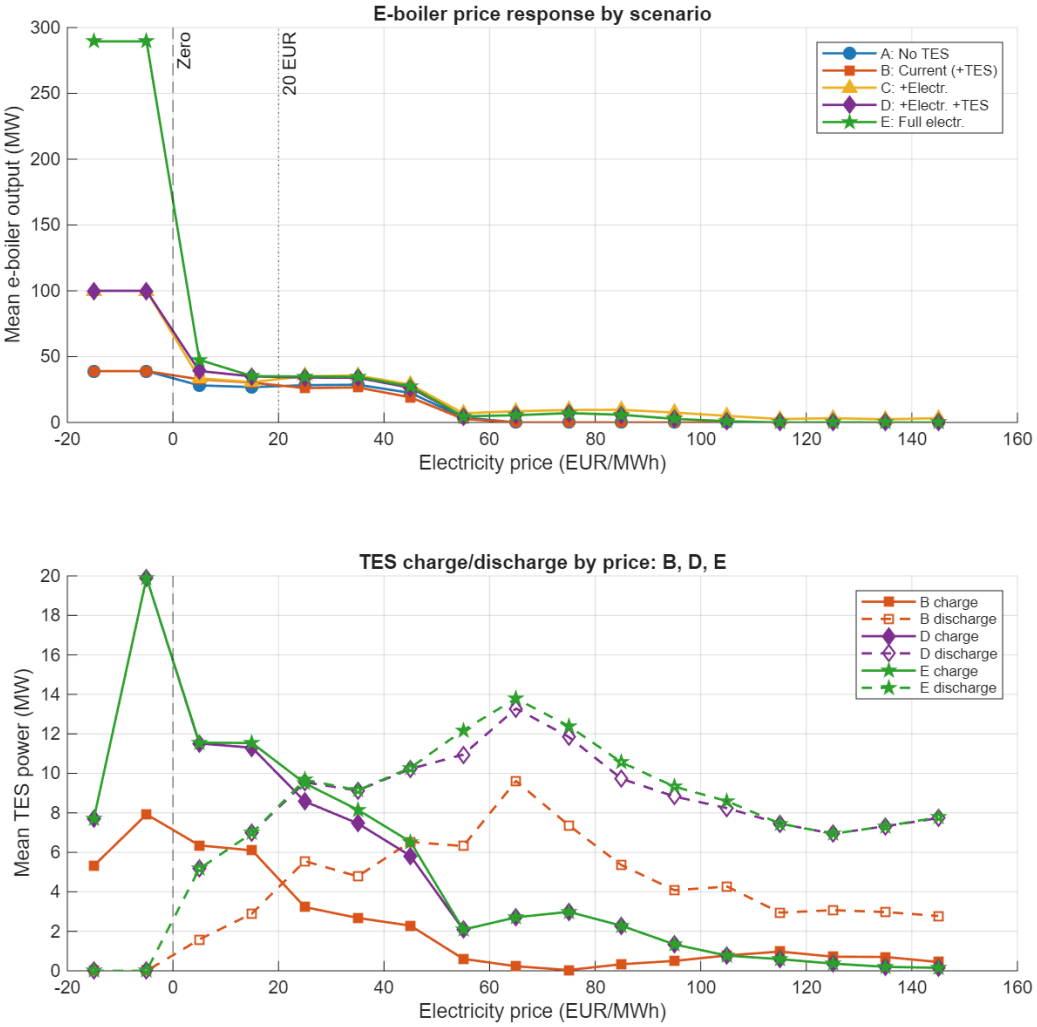

Figure 11. EB dispatch response to electricity price across all scenarios. Top: mean EB output versus electricity price. Bottom: mean TES charge and discharge power versus electricity price (solid lines: charging; dashed lines: discharging).

The concentration of consumption in low-price hours is confirmed by the breakdown by price band (Figure 12, left). In every scenario, the majority of EB energy is drawn in the 0 to 20 EUR/MWh band, with very little above 50 EUR/MWh. The electrified scenarios consume more in absolute terms across all bands, and Scenario E in particular draws a substantial amount in the below-zero price band, indicating that its large EB is able to take up electricity during periods of negative prices.

The corresponding electricity cost by band shows where spending is concentrated (Figure 12, right). Although most energy is consumed in the cheapest bands, a disproportionate share of cost falls in the higher-price bands, since each MWh there is more expensive. This effect

is most visible in Scenario C, which lacks storage and is therefore forced to consume in higher-price hours, incurring cost in the above 50 EUR/MWh band that the storage-enabled scenarios largely avoid.

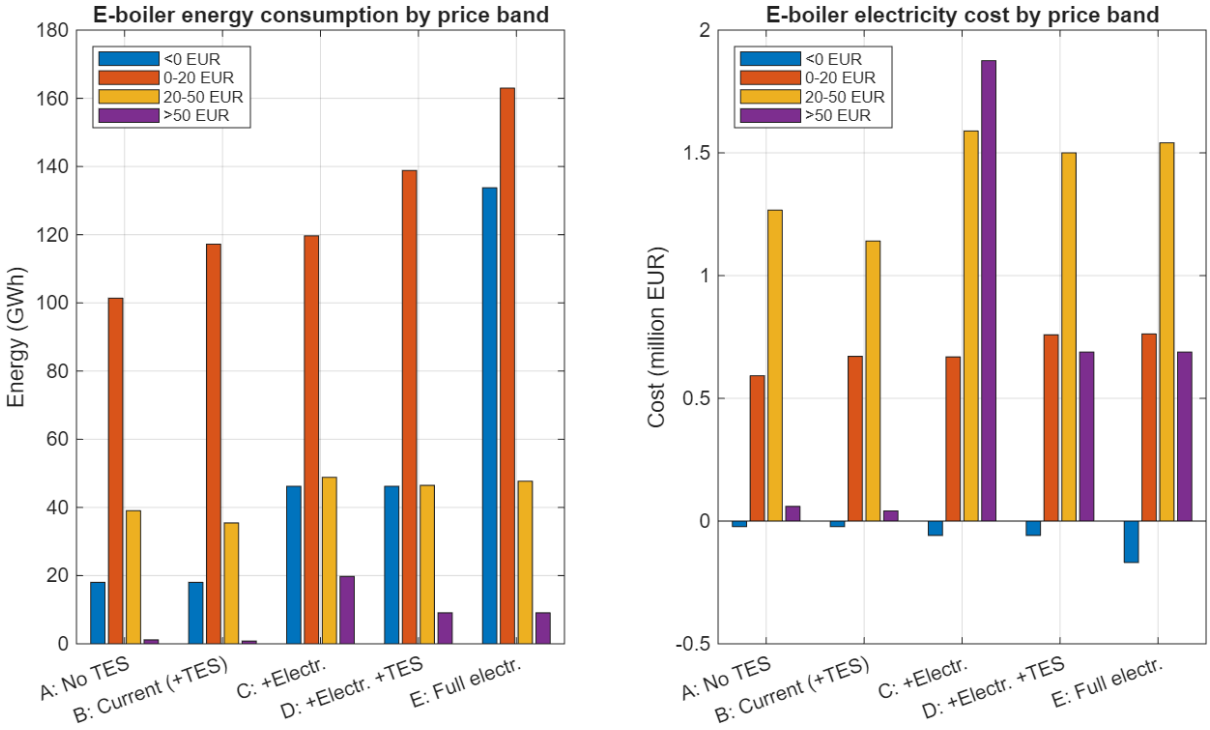

Figure 12. EB electricity consumption (left) and cost by price band across all scenarios (right).

4.3 Cost results

The annual cost results for all five scenarios are summarised in Table 10. Costs are reported at two levels. Operating cost is the basis on which the LP optimises the hourly dispatch, and comprises fuel cost and electricity cost. Total cost additionally includes the annualised capital cost (ACC) of investment, together with the variable and fixed operation and maintenance (O&M) costs; these apply only to the electrified scenarios C, D, and E, which require new EB capacity. Scenarios A and B build no new capacity and therefore carry no O&M or capital costs, so their operating and total costs coincide.

Figure 13 shows the cost composition by scenario, with operating cost broken into its fuel and electricity components and the investment-related costs (O&M and ACC) stacked

above. The dashed line marks operating cost, so the gap between it and the top of each bar represents the capital and O&M burden carried only by the electrified scenarios.

Table 10. Annual cost summary by scenario (MEUR).

Scenario	Operating cost (fuel/electricity)	VarOM	FixedOM	ACC	Total	vs A	vs B
A: No TES	22.54	-	-	-	22.54	-	0.89
B: Current (+TES)	21.65	-	-	-	21.65	- 0.89	-
C: +Electr.	23.16	0.03	0.07	0.33	23.59	1.05	1.94
D: +Electr. +TES	20.88	0.05	0.07	0.33	21.32	- 1.22	- 0.33
E: Full electr.	20.74	0.11	0.28	1.35	22.48	-0.06	0.83

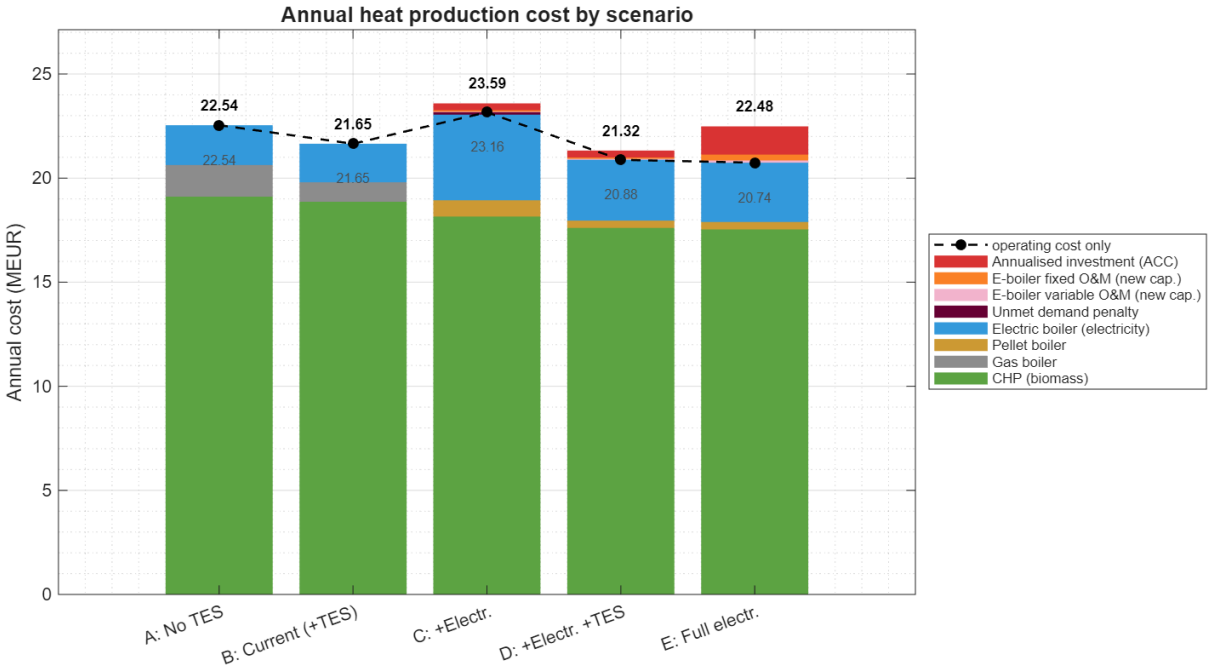

Figure 13. Annual cost by scenario: operating cost components with O&M and ACC stacked above; dashed line: operating cost.

4.3.1 Operating cost ordering

The cost ordering differs depending on which of the two cost levels is considered. On operating cost, the ordering is E < D < B < A < C, with the fully electrified Scenario E

cheapest to operate (20.74 MEUR) and Scenario C, electrification without storage, the most expensive (23.16 MEUR). This ordering reflects the dispatch economics in isolation: replacing gas with a large EB lowers fuel cost when electricity is favourably priced, and adding TES (D) lowers it further by shifting EB operation toward cheaper hours. Scenario C is the exception, more expensive to operate than the gas-based baseline B, because without storage its EB cannot avoid high-price hours and must either run at unfavourable prices or fall back on the slack penalty.

4.3.2 Total cost ordering

Once capital and O&M are included, the ordering changes to D < B < E < A < C on total cost. Scenario D is the only electrified scenario cheaper than the current system (Scenario B), at 21.32 MEUR against B's 21.65 MEUR, a reduction of 0.33 MEUR per year. Scenario C, despite removing gas, is the most expensive overall at 23.59 MEUR, 1.94 MEUR above B, since it combines the highest operating cost of any scenario with the EB investment. Scenario E, although cheapest to operate, becomes more expensive than B once its substantially larger capital cost is included (1.35 MEUR ACC for the 289.5 MW EB, against 0.33 MEUR for the 100 MW EB in C and D), ending 0.83 MEUR above B in total. Full electrification (E) ends up costing approximately the same overall as the fossil, no-storage counterfactual (A), because E's operating savings are almost exactly offset by its large capital cost.

The contrast between the two orderings is the central cost result: operating cost favours electrification, with the full-scale electrified Scenario E lowest, whereas total cost favours Scenario D, the storage-enabled, grid-constrained configuration. The economic effect of TES is visible in the C-to-D comparison, where adding storage to the electrified system reduces operating cost from 23.16 to 20.88 MEUR, a reduction of approximately 9.8%, while capital and O&M remain identical between the two. This is the storage value mechanism identified in the literature (Nuytten et al., 2013). The effect of storage on the baseline system is given by the A-to-B comparison, where adding the planned TES reduces cost from 22.54 to 21.65 MEUR, a saving of around 3.9% per year.

4.3.3 Cost savings against the baseline

The total-cost differences against the baseline B are reported in the final column of Table 10. Only Scenario D shows a saving against B; Scenarios C and E, and the no-storage counterfactual A, are all more expensive. The carbon price at which the electrified scenarios become cost-competitive with B, given that the base case applies no explicit carbon price, is examined in the sensitivity analysis in Section 4.5.6 .

4.4 Emissions results

4.4.1 Emissions by scenario

The annual CO2 emissions for all five scenarios are summarised in Table 11. Emissions from EB consumption are calculated using real-time hourly grid CO2 intensity, while direct fuel combustion uses fixed emission factors (see Section 3.5.2). Biomass combustion in the CHP unit and the pellet boiler is treated as carbon-neutral under EU and Finnish accounting, and therefore contributes zero emissions in all scenarios. Savings are reported against both Scenario A and the baseline Scenario B. Figure 14 shows the total annual CO2 emissions for the five scenarios. The emission ordering is C < D < E < B < A, from lowest to highest. Scenario C has the lowest emissions (approximately 4,700 tCO2), followed closely by Scenario D; Scenario E lies slightly below B, and Scenario A is the highest of all at 9,196 tCO2. All three electrified scenarios (C, D, and E) emit less than the baseline B, confirming that electrification reduces emissions overall.

Table 11. Total annual CO2 emissions comparison (with real-time grid CO2 intensity)

Source	A	B	C	D	E	unit
CHP (biomass)	0	0	0	0	0	tCO2
Gas boiler	6152.6	3794.8	0	0	0	tCO2
Oil boiler	0	0	0	0	0	tCO2
Pellet (biomass)	0	0	0	0	0	tCO2
EB (grid)	3043.5	3249.3	4608.4	4694.2	6809.0	tCO2
Slack (gas proxy)	0	0	84	0	0	tCO2
Total	9196.2	7044.0	4692.4	4694.2	6809.0	tCO2
Saving vs A	0	-2152.1	-4503.8	-4502.0	-2387.2	tCO2
Saving vs B	2152.1	0	-2351.6	-2349.9	-235.1	tCO2

System emission intensity	15.68	12.01	8.00	8.00	11.61	kgCO2/MWh

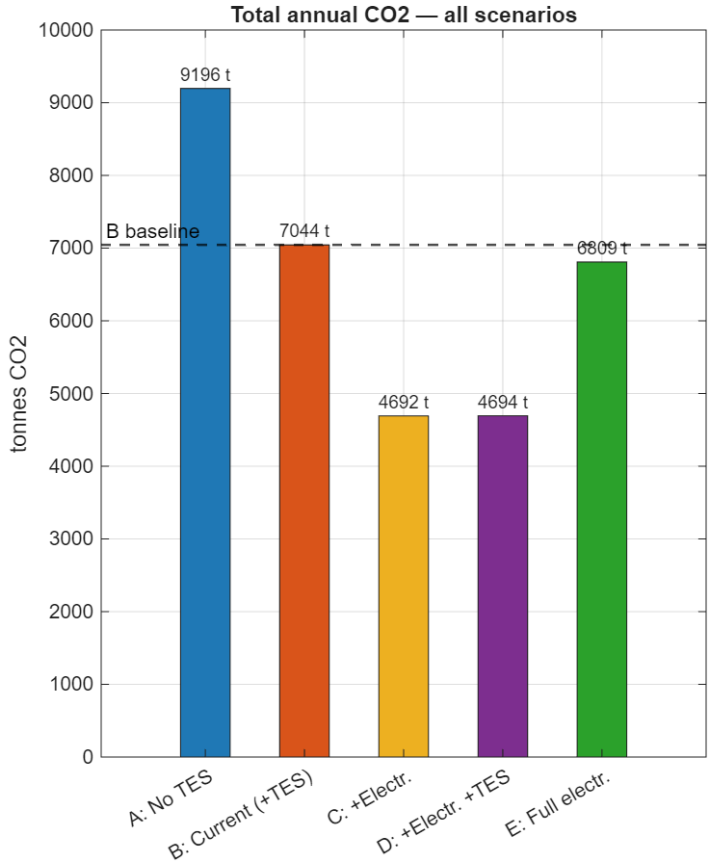

Figure 14. Total annual CO2 emissions for all five scenarios.

4.4.2 The roles of fuel switching and storage

The reduction in emissions is driven by the fuel switch (gas to EB) rather than by storage. Moving from B to either Scenario C or D cuts emissions by approximately 33% (B→D: −2,350 tCO2, −33.4%; C comparable), entirely through removing the gas boiler. Adding TES on top of electrification (C→D) changes emissions by only 1.8 tCO2 (less than 0.1%), and slightly increases rather than decreases them. The emissions reduction therefore comes from the fuel switch, not from storage: Scenario C, without TES, achieves essentially the same cut as the storage-enabled Scenario D.

The role of TES in emissions depends on whether fossil fuel remains in the system to displace. In the current system, comparing Scenario A (without TES) to Scenario B shows

TES cutting emissions by 23.4% (−2,152.1 tCO2), achieved by displacing gas, whose average output falls from 3.1 to 1.9 MW. Once gas has been removed, however, TES has almost no effect on emissions, as the C→D comparison shows. The distinction is whether fossil fuel is present to displace: TES reduces emissions only when it offsets fossil generation, not when the system is already decarbonised.

4.4.3 Emissions of full electrification

Scenario E, although fully fossil-free, emits more than both C and D, at 6,809 tCO2, and lies only 3.3% below B. The reason is volume rather than intensity. All three electrified scenarios retain the same carbon-neutral biomass capacity; what distinguishes E is its 289.5 MW EB, which is large enough to displace output from the CHP as well as the gas boilers whenever electricity is cheap, and which must also cover peak hours that exceed the biomass capacity. Scenario E therefore draws approximately 357 GWh of grid electricity over the year, against roughly 243 GWh in D and 237 GWh in C. Each of these megawatt-hours carries real grid emissions, whereas the biomass heat it replaces is accounted as zero-carbon, so total emissions grow with the volume of grid electricity consumed even though no fossil fuel is burned. This contrast with electrification studies conducted against fossil-fuelled reference systems is examined in Section 5.6 . The weighted intensity of E's consumption is in fact slightly lower than that of C and D, as Section 4.4.4 shows, so the higher total is entirely a volume effect.

4.4.4 Emissions intensity of electric boiler operation

The EB weighted CO2 intensity, defined as total EB emissions divided by total EB electricity consumption, is shown in Table 12. In every scenario it lies well below the grid annual average of 26.75 kgCO2/MWh, because the EB is dispatched on price, and low-price hours in the Finnish system typically coincide with high wind output and low grid intensity. The differences between scenarios then reflect how selectively each configuration can consume. The small 39 MW EB in Scenarios A and B runs only in the very cheapest hours, giving the lowest intensities, and the TES lowers B slightly below A by shifting consumption further towards those hours. The larger EBs in the electrified scenarios must draw power across a

wider range of hours, so their weighted intensities are somewhat higher, with the same storage effect visible in D relative to C. Scenario E sits between the two groups: although its EB must also run in high-demand winter hours of higher grid intensity, its scale combined with storage allows it to place a large share of its much greater consumption in the cheapest, and typically cleanest, hours, including periods of negative prices. This lower weighted intensity does not translate into lower total emissions, because total emissions are the product of intensity and volume, and E's volume is by far the largest (Section 4.4.3). The dependence of these results on grid intensity, that is, how they change as the grid decarbonises, is examined in Section 4.4.5

Table 12. EB weighted CO2 intensity

Scenarios	EB weighted CO2 intensity (kgCO2/MWh)	EB capacity
A: No TES	18.88	39 MW
B: Current (+TES)	18.76	39 MW
C: +Electr.	19.46	100 MW
D: +Electr. +TES	19.32	100 MW
E: Full electr.	19.07	289.5 MW

4.4.5 Emissions under grid decarbonisation

The emissions results above are evaluated at real time intensity, so their dependence on that intensity is tested by scaling the hourly Fingrid profile from zero to three times its current level, with dispatch unchanged in every case, since grid intensity does not enter the optimisation at zero carbon price (Section 3.5.2). Figure 15 shows the result. As the grid decarbonises, the electrified scenarios converge towards zero emissions, C retaining only its 84 tCO2 slack residual, whereas A and B approach the floors set by their gas combustion (6,153 and 3,795 tCO2). The ranking at current intensity is, however, not robust upwards: Scenario E exceeds B once intensity rises above approximately 1.07 times the current level, and above roughly 2.6 times even C and D emit more than B. The emissions benefit of electrification in this biomass-based system is therefore conditional on grid intensity, strengthening as the Finnish grid decarbonises and reversing under a more carbon-intensive grid.

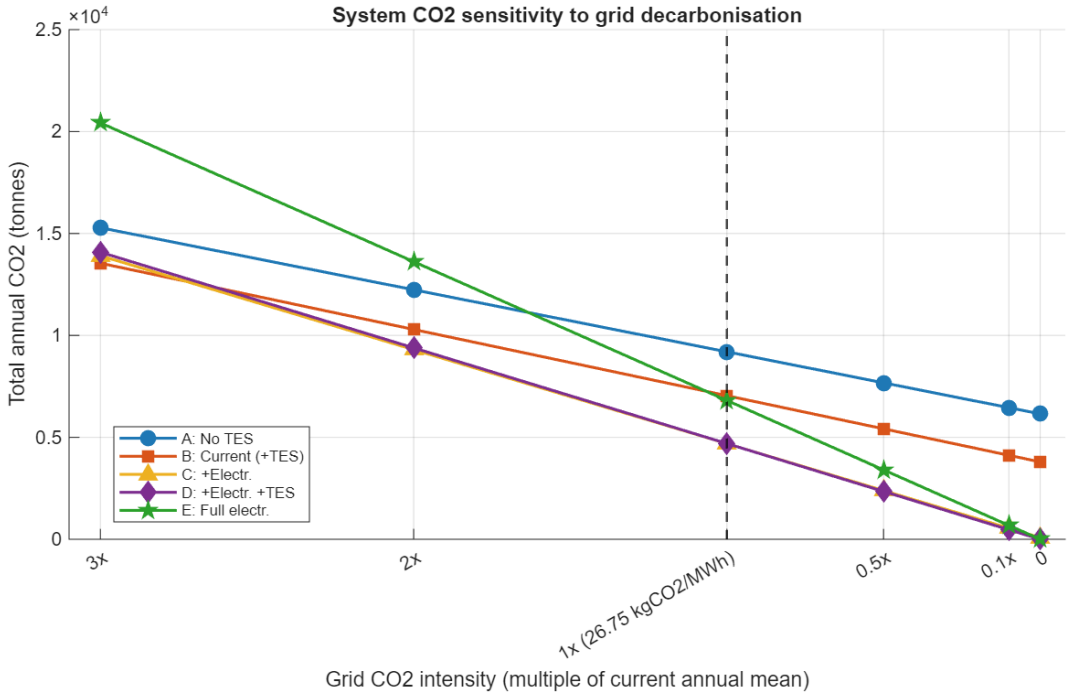

Figure 15. Total annual CO2 emissions as the hourly grid intensity profile is scaled from zero to three times its current level (dashed line: current mean).

4.5 Sensitivity analysis

The robustness of the base-case results is tested through three sensitivity sweeps. Sweep 1 varies electricity price, gas price, and TES capacity; Sweep 2 varies the TES charge and discharge power limits; and Sweep 3 varies the CHP electricity credit (alpha_chp) and the CO2 price. The parameter ranges and the rationale for each are described in Section 3.6 . The following subsections present each sweep in turn.

4.5.1 Sensitivity to electricity and gas prices

Sweep 1 tests the robustness of the operating-cost results to electricity price, gas price, and TES capacity. All comparisons in this subsection are based on operating cost (the LP objective) and therefore differ from the total-cost results in Section 4.3.2 , which include capital. As a result, both D and E appear cheaper than B here on operating cost, whereas only D is cheaper once capital is included.

As electricity price rises, the operating cost of all scenarios increases (Figure 16), with Scenario C rising most steeply because it has the largest grid draw and no storage to shift consumption away from high-price hours. On operating cost, D and E remain below B across most of the tested range; the D-vs-B advantage persists until electricity reaches approximately 218% of base, beyond which B's retained gas becomes competitive again. Scenario C is more expensive than B throughout.

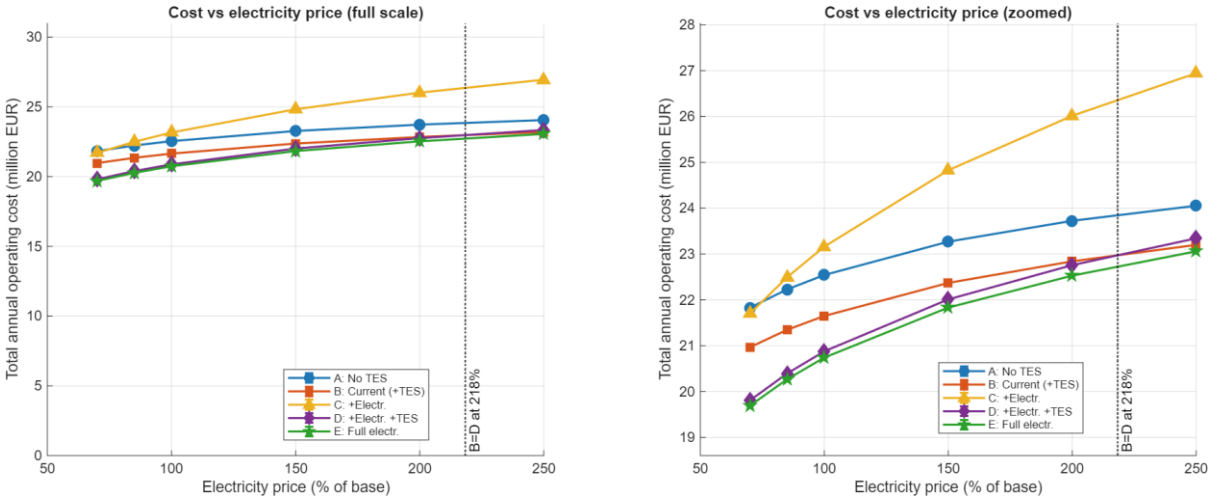

Figure 16. Total annual operating cost vs electricity price for all five scenarios (left: full scale; right: zoomed). Total operating cost B=D when electricity price at 218%.

The response to gas price is the mirror image (Figure 17). Scenarios C, D, and E are unaffected by gas price, as they use no gas, whereas A and B rise as gas becomes more expensive. The operating-cost value of electrification relative to B therefore grows with gas price, and D and E extend their advantage further.

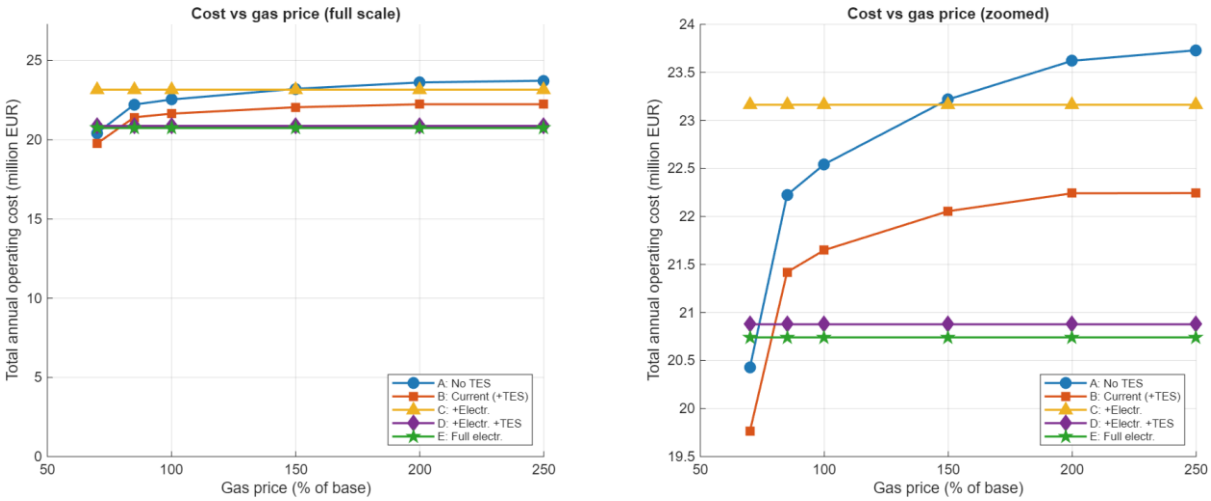

Figure 17. Total annual operating cost vs gas price for all five scenarios (left: full scale; right: zoomed).

The interaction of the two prices is shown in Figure 18. The D-vs-B operating saving is positive across almost the entire grid, turning negative only in the high-electricity, low-gas corner; at the base case it is 772 kEUR. This confirms that D's operating advantage over B is robust to joint price variation across most of the plausible range.

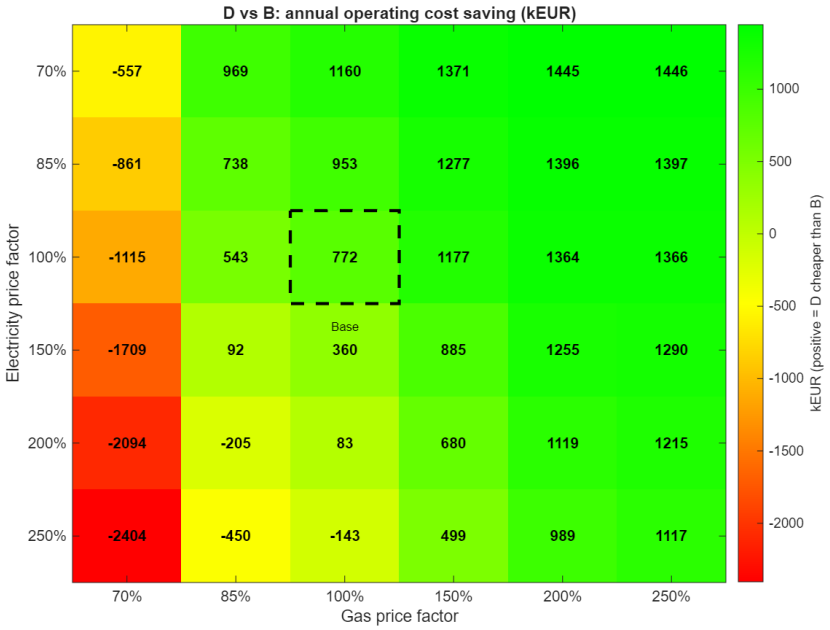

Figure 18. D-vs-B annual operating saving (kEUR) across the electricity and gas price grid; green: D cheaper.

Independent of price, TES capacity scales the operating-cost value of electrification (Figure 19). The D-vs-B saving rises from approximately 520 kEUR at 250 MWh to 770 kEUR at 500 MWh and 925 kEUR at 750 MWh, with E showing a similar but larger effect. A larger storage allows the EB to exploit a greater number of low-price hours.

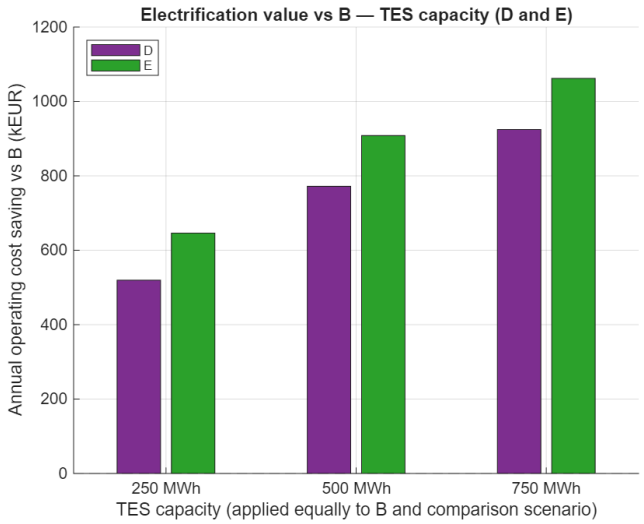

Figure 19. Annual operating cost saving of Scenarios D and E relative to Scenario B (kEUR), as TES capacity varies from 250 to 750 MWh.

Finally, the distribution of operating cost across all Sweep 1 cases confirms the stability of the ranking (Figure 20). Scenarios D and E show the lowest cost distributions and Scenario C the highest and widest, indicating that the operating-cost ordering is robust to price and capacity variation.

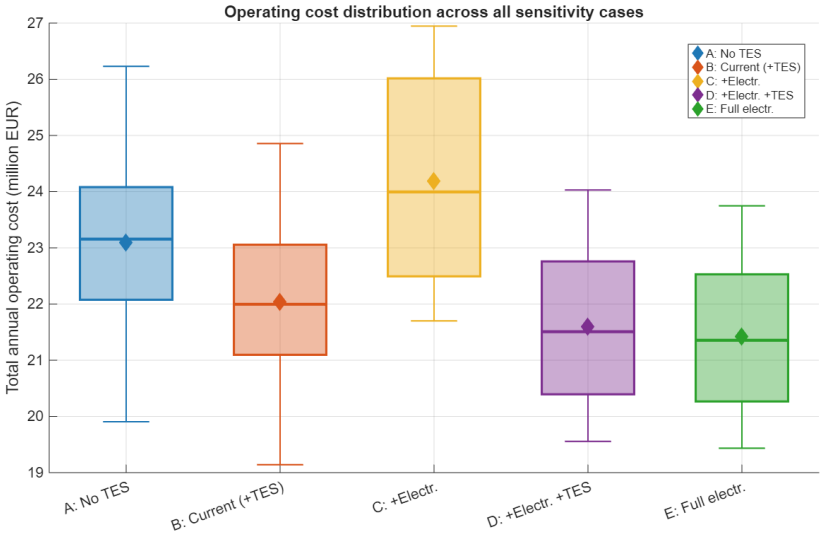

Figure 20. Distribution of annual operating cost across all Sweep 1 cases (box: interquartile range; line: median; diamond: mean; whiskers: full range).

4.5.2 Sensitivity to TES power limits

Sweep 2 varies the TES charge and discharge power limits, holding capacity and prices at base values. As with Sweep 1, the comparisons are on operating cost.

Increasing the power limits reduces operating costs for all three storage-enabled scenarios, but with diminishing returns (Figure 21). For Scenario B, raising both charge and discharge power from approximately 15 to 30 MW yields most of the available saving, after which the cost plateaus. Scenarios D and E follow the same pattern but with a much steeper initial reduction, reflecting the larger EB whose operation TES can buffer.

The effect is strongly asymmetric between charge and discharge power. For both D and E, raising charge power from approximately 18 to 32 MW (an increase of about 14 MW) produces roughly 0.05 MEUR more saving than raising discharge power over a comparable range (14 to 28 MW). Beyond about 30 MW, additional discharge power has little further effect, whereas additional charge power continues to lower cost. Charge power is therefore the binding constraint on the value of TES: the storage's ability to absorb cheap electricity matters more than its ability to release heat quickly.

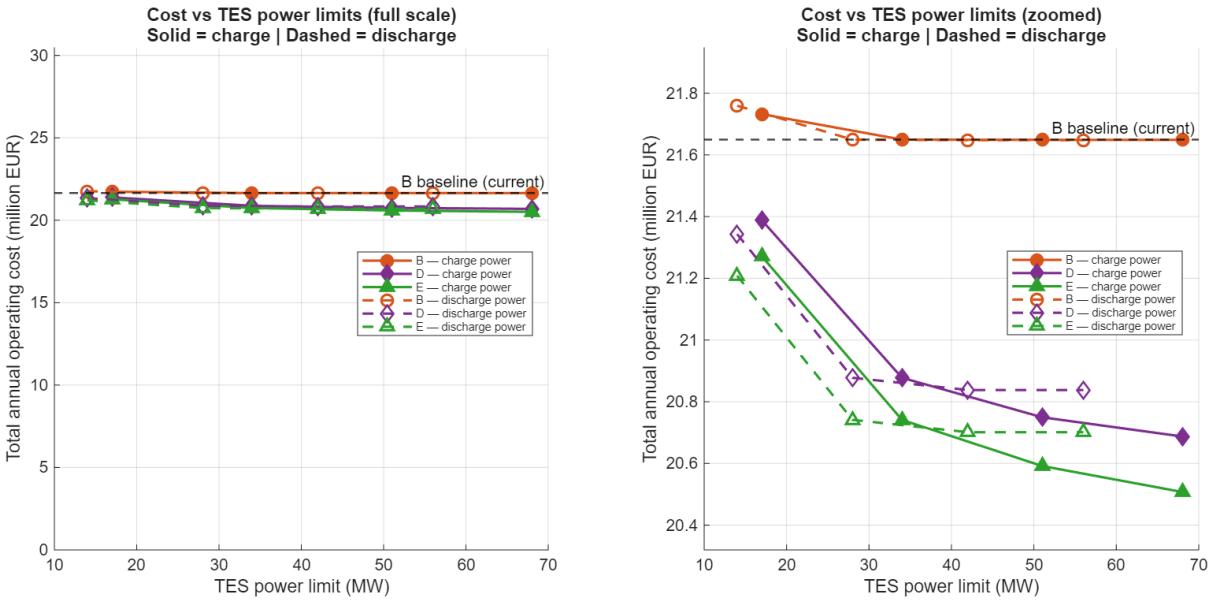

Figure 21. Annual operating cost against TES charge (solid) and discharge (dashed) power limits (left: full scale; right: zoomed).

This asymmetry is confirmed by the joint power sweep (Figure 22). The D-vs-B saving increases sharply along the charge-power axis, crossing from negative (B cheaper) to positive (D cheaper) as charge power rises, while movement along the discharge-power axis has comparatively little effect.

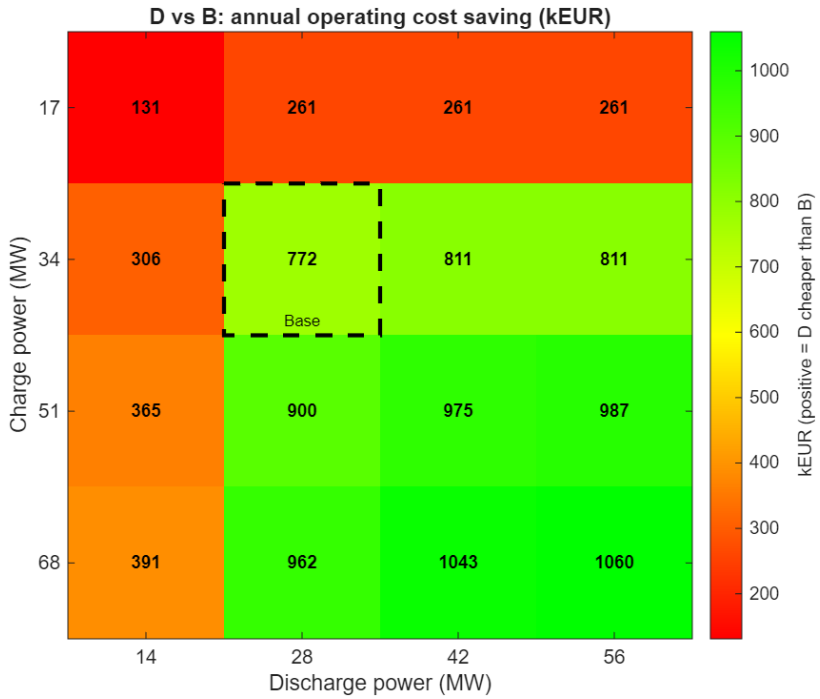

Figure 22. Annual operating cost saving of Scenario D relative to Scenario B (kEUR) across TES charge and discharge power limits.; B fixed at its current rating; base case outlined.

4.5.3 Optimal TES capacity

The sweeps above hold the storage at its existing size or vary it symmetrically across scenarios. This subsection instead asks what storage capacity would be optimal if the storage itself could be resized, with the annualised capital cost of any capacity above the existing 500 MWh charged against the operating saving. Figure 23 shows the resulting net annual saving relative to the baseline B for capacities from 250 to 4,000 MWh, under two assumptions about how the charge and discharge power limits scale with capacity: proportionally (linear) and with the square root of capacity, the latter reflecting that a larger storage's power rating typically grows more slowly than its volume.

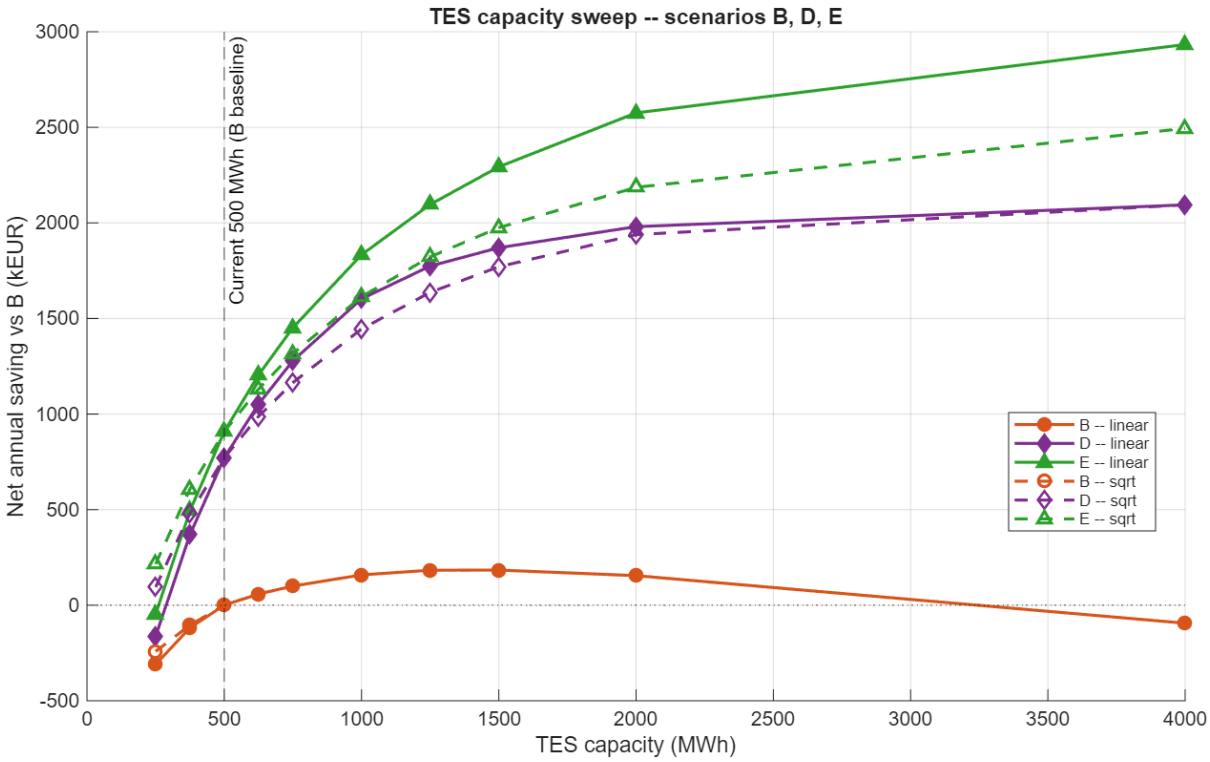

Figure 23. Net annual saving relative to B at the committed 500 MWh as TES capacity varies; capital charged on capacity above 500 MWh; solid: linear power scaling, dashed: square-root scaling.

For the current system (Scenario B), upsizing the storage yields only a modest gain. The net saving reaches a flat optimum of approximately 184 kEUR per year across 1,250 to 1,500 MWh and declines thereafter, turning negative between 2,000 and 4,000 MWh as the capital cost of additional capacity outweighs the diminishing operating benefit. The existing 500 MWh is therefore close to adequately sized for the current system: the potential gain from upsizing is modest relative to the investment involved.

Under electrification the storage is worth substantially more at every size. The D and E curves are measured against B at the committed 500 MWh, so their level combines two effects: the value of electrification itself (the curve's height at 500 MWh, 772 kEUR for D and 910 kEUR for E) and the value of additional storage (the rise beyond that point). Isolating the second effect, upsizing the storage from 500 to 4,000 MWh adds a further 1,323 kEUR per year for Scenario D and 2,025 kEUR for Scenario E under linear power scaling, with clear diminishing returns beyond roughly 1,500 to 2,000 MWh but no interior optimum within the tested range. In contrast to the current system, the net saving remains positive

throughout: the capital cost of a larger tank never overtakes its operating value when a large electric boiler is present to exploit it.

The conclusion is robust to the power-scaling assumption. The square-root variant lowers the saving at large capacities, as the relatively weaker charge and discharge power limits what the storage can exploit, but does not change the shape of the curves or the ordering of the scenarios. At small capacities the effect reverses: at 250 MWh, Scenario D is loss-making under linear scaling (−163 kEUR) but positive under square-root scaling (+95 kEUR), since a small storage with proportionally stronger power limits can cycle more effectively. This is consistent with the finding of Section 4.5.2 that power, particularly charge power, rather than energy capacity is the binding constraint on storage value.

4.5.4 Sensitivity to TES conversion efficiency

The validation in Section 3.7.2 adopted the DEA catalogue round-trip efficiency of 0.98, whereas the round-trip efficiency implied by the raw measured data was 0.937. Because this figure conflates conversion and standing losses, and is reduced by the TES closing the window at a higher SOC than it began, it was not adopted as a point estimate; instead, the sensitivity of the results to the conversion efficiency was tested directly. The round-trip efficiency was varied from the catalogue value of 0.98 down to 0.90, applied symmetrically as a charge and discharge efficiency of sqrt(round-trip) on each side, with the standing loss held at the validated 0.2% per day, so that a single mechanism is varied at a time (Figure 24).

Here, the TES saving is defined as the reduction in annual operating cost (fuel, CO2, and electricity) obtained by adding the TES to the system relative to the same configuration without it, with all other parameters held fixed; capital cost is excluded. Reducing the round-trip efficiency lowers this saving in Scenario B, as expected, since a less efficient unit recovers less useful heat. At the catalogue value of 0.98 the TES saving is 893 kEUR. It falls to 868 kEUR at 0.95 (a reduction of 2.8%) and to 826 kEUR at 0.90 (a reduction of 7.5%). Even at 0.90, which lies below the operational figure of 0.937, the TES remains clearly beneficial. Measured against the total system operating cost of approximately 22.5 MEUR,

the largest change across this range corresponds to a shift in total cost of about 0.3%. The scenario ranking is unchanged throughout, confirming that the headline results are robust to the residual uncertainty in the conversion efficiency between the catalogue value and the operational figure.

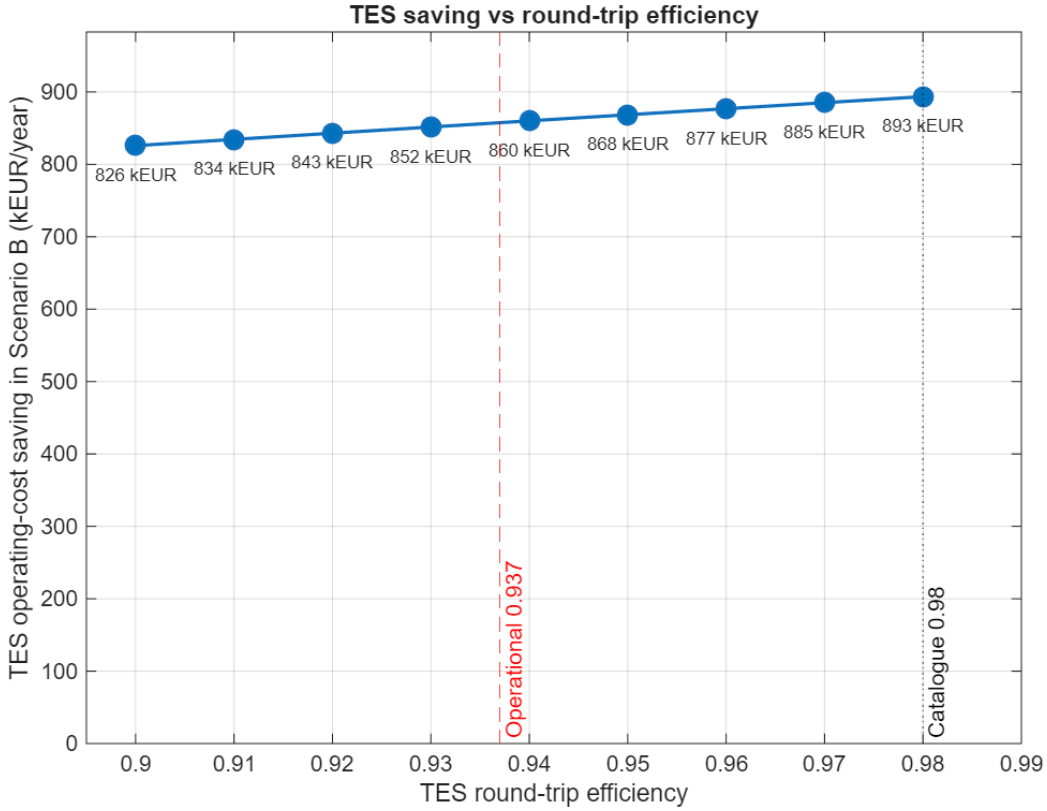

Figure 24. Annual TES operating-cost saving in Scenario B as a function of round-trip efficiency

4.5.5 Sensitivity to CHP electricity credit and carbon price

Sweep 3 tests robustness to the two least-certain assumptions: the CHP electricity credit (alpha_chp) and the CO2 price (c_co2). The base case uses alpha_chp = 0, the value confirmed by Lappeenrannan Energia and justified in Section 3.5.1 , and a CO2 price of zero. As in the previous sweeps, the comparisons are on operating cost; here the operating cost includes the carbon charge where the CO2 price is non-zero.

Figure 25 shows how operating cost varies with CO2 price at the default credit (alpha_chp = 0). Scenarios C, D, and E are flat, as they use no fossil fuel and the CO2 price therefore does not affect their cost, whereas the cost of A and B rises as the CO2 price increases. On

operating cost, D and E remain cheaper than B at every CO2 price, while C never beats B, consistent with the other sweeps.

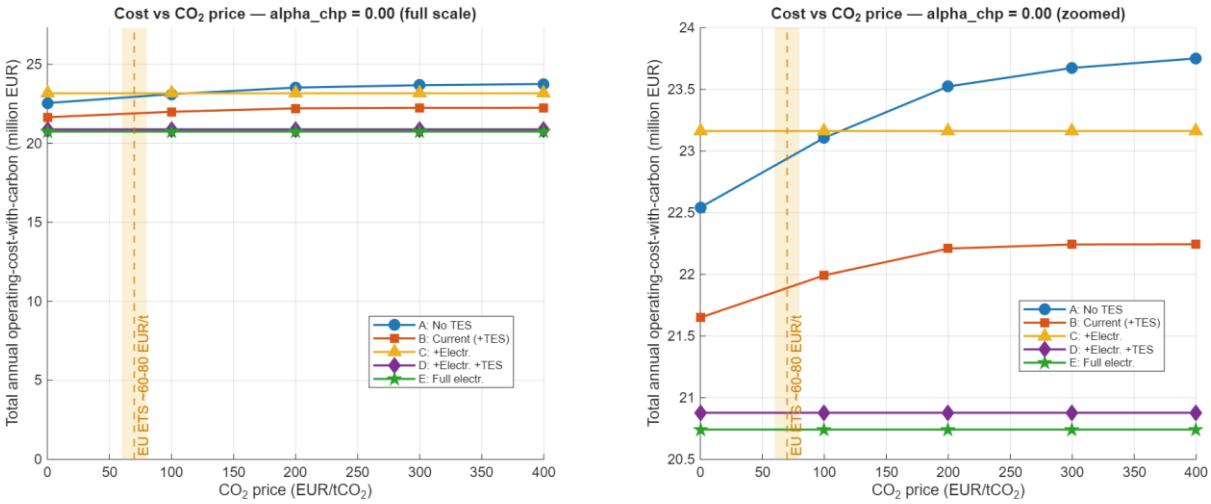

Figure 25. Total annual operating cost (including the carbon charge) versus CO2 price for all five scenarios, at alpha_chp = 0 (left: full scale; right: zoomed); shaded band: current EU ETS range.

Figure 26 shows operating cost against the CHP electricity credit at zero CO2 price. A higher credit lowers the cost of every scenario, since all of them rely on CHP, but it benefits the gas-using baseline B most. The D-vs-B crossover occurs at alpha_chp = 0.865: below this value D is cheaper, and above it B becomes cheaper. Scenarios A and C remain more expensive than B across the entire range.

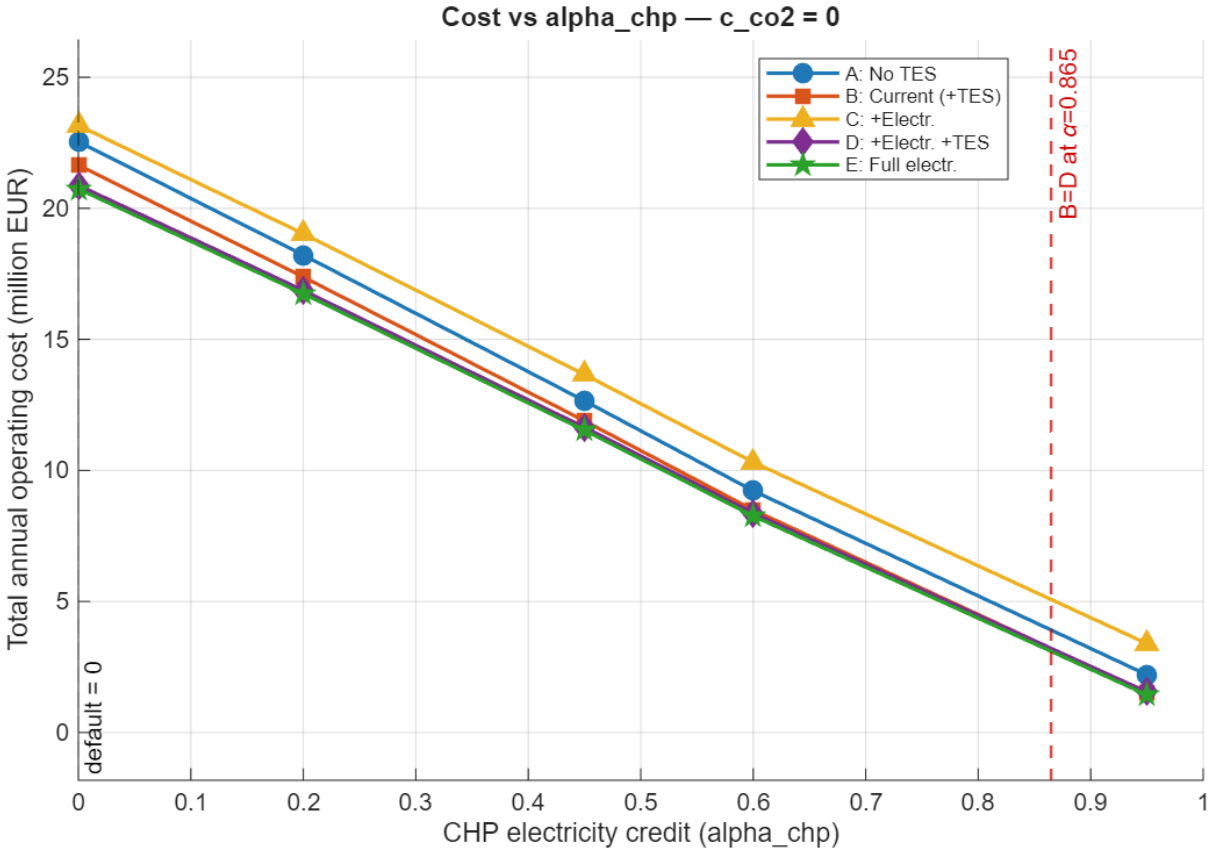

Figure 26. Total annual operating cost versus CHP electricity credit (alpha_chp), at zero CO2 price.

The combined effect of both parameters is shown in Figure 27. For Scenario D, the operating-cost saving over B is positive across almost the entire grid, becoming negative only at the highest credit (alpha_chp = 0.95) combined with zero CO2 price, where B is marginally cheaper (by 38 kEUR). The saving widens as the CO2 price rises, which penalises B's gas use, and narrows as alpha_chp rises, which lowers the cost of B's CHP. Scenario E shows the same pattern with consistently larger savings, while Scenario C is more expensive than B across the whole grid. This confirms that D's operating-cost advantage over B is robust to both assumptions except in the extreme corner of maximum CHP credit and zero carbon price.

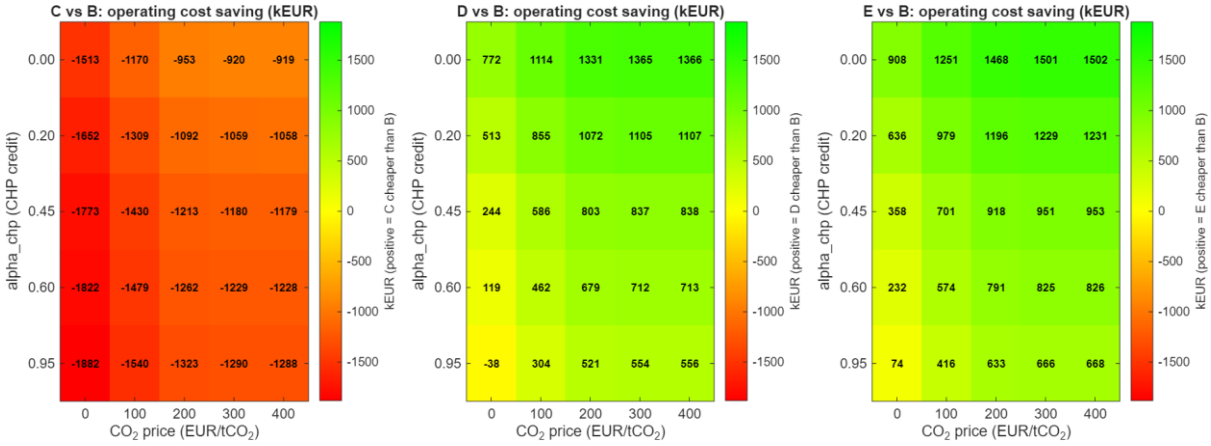

Figure 27. Operating saving of C, D and E relative to B (kEUR) across the alpha_chp (vertical) and CO2 price (horizontal) grid; green: electrified scenario cheaper.

These comparisons are on operating cost; once capital is included, the carbon price required to justify each investment differs markedly, as the following subsection shows.

4.5.6 Carbon price break-even for investment

The comparisons in Section 4.5.5 are on operating cost and therefore exclude the capital cost of new EB capacity. Because the investment decision depends on total cost, this subsection reports the CO2 price at which each electrified scenario's *total* cost (operating cost plus annualised capital and O&M) equals that of Scenario B. This is the carbon price that would be required to justify each investment, given that B builds no new capacity.

The CO2 price is applied only to direct fuel combustion, in practice Scenario B's gas emissions (3,794.8 tCO2), consistent with EU ETS scope; the indirect grid emissions in Table 11 are not charged, as the carbon cost of generation is already embedded in the electricity price.

It is important to distinguish this total-cost break-even from the operating-cost comparison above. On operating cost (Figure 25), D and E are already cheaper than B at zero CO2 price, and C never overtakes B within the tested range. On total cost, the picture differs because the electrified scenarios must also recover their capital cost. The break-even CO2 prices are shown in Table 13.

Table 13. Break-even CO2 price at which each electrified scenario's total cost equals Scenario B's.

Scenario	Break-even CO2 price vs Scenario B (EUR/tCO2)
C: +Electr.	511
D: +Electr. +TES	-86
E: Full electr.	219

A negative break-even for Scenario D means that D is already cheaper than B on total cost at zero carbon price, so no carbon price is required to justify it; this is consistent with D being the only scenario cheaper than B in the cost results of Section 4.3 . Scenario E, although cheaper than B on operating cost, requires a CO2 price of 219 EUR/tCO2 before its operating saving offsets its substantially larger capital cost. Scenario C requires the highest price, 511 EUR/tCO2, as it combines the highest operating cost with the EB investment.

These break-even prices assume Scenario B's dispatch, and hence its gas emissions, remain at base-case levels as the carbon price rises; since B would partially substitute away from gas at high prices, as Figure 25 shows, the true break-even values for C and E are somewhat higher; the figures reported here therefore represent lower bounds. Scenario D's negative break-even is unaffected.

These break-even prices can be read against current and projected carbon prices. The EU ETS price is currently in the range of approximately 60 to 80 EUR/tCO2 (European Commission, 2025), well below the thresholds for C and E, but scenario projections reach approximately 130 to 190 EUR/tCO2 by 2030 to 2040 (IEA, 2023). On this trajectory, Scenario E approaches its break-even within the projection horizon, whereas Scenario C remains uneconomic across the tested range. Scenario D is justified at any carbon price, including zero.

4.6 Summary of results

This chapter compared five configurations of the Lappeenranta district heating system against the current system with storage (Scenario B), examining cost, emissions, dispatch behaviour, and the sensitivity of the results to key parameters.

On cost, the central finding is the distinction between operating and total cost. On operating cost, electrification is favourable, and the fully electrified Scenario E is cheapest to operate. Once annualised capital is included, only Scenario D, electrification combined with the existing storage, is cheaper than B in total, by approximately 0.33 MEUR per year. Scenario C is the most expensive on both measures, and Scenario E's large capital cost offsets its operating advantage.

On emissions, the fuel switch from gas to the EB is the dominant decarbonisation lever, cutting emissions by approximately 33% relative to B in Scenarios C and D. Storage itself does not decarbonise once gas has been removed: it reduces emissions only when it displaces fossil generation, as in the current system. Scenario E, although fossil-free, emits more than C and D because its larger grid draw occurs partly in higher-intensity hours.

The dispatch results show that both the EB and the TES respond strongly to electricity price, concentrating consumption and charging in low-price hours. The sensitivity analysis confirms that these results are robust across plausible electricity and gas prices, that charge power rather than discharge power is the binding constraint on TES value, and that the operating-cost ranking is stable under price variation. On a total-cost basis, Scenario D is justified at any carbon price, Scenario E approaches its break-even within projected carbon price ranges, and Scenario C remains uneconomic across the tested range.

Taken together, the results indicate that under current conditions the combination of electrification with the existing storage (Scenario D) is the only configuration that improves on the current system in both cost and emissions, while the case for full electrification (Scenario E) strengthens as carbon prices rise and the electricity grid decarbonises. This is in line with literature findings that hybrid configurations outperform purely fuel-based or purely electric systems (Taylor, Atkins and Walmsley, 2025).

5 Discussion

The results of this study answer the central research question as follows: electric boilers and thermal energy storage improve the cost-efficiency and emissions of the Lappeenranta district heating system most effectively in combination, and at grid-constrained rather than

full scale. Under current conditions, the fuel switch from gas to electricity is what decarbonises, while storage is what makes that switch affordable; storage itself is an economic instrument, not a decarbonisation measure. The configuration combining both (Scenario D) is the only one that improves on the current system in both cost and emissions today, while full electrification is a conditional future stage whose case strengthens with the carbon price and grid decarbonisation.

This chapter interprets these findings and examines their basis. Sections 5.1 and 5.2 discuss the two technologies in turn: the role and appropriate scale of the electric boiler, and the economic value of TES. Sections 5.3 and 5.4 develop the two central interpretive findings, the separation of the cost and carbon levers, and the counterintuitive emissions behaviour of full electrification in a biomass-based system. Section 5.5 examines the robustness of the conclusions to the key assumptions, Section 5.6 relates the findings to the existing literature, and Section 5.7 draws the practical implications for Lappeenrannan Energia and states the limitations of the study.

5.1 Role and optimal capacity of electric boilers

The role of the electric boiler changes fundamentally across the scenarios. In the current system it is an opportunistic marginal unit: at 39 MW, it absorbs cheap electricity when the spot price falls below the biomass alternative, but it cannot carry significant load. At 100 MW (Scenarios C and D) it becomes the primary flexible unit, replacing the gas boilers, and at 289.5 MW (Scenario E) it is deployed as the largest heat source. The dispatch logic remains constant across all three roles: the EB runs almost exclusively when electricity is cheap, with consumption concentrated below 50 EUR/MWh in every scenario, and its weighted CO2 intensity consequently remains below the grid annual average.

The results indicate that the near-term optimal capacity is the 100 MW level rather than full electrification. This capacity, which corresponds to the grid connection Lappeenrannan Energia can use without significant reinforcement, captures most of the achievable saving: Scenario D undercuts the baseline B on total cost by approximately 0.33 MEUR per year. Scenario E achieves a lower operating cost still, but its annualised capital cost of 1.35 MEUR, together with the required 400 kV grid upgrade, whose investment cost is not

included in this study, more than offsets the additional operating advantage, leaving E approximately 0.83 MEUR per year above B in total.

The value of EB capacity is, however, conditional on storage. Scenario C shows that a large EB without a buffer is exposed to electricity price risk: it must either consume in high-price hours or fall short, and it records 378 MWh of unmet demand in the most extreme price hours while being the most expensive configuration overall. The question of optimal EB capacity therefore cannot be answered independently of storage, which is the subject of the next section.

5.2 Economic value of thermal energy storage

The TES contributes clear economic value in the current system, but its real significance lies in what it enables under electrification. In the current configuration, the TES saves approximately 893 kEUR per year (the A to B comparison), by shifting EB consumption towards cheaper hours and displacing part of the gas boiler output. When the system is electrified, the same TES becomes considerably more valuable: adding it to the electrified system (C to D) reduces operating cost by approximately 2.3 MEUR per year, roughly 2.6 times its value in the current system.

The mechanism is that storage decouples the timing of electricity purchase from the timing of heat delivery. Without it, a large EB must follow demand in real time even when the electricity price is high, which is precisely Scenario C's weakness; with it, consumption concentrates in the cheapest hours and the exposure to price spikes is largely removed, as shown by the elimination of C's unmet demand in Scenario D.

The sizing analysis identifies where additional storage investment would yield the most, and the answer differs clearly between the current and the electrified system. For the current system, the existing 500 MWh tank is close to optimally sized: net of capital, upsizing yields at most around 184 kEUR per year, with the optimum reached at 1,250 to 1,500 MWh and the net value turning negative beyond roughly 3,000 MWh. For the electrified system, by contrast, additional capacity remains net-positive across the entire tested range, up to eight times the existing tank: upsizing from 500 to 4,000 MWh is worth a further 1.3 MEUR per year in Scenario D, although returns diminish clearly beyond 1,500 to 2,000 MWh. The same

asymmetry appears in the power dimension: the saving responds far more strongly to charge power than to discharge power, and beyond roughly 30 MW additional discharge capability adds little, whereas additional charge capability continues to lower cost. The binding constraint on the storage's value is therefore its ability to absorb cheap electricity, rather than its energy capacity or its ability to release heat quickly.

Two qualifications apply to this value. First, the contribution of the TES is economic rather than environmental: the store is dispatched on price, not on emissions, so adding it to the electrified system slightly increases emissions (by 1.8 tCO2). Second, because the TES is already operational and its capital cost is sunk, the practical question for the operator is not whether storage is worthwhile, but how it should be developed as electrification proceeds. The results give a two-part answer: under the current system, no further development is warranted, since the existing size is close to optimal; under electrification, both a larger store and, in particular, greater charge power become clearly justified. Storage investment should therefore be sequenced with the electrification decision, not ahead of it.

5.3 Decoupling decarbonisation from economics

A central finding of this study is that the decarbonisation and cost benefits of the investigated measures come from different levers, which are usually conflated. The fuel switch from gas to the EB is the carbon lever: moving from B to D cuts emissions by 33.4%, and Scenario C, which makes the same fuel switch without storage, achieves essentially the same cut. Storage is the cost lever: adding it to the electrified system reduces operating cost by approximately 9.8% while emissions remain almost unchanged. Neither lever can substitute for the other. Storage decarbonises only where fossil fuel remains to be displaced, as the A to B comparison shows, where a 23.4% reduction is achieved through gas displacement; once the gas is gone, further storage does nothing for emissions. Conversely, the fuel switch without storage delivers the emissions cut, but at the highest cost of any configuration (A to C).

Scenario D improves on the current system precisely because it combines the two levers: the fuel switch delivers the emissions reduction, and the storage makes that reduction affordable by protecting the EB from price risk. The practical implication is that investment appraisal in district heating should assign each technology to its correct objective. Thermal storage

should be justified on its economic merits, not presented as a decarbonisation measure; an electrification investment should be justified on its emissions merits, with storage as the enabling complement that improves its economics.

5.4 The emissions trade-off of electrification in a biomass-CHP system

The most counterintuitive result of this study is that the fully fossil-free Scenario E emits more CO2 than the partially electrified Scenarios C and D, and lies only 3.3% below the gas-using baseline B. The mechanism follows directly from what electrification displaces in this system. In Scenarios C and D, the EB replaces the gas boilers, substituting grid electricity for fossil combustion, and emissions fall by roughly a third. In Scenario E, the further enlarged boiler additionally displaces output from the biomass CHP, which is counted as carbon-neutral under EU and Finnish accounting. Every MWh shifted from the CHP to the grid therefore replaces zero accounted emissions with the real hourly intensity of the electricity mix. The effect is volume rather than intensity: Scenario E's weighted CO2 intensity (19.07 kgCO2/MWh) is in fact slightly lower than that of C and D, since the larger boiler combined with storage can concentrate consumption in the cheapest and typically cleanest hours, but the far greater quantity of electricity drawn outweighs this advantage. Electrification beyond the fossil share of the system therefore adds emissions rather than removing them.

This outcome is not a modelling artefact but a property of cost-optimal operation in this system. The dispatch is optimal under the operator's own cost accounting, in which CHP electricity revenue is excluded from heat production cost (alpha_chp = 0). This convention makes CHP heat comparatively expensive, so the optimiser shifts load to the EB whenever electricity is cheap, and the emissions consequence follows from the accounting asymmetry: the displaced biomass is counted as zero-carbon while the grid electricity carries real emissions. Cost optimisation alone can therefore move the system away from its lowest-emission configuration, driven by the combination of a revenue convention and a carbon-accounting convention.

The finding is conditional on two assumptions, both examined in this thesis. The first is the biomass carbon-neutrality convention: under a lifecycle accounting that assigned supply-chain emissions to forest chips, typically 40 to 110 kgCO2 per MWh (Repo, Tuomi and

Liski, 2011), the CHP would no longer be zero-carbon and displacing it would look correspondingly better, so the convention used here is conservative against electrification. The second is the current Finnish grid intensity: as the grid decarbonises, the penalty for drawing electricity in any hour shrinks and Scenario E's position improves, as the grid decarbonisation sensitivity in Section 4.4.5 confirms.

The key point is that the emissions case for electrification depends on what is being displaced, not only on what is being installed. In a fossil-heavy system, electrification decarbonises almost by definition; in a biomass-incumbent system such as Lappeenranta, it must be targeted at the remaining fossil share to deliver its expected benefit.

5.5 Sensitivity to carbon price and key assumptions

The sensitivity analysis establishes which conclusions are robust and which are conditional. The central result, that Scenario D improves on the baseline, is robust across every dimension tested: it holds over most of the electricity and gas price grid, across the CHP electricity credit up to approximately 0.865 (far above the confirmed value of zero), and at any carbon price, since D's total-cost break-even of −86 EUR/tCO2 means it is already cheaper than B with no carbon pricing at all. The conclusion for Scenario E is explicitly conditional: its break-even of 219 EUR/tCO2 lies well above the current EU ETS range of roughly 60 to 80 EUR/tCO2 (European Commission, 2025), but within the range projected for 2030 to 2040, making full electrification a plausible second stage rather than a present-day option. Scenario C is not justified within the tested range, with a break-even of 511 EUR/tCO2. This also verifies that electrification without TES cannot be justified.

Two of the conventions adopted in this study act on the results in opposite directions, and their effects should be separated. The carbon-neutral treatment of biomass favours the incumbent system: the CHP is assigned zero emissions. A lifecycle accounting of forest chip supply chains would raise the emissions of the biomass-dependent scenarios most and improve the relative position of the electrified ones. The emissions findings are therefore conservative against electrification. The zero CHP electricity credit works the other way. At alpha_chp = 0, the CHP carries its full fuel cost, which makes the EB comparatively attractive and weighs most heavily on Scenario B, whose dispatch retains the largest CHP output. Part of D's base-case cost advantage over B is therefore a product of this convention,

whose justification is empirical rather than theoretical: it is the accounting practice confirmed by Lappeenrannan Energia.

The sensitivity analysis bounds this dependence. On operating cost, D remains cheaper than B for any credit below alpha_chp = 0.865. Across the joint sweep of CHP credit and carbon price, D loses to B only in one extreme corner, where the highest tested credit (alpha_chp = 0.95) coincides with a zero carbon price. Scenario E shows the same pattern with larger margins, and Scenario C never beats B under any tested combination. The one genuine price fragility is the combination of sustained high electricity prices with low gas prices, the single corner of the price grid in which B regains its advantage over D; at unchanged gas prices this requires electricity prices of roughly 218% of the base level. The conclusion that electrification with storage improves on the current system therefore rests on two things: the operator's confirmed cost accounting, and broadly current price relationships between electricity and gas. Both are shown by the sensitivity results to be mild assumptions.

5.6 Comparison with existing literature

The results of this thesis largely align with the literature reviewed in Chapter 2, while diverging from it at one significant point. The alignment spotlights the operating logic. The price-threshold-driven dispatch is described by Trømborg et al. (2017) and Kirkerud, Trømborg and Bolkesjø (2016), and the dispatch results of this study directly reproduce it: EB output concentrates in the lowest price bands and approaches zero above approximately 50 EUR/MWh in every scenario. The value of TES in CHP-based systems, demonstrated by Nuytten et al. (2013) and Guelpa and Verda (2019), shares the same pattern here in quantified form: storage reduces cost by 3.9% in the current system and by 9.8% in the electrified one, with the value of storage scaling by a factor of approximately 2.6 under electrification. This also corresponds to the finding of Taylor, Atkins and Walmsley (2025) that hybrid fuel-plus-electric configurations outperform pure configurations, as the hybrid Scenario D is the only configuration cheaper than the current system. The literature's consistent pairing of the EB with storage is matched by the numbers here. Electrification without storage (Scenario C) is the most expensive configuration examined, requiring a carbon price of 511 EUR/tCO2 to break even. The viability of electrified district heating

under Finnish conditions reported by Javanshir, Syri and Hiltunen (2024) is likewise confirmed at the total-cost level, since Scenario D is justified without any carbon price.

However, the divergence concerns emissions. The electrification studies reviewed in Chapter 2 evaluate power-to-heat against fossil-fuelled incumbents (Bloess, Schill and Zerrahn, 2018; Javanshir et al., 2022), showing that replacing combustion with electricity reduces emissions almost by default. In the system examined here, by contrast, the key difference is that the incumbent heat source is biomass CHP, which is accounted as carbon-neutral under EU and Finnish accounting conventions, and the emissions calculation inverts.

The emissions reduction achieved by Scenarios C and D arises entirely from removing the residual gas of the current system. Electrification beyond that point increases emissions, as the fully electrified Scenario E emits more than Scenario D and only 3.3% less than the current system (Scenario B). This is mainly because grid electricity carrying real hourly emissions displaces heat that is accounted as zero-carbon. The conclusions of the fossil-baseline literature are therefore scope-dependent rather than general.

This thesis identifies this boundary condition: electrification decarbonises where it displaces fossil fuel, and when the displaced source is not fossil, the result differs according to how emissions are accounted. Two further key points follow. First, storage is frequently bundled with decarbonisation benefits in the literature, but it is shown here to be emissions-neutral once the fossil fuel is gone, cutting 2,152 tCO2 in the current system but changing emissions by less than 2 tCO2 in the electrified one. This separates the effect of the fuel switch, the carbon lever, from that of the storage, the cost lever. Second, whereas the reviewed investment literature focuses mainly on justifying EB investment through reserve-market revenues (Böttger et al., 2015; Javanshir and Syri, 2023), the investment in Scenario D pays for itself on spot-market operation alone, making reserve revenue an addition rather than a decisive factor. Similarly, against the capacity-sizing literature (Liu et al., 2016; Li et al., 2022), the results show that larger capacity is not ultimately better once capital is counted, as the grid-constrained 100 MW configuration outperforms the full-scale build, whose operating advantage is consumed by its capital cost.

5.7 Practical implications for Lappeenrannan Energia and study limitations

For Lappeenrannan Energia, the results indicate a practical near-term pathway. The expansion of the electric boiler to the 100 MW grid connection limit, operated together with the existing thermal energy storage, improves on the current system in both cost (by 0.33 MEUR per year in total) and emissions (by 33.4%), and this holds under current market conditions without any carbon price support. If the storage is upgraded, the results indicate that charge power is where additional investment yields the most. Full electrification should be treated as a staged future option rather than a present decision: it becomes cost-competitive at a carbon price of 219 EUR/tCO2, and its emissions position improves as the grid decarbonises, but it additionally requires the 400 kV connection upgrade. Throughout, the removal of gas remains the emissions priority; storage and boiler sizing are economic instruments.

These conclusions are subject to several limitations. The model has perfect foresight of prices over the full year, so the reported storage savings are an upper bound on what realisable forecasting could achieve; the sub-daily cycling of the storage limits this effect, however, and all scenarios share the bias equally. The linear formulation omits start-up costs and commitment dynamics. The validation nevertheless shows that the model reproduces observed operation closely, including the shoulder seasons, where these omitted dynamics would be expected to matter most. The analysis rests on a single price year, March 2025 to March 2026, and the price relationships of that year shape the results, as the sensitivity analysis makes explicit. The existing storage capital is treated as sunk. This is correct for the marginal decision studied here, but it means the reported TES savings do not generalise to a brand-new TES investment. Biomass is treated as carbon-neutral by convention, which is conservative against electrification. So is the exclusion of electricity reserve markets: both the EB and the TES could participate in them, and including these revenues would add value to precisely the assets this study finds most valuable. Finally, the operational data underlying the model are confidential, which limits the direct reproducibility of the inputs, although the methods and all derived results are fully reported.

6 Conclusion

6.1 Answers to the research questions

This thesis asked how electric boilers and thermal energy storage can be integrated into the Lappeenranta biomass-CHP district heating system to improve its cost-efficiency and reduce emissions, and under what conditions each configuration becomes justified. The answer is that the two technologies are most effective in combination and at grid-constrained scale: expanding the electric boiler to 100 MW and operating it with the existing storage (Scenario D) improves on the current system in both total cost and emissions under present market conditions, without requiring any carbon price support. The conditions for the other configurations are explicit: electrification without storage (Scenario C) is not justified within any tested carbon price range, and full electrification (Scenario E) becomes justified only as the carbon price approaches roughly 220 EUR/tCO2, making it a future stage rather than a present option.

The first sub-question asked what role the electric boiler can play and how its capacity affects dispatch, cost, and emissions. The boiler's role expands with its capacity: at the existing 39 MW it is an opportunistic marginal unit absorbing cheap electricity; at 100 MW it becomes the system's primary flexible unit, replacing the gas boilers; and at 289.5 MW it carries the full heat load outside the CHP. Its dispatch remains price-driven in every configuration, concentrated in low-price hours with a CO2 intensity below the grid average. Larger capacity lowers operating cost consistently but raises emissions once electrification extends beyond the fossil share of the system, and the capital cost of the largest boiler outweighs its operating advantage.

The second sub-question asked the economic value of storage, the appropriate size, and how the value changes under electrification. The existing TES saves around 893 kEUR per year in the current system. Its value grows to roughly 2.6 times that when the system is electrified, because storage then protects a much larger price-exposed boiler from high-price hours. The existing 500 MWh capacity is appropriate: value continues to grow with size but with diminishing returns, and the binding constraint is charge power rather than capacity or

discharge power. Storage value is economic rather than environmental, and it is greatest precisely where electrification makes the system most price-exposed.

The third sub-question asked how the electrified configurations compare with the baseline. On operating cost, both electrified-with-storage configurations undercut the baseline, with full electrification cheapest to run; on total cost, only Scenario D remains cheaper, by 0.33 MEUR per year, while Scenarios C and E are more expensive once capital is included. On emissions, all electrified configurations emit less than the baseline, but the ordering is not linear with the degree of electrification: the partially electrified configurations cut emissions by around a third, whereas the fully electrified system, despite being fossil-free, sits only 3.3% below the baseline because it displaces carbon-neutral biomass with grid electricity.

The fourth sub-question asked at what carbon price each configuration becomes cost-competitive with the baseline. Scenario D requires none: its break-even of −86 EUR/tCO2 means it is already cheaper at a zero carbon price. Scenario E breaks even at 219 EUR/tCO2, above the current EU ETS range but within levels projected for the 2030s. Scenario C breaks even only at 511 EUR/tCO2, well beyond any projected range, confirming that electrification without storage is not an economically viable path for this system.

6.2 Practical recommendations

Five recommendations follow for Lappeenrannan Energia. First, proceed with the expansion of electric boiler capacity to the 100 MW grid connection limit, operated together with the existing thermal energy storage, as this configuration improves on the current system in both cost and emissions under present conditions. Second, if the storage is upgraded, invest in charge power before discharge power or additional capacity, as this is where the analysis locates the binding constraint on storage value. Third, treat full electrification as a staged option rather than a present decision, to be revisited when the carbon price approaches 220 EUR/tCO2 or when the 400 kV grid upgrade is undertaken for other reasons. Fourth, in internal investment appraisal, assess storage on economic grounds and fuel-switching on emissions grounds, as the two measures serve different objectives and neither substitutes for the other. Fifth, monitor the relationship between electricity and gas prices, since a sustained combination of high electricity and low gas prices is the one market condition identified in which the current system regains its cost advantage.

6.3 Future research

Several directions follow naturally from this work. The most immediate is a rolling-horizon formulation with a 24 to 48 hour look-ahead, which would quantify the storage value realisable under day-ahead information and convert this study's upper bound into an operational estimate. The attempt made here did not integrate with the optimisation structure in the available time, but the framework is otherwise in place. Reserve and balancing markets are a second direction. Participation of the EB and the storage in these markets, excluded from the present scope, is likely to add revenue to the assets found attractive here and deserves quantification. The single price year is a third. Testing the results against multi-year price data would be particularly valuable for the electricity-to-gas price relationship identified as the one genuine fragility. Heat pumps, de-scoped from this study, warrant comparison as an alternative or complement to EBs, since their higher efficiency trades against higher capital cost in ways this framework could readily evaluate. On the emissions side, a lifecycle treatment of biomass supply-chain emissions would test the sensitivity of the biomass-inversion finding to the carbon-neutrality convention. Two extensions would carry the framework furthest. The joint optimisation of storage sizing and boiler capacity, including the brand-new storage case this study's marginal framing deliberately excludes, would generalise the investment question; and the effect of projected grid decarbonisation trajectories on the full-electrification case would extend the decision framework from the present system to its longer-term development.

References

Bastos, J., Monforti-Ferrario, F. and Melica, G. (2026) “GHG Emission Factors for Electricity Consumption.” European Commission, Joint Research Centre. Available at: https://doi.org/10.2905/JRC.4800KC0.

Beiron, J., Normann, F. and Johnsson, F. (2023) “Carbon capture from combined heat and power plants – Impact on the supply and cost of electricity and district heating in cities,” *International Journal of Greenhouse Gas Control*, 129, p. 103973. Available at: https://doi.org/10.1016/j.ijggc.2023.103973.

Bird, L. *et al.* (2016) “Wind and solar energy curtailment: A review of international experience,” *Renewable and Sustainable Energy Reviews*, 65, pp. 577–586. Available at: https://doi.org/10.1016/j.rser.2016.06.082.

Blarke, M.B. (2012) “Towards an intermittency-friendly energy system: Comparing electric boilers and heat pumps in distributed cogeneration,” *Applied Energy*, 91(1), pp. 349–365. Available at: https://doi.org/10.1016/j.apenergy.2011.09.038.

Bloess, A., Schill, W.-P. and Zerrahn, A. (2018) “Power-to-heat for renewable energy integration: A review of technologies, modeling approaches, and flexibility potentials,” *Applied Energy*, 212, pp. 1611–1626. Available at: https://doi.org/10.1016/j.apenergy.2017.12.073.

Boldrini, A. *et al.* (2022) “The role of district heating systems to provide balancing services in the European Union,” *Renewable and Sustainable Energy Reviews*, 154, p. 111853. Available at: https://doi.org/10.1016/j.rser.2021.111853.

Borsche, T., Oldewurtel, F. and Andersson, G. (2014) “Scenario-based MPC for Energy Schedule Compliance with Demand Response,” *IFAC Proceedings Volumes*, 47(3), pp. 10299–10304. Available at: https://doi.org/10.3182/20140824-6-ZA-1003.01284.

Böttger, D. *et al.* (2015) “Control power provision with power-to-heat plants in systems with high shares of renewable energy sources – An illustrative analysis for Germany based on the use of electric boilers in district heating grids,” *Energy*, 82, pp. 157–167. Available at: https://doi.org/10.1016/j.energy.2015.01.022.

Chaudry, M. *et al.* (2023) “Simulating flexibility, variability and decentralisation with an integrated energy system model for Great Britain,” *Scientific Reports*, 13(1), p. 4772. Available at: https://doi.org/10.1038/s41598-023-31257-9.

Cheng, X. *et al.* (2021) “Coordinated wind power dispatch model for an integrated heat and power system by a novel scenario-dependent algorithm,” *2021 Power System and Green Energy Conference (PSGEC)*. *2021 Power System and Green Energy Conference (PSGEC)*, Shanghai, China: IEEE, pp. 765–774. Available at: https://doi.org/10.1109/PSGEC51302.2021.9542402.

Cramton, P. (2017) “Electricity market design,” *Oxford Review of Economic Policy*, 33, pp. 589–612. Available at: https://doi.org/10.1093/oxrep/grx041.

Dahl, M., Brun, A. and Andresen, G.B. (2019) “Cost sensitivity of optimal sector-coupled district heating production systems,” *Energy*, 166, pp. 624–636. Available at: https://doi.org/10.1016/j.energy.2018.10.044.

Dancker, J. *et al.* (2019) “Optimal design and operation of a CHP based district heating system including a heat storage and electrode boiler to increase self-consumption,” *2019 IEEE PES Innovative Smart Grid Technologies Conference - Latin America (ISGT Latin America)*. *2019 IEEE PES Innovative Smart Grid Technologies Conference - Latin America (ISGT Latin America)*, Gramado, Brazil: IEEE, pp. 1–6. Available at: https://doi.org/10.1109/ISGT-LA.2019.8895427.

Danish Energy Agency (2024) *Technology Data for Energy Storage | Energistyrelsen*. Available at: https://ens.dk/en/analyses-and-statistics/technology-data-energy-storage (Accessed: July 18, 2026).

Danish Energy Agency (2026a) “Data sheet for Electricity and district heat production.” Available at: https://ens.dk/en/analyses-and-statistics/technology-data-generation-electricity-and-district-heating (Accessed: June 15, 2026).

Danish Energy Agency (2026b) *Technology Data Catalogue for Electricity and District Heating Production*. Available at: https://ens.dk/en/analyses-and-statistics/technology-data-generation-electricity-and-district-heating (Accessed: May 1, 2026).

European Commission (2022) *REPowerEU Plan*. Available at: https://eur-lex.europa.eu/legal-content/EN/TXT/?uri=COM%3A2022%3A230%3AFIN (Accessed: July 17, 2026).

European Commission (2025) *Trends in carbon intensity and the macroeconomic role of the EU Emissions Trading System - Economy and Finance*. Available at: https://economy-finance.ec.europa.eu/trends-carbon-intensity-and-macroeconomic-role-eu-emissions-trading-system_en (Accessed: July 18, 2026).

European Commission (2026) *European Climate Law - Climate Action*. Available at: https://climate.ec.europa.eu/eu-action/european-climate-law_en (Accessed: July 13, 2026).

European Union (2018) *Commission Implementing Regulation (EU) 2018/2066 of 19 December 2018 on the monitoring and reporting of greenhouse gas emissions pursuant to Directive 2003/87/EC of the European Parliament and of the Council and amending Commission Regulation (EU) No 601/2012*, *OJ L*. Available at: http://data.europa.eu/eli/reg_impl/2018/2066/oj (Accessed: July 18, 2026).

Fingrid (2025) *Power system reserves*. Available at: https://www.fingrid.fi/en/electricity-market/reserves/power-system-reserves/ (Accessed: July 15, 2026).

Fingrid (2026) “Emission factor for electricity consumed in Finland.” Available at: https://data.fingrid.fi/en/data?datasets=396 (Accessed: May 28, 2026).

Finnish Energy (2026) *District heating statistics*. Available at: https://energia.fi/en/statistics/district-heating-statistics/ (Accessed: July 13, 2026).

Finnish Meteorological Institute (2026) “Air Temperature observations.” Available at: https://en.ilmatieteenlaitos.fi/download-observations (Accessed: May 28, 2026).

Finnish Ministry of the Environment (2022) *Finnish Climate Act*. Available at: https://ym.fi/en/-/climate-change-legislation (Accessed: July 4, 2026).

Frederiksen, S. and Werner, S. (2013) *District Heating and Cooling*. Studentlitteratur.

Gao, S. *et al.* (2023) “Benefits of integrating power-to-heat assets in CHPs,” *Applied Energy*, 335, p. 120763. Available at: https://doi.org/10.1016/j.apenergy.2023.120763.

Gonzalez-Salazar, M. *et al.* (2023) “Portfolio optimization in district heating: Merit order or mixed integer linear programming?,” *Energy*, 265, p. 126277. Available at: https://doi.org/10.1016/j.energy.2022.126277.

Guelpa, E. and Verda, V. (2019) “Thermal energy storage in district heating and cooling systems: A review,” *Applied Energy*, 252, p. 113474. Available at: https://doi.org/10.1016/j.apenergy.2019.113474.

Henchoz, S. *et al.* (2016) “Key energy and technological aspects of three innovative concepts of district energy networks,” *Energy*, 117, pp. 465–477. Available at: https://doi.org/10.1016/j.energy.2016.05.065.

Hiltunen, P., Lindroos, T.J. and Rämä, M. (2025) “The impact of electric boilers and heat storages in the Nordic power markets and district heating systems,” *Cleaner Engineering and Technology*, 27, p. 101028. Available at: https://doi.org/10.1016/j.clet.2025.101028.

Ibrahim, H., Ilinca, A. and Perron, J. (2008) “Energy storage systems—Characteristics and comparisons,” *Renewable and Sustainable Energy Reviews*, 12(5), pp. 1221–1250. Available at: https://doi.org/10.1016/j.rser.2007.01.023.

IEA (2023) *World Energy Outlook 2023*. Paris: International Energy Agency. Available at: https://www.iea.org/reports/world-energy-outlook-2023 (Accessed: July 18, 2026).

Impram, S., Varbak Nese, S. and Oral, B. (2020) “Challenges of renewable energy penetration on power system flexibility: A survey,” *Energy Strategy Reviews*, 31, p. 100539. Available at: https://doi.org/10.1016/j.esr.2020.100539.

Ivanova, P., Sauhats, A. and Linkevics, O. (2017) “Cost — Benefit analysis of electric boiler at combined heat and power plants,” *2017 IEEE 58th International Scientific Conference on Power and Electrical Engineering of Riga Technical University (RTUCON)*. *2017 IEEE 58th International Scientific Conference on Power and Electrical Engineering of Riga Technical University (RTUCON)*, pp. 1–6. Available at: https://doi.org/10.1109/RTUCON.2017.8124747.

Javanshir, N. *et al.* (2022) “Abandoning peat in a city district heat system with wind power, heat pumps, and heat storage,” *Energy Reports*, 8, pp. 3051–3062. Available at: https://doi.org/10.1016/j.egyr.2022.02.064.

Javanshir, N. *et al.* (2023) “Operation of district heat network in electricity and balancing markets with the power-to-heat sector coupling,” *Energy*, 266, p. 126423. Available at: https://doi.org/10.1016/j.energy.2022.126423.

Javanshir, N. and Syri, S. (2023) “Techno-Economic Analysis of a Highly Renewable and Electrified District Heating Network Operating in the Balancing Markets,” *Energies*, 16(24), p. 8117. Available at: https://doi.org/10.3390/en16248117.

Javanshir, N., Syri, S. and Hiltunen, P. (2024) “The risks of electrified district heating in Finland’s cold climate,” *Renewable and Sustainable Energy Reviews*, 202, p. 114652. Available at: https://doi.org/10.1016/j.rser.2024.114652.

Ketterer, J.C. (2014) “The impact of wind power generation on the electricity price in Germany,” *Energy Economics*, 44, pp. 270–280. Available at: https://doi.org/10.1016/j.eneco.2014.04.003.

Kirkerud, J.G., Trømborg, E. and Bolkesjø, T.F. (2016) “Impacts of electricity grid tariffs on flexible use of electricity to heat generation,” *Energy*, 115, pp. 1679–1687. Available at: https://doi.org/10.1016/j.energy.2016.06.147.

Knorr, L., Schlosser, F. and Meschede, H. (2023) “Assessment of Energy Efficiency and Flexibility Measures in Electrified Process Heat Generation Based on Simulations in the Animal Feed Industry,” *Journal of Sustainable Development of Energy, Water and Environment Systems*, 11(3), pp. 1–16. Available at: https://doi.org/10.13044/j.sdewes.d11.0444.

Lappeenrannan Energia (2025) *New district heating battery put into operation – the city was heated solely with stored thermal energy | Lappeenrantan Energia*. Available at: https://www.lappeenrannanenergia.fi/ajankohtaista/uusi-kaukolampoakku-kayttoon-kaupunkia-lammitettiin-pelkastaan-varastoidulla (Accessed: June 3, 2026).

Li, L. *et al.* (2022) “Analysis on optimal capacity and parameter configuration of electrode type boiler for improving wind power consumption capacity,” *2022 IEEE 4th International Conference on Power, Intelligent Computing and Systems (ICPICS)*. *2022 IEEE 4th International Conference on Power, Intelligent Computing and Systems (ICPICS)*, pp. 768–772. Available at: https://doi.org/10.1109/ICPICS55264.2022.9873682.

Liu, B. *et al.* (2020) “Economic Dispatch of Combined Heat and Power Energy Systems Using Electric Boiler to Accommodate Wind Power,” *IEEE Access*, 8, pp. 41288–41297. Available at: https://doi.org/10.1109/ACCESS.2020.2968583.

Liu, D. *et al.* (2016) “Optimum Electric Boiler Capacity Configuration in a Regional Power Grid for a Wind Power Accommodation Scenario,” *Energies*, 9(3), p. 144. Available at: https://doi.org/10.3390/en9030144.

Lu, J. *et al.* (2023) “A dynamic demand response control strategy for isolated microgrid with primary frequency regulation,” *Electric Power Systems Research*, 224, p. 109691. Available at: https://doi.org/10.1016/j.epsr.2023.109691.

Lund, H. *et al.* (2012) “From electricity smart grids to smart energy systems – A market operation based approach and understanding,” *Energy*, 42(1), pp. 96–102. Available at: https://doi.org/10.1016/j.energy.2012.04.003.

Lund, H. *et al.* (2014) “4th Generation District Heating (4GDH): Integrating smart thermal grids into future sustainable energy systems,” *Energy*, 68, pp. 1–11. Available at: https://doi.org/10.1016/j.energy.2014.02.089.

Lund, P.D. *et al.* (2015) “Review of energy system flexibility measures to enable high levels of variable renewable electricity,” *Renewable and Sustainable Energy Reviews*, 45, pp. 785–807. Available at: https://doi.org/10.1016/j.rser.2015.01.057.

Mazhar, A.R., Liu, S. and Shukla, A. (2018) “A state of art review on the district heating systems,” *Renewable and Sustainable Energy Reviews*, 96, pp. 420–439. Available at: https://doi.org/10.1016/j.rser.2018.08.005.

Meibom, P. *et al.* (2007) “Value of electric heat boilers and heat pumps for wind power integration,” *Wind Energy*, 10(4), pp. 321–337. Available at: https://doi.org/10.1002/we.224.

Nielsen, M.G. *et al.* (2016) “Economic valuation of heat pumps and electric boilers in the Danish energy system,” *Applied Energy*, 167, pp. 189–200. Available at: https://doi.org/10.1016/j.apenergy.2015.08.115.

Nord Pool (2025) *Market Coupling Steering Committee confirms go-live of 15-Minute MTU in SDAC on trading day 30 September 2025 for delivery day 1 October 2025*. Available at: https://www.nordpoolgroup.com/en/message-center-container/newsroom/exchange-message-list/2025/q3/market-coupling-steering-committee-confirms-go-live-of--15-minute-mtu-in-sdac-on-trading-day-30-september-2025-for-delivery-day-1-october-2025/ (Accessed: July 15, 2026).

Nord Pool (2026) *Nord Pool | Day-ahead prices*. Available at: https://data.nordpoolgroup.com/auction/day-ahead/prices?deliveryDate=latest&currency=SEK&aggregation=DeliveryPeriod&deliveryAreas=AT,FI (Accessed: July 18, 2026).

Novikov, P. *et al.* (2023) "Review of Technologies of Thermal Energy Generation Using High Voltage Electrode Boilers in the Context of Their Application as Energy Load Regulator," *Systems, Decision and Control in Energy V*. Cham: Springer Nature Switzerland, pp. 355–370. Available at: https://doi.org/10.1007/978-3-031-35088-7_18.

Nuytten, T. *et al.* (2013) "Flexibility of a combined heat and power system with thermal energy storage for district heating," *Applied Energy*, 104, pp. 583–591. Available at: https://doi.org/10.1016/j.apenergy.2012.11.029.

Ommen, T., Markussen, W.B. and Elmegaard, B. (2014) "Comparison of linear, mixed integer and non-linear programming methods in energy system dispatch modelling," *Energy*, 74, pp. 109–118. Available at: https://doi.org/10.1016/j.energy.2014.04.023.

Pini, N. *et al.* (2018) *Magnitude D1.2 Technology and case studies factsheets*. Europaisches Institut für Energieforschung EDF-KIT EWIV. Available at: https://www.magnitude-project.eu/wp-content/uploads/2019/07/MAGNITUDE_D1.2_EIFER_Final_Submitted.pdf (Accessed: July 16, 2026).

Renewables Finland (2026) *Wind power statistics 2025*. Available at: https://suomenuusiutuvat.fi/en/wind-power-statistics-2025/ (Accessed: July 17, 2026).

Repo, A., Tuomi, M. and Liski, J. (2011) "Indirect carbon dioxide emissions from producing bioenergy from forest harvest residues," *GCB Bioenergy*, 3(2), pp. 107–115. Available at: https://doi.org/10.1111/j.1757-1707.2010.01065.x.

Sinha, R., Jensen, B.B. and Radhakrishnan Pillai, J. (2018) "Impact Assessment of Electric Boilers in Low Voltage Distribution Network," *2018 IEEE Power & Energy Society General Meeting (PESGM). 2018 IEEE Power & Energy Society General Meeting (PESGM)*, Portland, OR: IEEE, pp. 1–5. Available at: https://doi.org/10.1109/PESGM.2018.8586236.

Sinsel, S.R., Riemke, R.L. and Hoffmann, V.H. (2020) "Challenges and solution technologies for the integration of variable renewable energy sources—a review," *Renewable Energy*, 145, pp. 2271–2285. Available at: https://doi.org/10.1016/j.renene.2019.06.147.

Soysal, E.R. *et al.* (2016) "Electric Boilers in District Heating Systems: A Comparative Study of the Scandinavian market conditions," *Swedish Association for Energy Economics Conference 2016* [Preprint]. Available at: https://backend.orbit.dtu.dk/ws/portalfiles/portal/126597670/Electric_boilers_in_district_heating_systems_Lule_2016_2_.pdf.

Statistics Finland (2026a) "Fuel Classification 2026 | Statistics Finland." Available at: https://stat.fi/en/luokitukset/polttoaineet/polttoaineet_1_20260101 (Accessed: July 18, 2026).

Statistics Finland (2026b) “Fuel prices in electricity production by Month, Fuel price in electricity production and Information. PxWeb.” Available at: https://pxdata.stat.fi/PxWeb/pxweb/en/StatFin/StatFin__ehi/statfin_ehi_pxt_13p7.px/table/tableViewLayout1/ (Accessed: May 28, 2026).

Sun, B. *et al.* (2022) “Research on Demand Side Response Strategy Considering Operation Flexibility of Thermal Storage Electric Boiler,” *2022 4th International Conference on Smart Power & Internet Energy Systems (SPIES)*. *2022 4th International Conference on Smart Power & Internet Energy Systems (SPIES)*, Beijing, China: IEEE, pp. 2134–2139. Available at: https://doi.org/10.1109/SPIES55999.2022.10082418.

Taylor, M., Atkins, M. and Walmsley, T. (2025) “Hybrid Industrial Utility Systems with Biomass and Electrode Boilers: A Techno-Economic Investigation.” SSRN. Available at: https://doi.org/10.2139/ssrn.5119642.

Trømborg, E. *et al.* (2017) “Flexible use of electricity in heat-only district heating plants,” *International Journal of Sustainable Energy Planning and Management*, pp. 29-46 Pages. Available at: https://doi.org/10.5278/IJSEPM.2017.12.4.

Wang, X., Gui, J. and Cai, H. (2023) “Optimization Method for Demand Response of Thermal Storage Electric Boilers,” *2023 6th International Conference on Intelligent Autonomous Systems (ICoIAS)*. *2023 6th International Conference on Intelligent Autonomous Systems (ICoIAS)*, Qinhuangdao, China: IEEE, pp. 379–384. Available at: https://doi.org/10.1109/ICoIAS61634.2023.00070.

Werner, S. (2017) “International review of district heating and cooling,” *Energy*, 137, pp. 617–631. Available at: https://doi.org/10.1016/j.energy.2017.04.045.

Witkowski, K. *et al.* (2020) “Role of thermal technologies for enhancing flexibility in multi-energy systems through sector coupling: technical suitability and expected developments,” *IET Energy Systems Integration*, 2(2), pp. 69–79. Available at: https://doi.org/10.1049/iet-esi.2019.0061.

Yang, L., Zhang, X. and Gao, P. (2018) “Research on heat and electricity coordinated dispatch model for better integration of wind power based on electric boiler with thermal storage,” *IET Generation, Transmission & Distribution*, 12(15), pp. 3736–3743. Available at: https://doi.org/10.1049/iet-gtd.2017.2032.

Yilmaz, H.Ü. *et al.* (2018) “Analysis of the power-to-heat potential in the European energy system,” *Energy Strategy Reviews*, 20, pp. 6–19. Available at: https://doi.org/10.1016/j.esr.2017.12.009.

Zhang, L. *et al.* (2024) “Theoretical analysis and economic evaluation of wind power consumption by electric boiler and heat storage tank for distributed heat supply system,” *Electric Power Systems Research*, 228, p. 110060. Available at: https://doi.org/10.1016/j.epsr.2023.110060.

Zhou, N. and Zhong, H. (2019) “Coordination Dispatch for the Wind Farm-Combined Heat and Power-Electric Boiler Considering Real-Time Pricing,” *2019 4th International Conference on Intelligent Green Building and Smart Grid (IGBSG)*. *2019 4th International Conference on Intelligent Green Building and Smart Grid (IGBSG)*, Hubei, Yi-chang, China: IEEE, pp. 552–556. Available at: https://doi.org/10.1109/IGBSG.2019.8886285.